

The Journal of Refractory Innovations

bulletin

2018



32 Benefits of Modern
Doloma Magnesita Linings

58 Investigation
of Ladle

72 Tundish Furniture
Optimisation



RHI MAGNESITA



bulletin

The Journal of Refractory Innovations

2018

Published by	RHI Magnesita GmbH, Vienna, Austria
Chief Editor	Stefan Schriebl
Executive Editors	Markus Dietrich, Roland Krischanitz, Alexander Maranitsch, Alfred Spanring, Marcos Tomas
Raw Materials Expert	Gerald Gelbmann, Paschoal Bonadia
Lingual Proofreader	Janine Pink
Project Manager	Ulla Kuttner
Photography, Graphics and Production	Markus Kohlbacher, Christoph Brandner
Design and Typesetting	Universal Druckerei GmbH, Leoben, Austria
Contact	Ulla Kuttner RHI Magnesita GmbH, Technology Center Magnesitstrasse 2 8700 Leoben, Austria
E-mail	bulletin@rhimaginesita.com
Phone	+43 50213 5323
Website	rhimaginesita.com

The products, processes, technologies, or tradenames in the bulletin may be the subject of intellectual property rights held by RHI Magnesita N.V. or its affiliated companies.

Cover picture: The image depicts an RH degasser, a secondary metallurgical unit used in steel plants. It shows the two RH snorkels shortly after the end of the process and the steel level in the casting ladle. In the RH process the snorkels are submerged in the liquid steel of the steel casting ladle. Through the argon-purged inlet snorkel, the steel is sucked up into the lower vessel of the RH degasser, to which a vacuum is applied. The steel treated in the lower vessel flows back to the ladle through the outlet snorkel. A continuous steel circulation between the ladle and the RH degasser is created. In the RH degasser there is a strong negative pressure (vacuum), leading to different metallurgical processes, which have a positive influence on the steel quality. Degassing, decarburization, deoxidation and alloying under vacuum are the most important process steps. Rail steel, flat steel for the automotive industry and steel plates for shipbuilding are only a few products that are advantageously made in the RH degasser.

Prefabricated snorkels, which RHI MAGNESITA manufactures ready for use and delivers to our globally operating customers, are essential components of the RH degasser.

RHI Magnesita Worldwide news

UK

RHI Magnesita Included in the FTSE 250 Index

Since December 2017 RHI Magnesita has been included in the FTSE 250 Index. The inclusion marked an important milestone for the company and will further open up the stock to a wide audience of investors. “The inclusion in the FTSE 250 index is another significant step towards the strategic repositioning of RHI Magnesita as the global leader in the refractory industry. Our focus now is to complete the integration, build the business in regions and products where we don’t have a significant presence, and use our combined best in class technological know-how to find new solutions for our customers.”

China

Major Investment in China to Strengthen Market Position and Address Global Supply Shortages

In June 2017 RHI Magnesita announced an increased investment in the strategically important Chinese market by investing more than €20 million in its dolomite plant in Chizhou, China. This investment

marked a decisive response to address global pressures in the supply of raw materials to the refractory industry and provide additional volumes rapidly to customers worldwide.

The Chizhou site includes an extensive dolomite mine and raw material production as well as facilities for the production of high-quality dolomite-based finished products.

With the investment, RHI Magnesita also ensures long-term raw material availability. RHI Magnesita will offer fully integrated dolomite production in China. The Chizhou dolomite mine is considered in quality terms one of the best mines in China and the location in the Anhui Province is located very close to our largest key customers and steel producers.

“One of the reasons for the merger of RHI and Magnesita last year was to create a global leader in the refractory industry capable of capitalizing on growth potential including in China and Asia. After the completion of the investment, our company will be able to offer a fully integrated dolomite source in each of the big regions of the world to our customers and simultaneously offer dual sourcing options.”

Worldwide

Trade Fair Highlights 2019

With around 50 trade fair appearances per year round the globe, RHI Magnesita is eager to present at these international events. With the new design, the RHI Magnesita exhibition stands out. The trade fairs provide an excellent opportunity to talk to experts and to network internationally within the industry.

AISTECH 2019

The Iron & Steel Technology Conference and Exposition
May 6–9, 2019
Pittsburgh/USA

China Glass 2019

The 30th China International Glass Industrial Technical Exhibition
May 22–25, 2019
Beijing/China

METEC international

10th International Metallurgical Trade Fair with Congresses
June 25–29, 2019
Düsseldorf/Germany

Copper CU2019

The 10th International Copper Conference
August 18–21, 2019
Vancouver / Canada

RHI Magnesita Worldwide news (continued)

Germany

Outstanding Furnace Lifetime Record at Stahlwerk Thüringen GmbH in Germany

With the introduction of a newly developed “high performance” refractory concept for the 120 t DC FIN type furnace at one of our FLS (Full Line Service) customers Stahlwerk Thüringen GmbH (Germany) it was possible to achieve an outstanding furnace lifetime record of 2066 heats. The “high performance” refractory concept involves state-of-the-art refractories (e.g., dense pressed bricks, special hearth mix for DC furnaces,) and was specifically designed for Stahlwerk Thüringen GmbH. Compared to the initial situation it was possible to operate the furnace continuously and above all safely for 15 weeks. With this excellent result, it will be possible to save one complete refractory lining per year!

India

JSW T — RHI Magnesita BOF Partnership Contract Reaches new level of Success

JSW Steel Plant, Toranagallu India, is in a Partnership contract with RHI Magnesita for complete BOF management inclusive of technical supervision to ensure highest possible purging efficiency. BOF3 in SMS2 was stopped on June 25th 2018, at a life of 4794 heats. The BOF was stopped due to logistic reasons and had a potential to reach a life of 6000 heats. This is the best result for RHI Magnesita and at the same time the most productive campaign for JSW T SMS2. All 8 purging plugs were operating until the end of campaign and no mix maintenance was required to reach this excellent result with 100% safety. This was the third campaign in a row, where this excellent performance was achieved without mix maintenance, due to close cooperation between RHI Magnesita team and JSW T.

Worldwide

Expanding our Portfolio to Better Serve the Industry!

One of the latest additions to the RHI Magnesita portfolio is advanced systems for process control and safety of operation. In November of last year, the Swedish company AGELLIS® was acquired and included into the department for Systems and Advanced Technologies. AGELLIS® develop measurement solutions based on electromagnetic and vision technologies for steel and nonferrous customers. The products developed in Sweden are a perfect match to the flow control solutions as well as to the extensive refractory portfolio.

RHI Magnesita is now able to offer complete solutions stretching beyond the scope of refractories to ensure process excellence and the highest level of safety for all our customers. The products based on the VISIR (Vision and InfraRed) platform help monitor and track the refractory performances and ensuring “hot-spots” are detected long before they can be seen by the naked eye. As such, these systems increase operational safety by avoiding accidents and unplanned repairs or production stops. By including these systems and solutions into our portfolio, we act customer focused and innovatively.

Because we all want to work in a safe environment, we can pride ourselves by offering the highest safety level in the industry, distinguishing the company from other suppliers. As the driving force of the refractory industry, we must continuously improve our standards and offer nothing but the best to our customers. Selecting RHI Magnesita as one's supplier is synonym with taking the right steps towards operating excellence. The concept of excellence is to be applied not only to refractory related segments, but also to the production process in general.

With the introduction of the EMLI (ElectroMagnetic Level Indication) platform into the steel industry, we are ensuring the customers get in control of their processes by, monitoring slag carry over from furnaces and ladles and measure critical casting levels in tundishes and moulds. The EMLI systems go hand-in-hand with the "Ladle to Mould" concept, joining the flow control portfolio with critical measurement solutions improving process control and creating extensive additional values.

Revolutionizing the nonferrous industry by providing new measurement solutions allowing users to better understand their process in real time. The unique furnace profiling system and the on-line furnace level system are new tools available for Flash, TSL, SAF, converters and holding furnaces, bringing process efficiency and improving operational safety. At this moment, we are working intensively to reach all parts of the company, highlighting the new opportunities created by this acquisition, in both the steel and nonferrous segments. The value creation of combining refractories, flow control solutions and precise process measurement tools is enormous as customers continuously strive towards process excellence.

India

Proposed Merger of Indian Subsidiaries to Better Capture Growth Opportunities in India

RHI Magnesita announced the proposed merger of its three Indian subsidiaries in August 2018. The merger is designed to optimally position RHI Magnesita's operations in the strategically important Indian market to capture growth opportunities more effectively and efficiently. Orient Refractories, a leading manufacturer and supplier of special refractory products, systems and services for the steel industry. RHI India, is the Indian sales company of RHI Magnesita group offering a full range of refractories and related services sourced from various RHI Magnesita group entities to Indian customers. RHI Clasil, is a manufacturer and supplier of mainly alumina-based refractories for steel and cement.

The key objective is to combine the strengths and competencies of all three companies to establish one consolidated listed company that is well positioned to seize future growth opportunities, create value-add for the customers and enhance shareholder value. "The proposed merger of our Indian subsidiaries marks an important milestone towards expanding our market leadership in the refractory market in India. One strong, integrated organization and management will increase long term value for all stakeholders and efficiently combine resources and capabilities. This merger will significantly enhance the profile of our company in India and creates a stronger foundation to tap the immense growth potential we see in the Indian market."

Austria

RHI Magnesita Supports Young Talent: Metaldays 2018

Every year, RHI Magnesita supports the Metaldays of the Montanuniversität Leoben, Austria. The aim of the event is to make metallurgy more tangible and underline the indispensability of metals for a range of high-tech products, like airplanes, cars, mobile phones and computers. To continuously develop this exciting field of research, there is a high demand for young people with enthusiasm for technology and innovation. This year, in June, 30 pupils from all over Austria had the opportunity to get to know various areas of metallurgy and experiencing metallurgy up close, e.g., through visits to laboratories, the steel plant of voestalpine in Donawitz and the Styrian Erzberg. In addition to gaining insights into current research projects and the university environment, the lively exchange of experience with teachers and students of metallurgy was an essential component.

The Metaldays are a great initiative to increase the number of metallurgy students. According to an analysis of Montanuniversität Leoben, approximately 50% of the pupils participating in the Metaldays begin to study at the University afterward. The initiative gives RHI Magnesita a better chance of recruiting highly qualified young specialists and securing the demand for specialists of tomorrow.

RHI Magnesita Worldwide news (continued)

Worldwide

INNOREG — The New Regenerator System for Glass Furnaces

The performance of the glass furnace regenerator has a direct effect on the energy efficiency of the glass production process. To achieve the best performance with optimum regenerator design, the operational conditions and customer expectations have to be considered. RHI Magnesita's INNOREG system has captured all features of top performing regenerators into an innovative and flexible regenerator solution. INNOREG is a tool box, combining well-known and proven material solutions for the checkers, the casing, and the rider arches, with new optimized checker shapes, providing improved characteristics. The heat exchange surface of the checker work is one of the key factors influencing the energy efficiency of the regenerator. Therefore, the INNOREG system introduces a new fluted chimney block solution with 15% increased heat exchange surface area (TLW shape), leading to a calculated increase in efficiency of more than 1%. At the same time the new format maintains all advantages of today's chimney blocks

Another concern of glass producers is the clogging of regenerator channels at the condensation zone level, in presence of a high load of sulphur and

particulates in the flue gas. In this case channels with a larger flue size may prevent such problems. The INNOREG system provides a new checker format, the innovative Large Channel Pieces (LCP), allowing the necessary increase of the flue size of the regenerator channels by two. This reduces the risk for clogging and at the same time facilitates the cleaning of the channels from condensates. Rounding out the INNOREG system are the proven chimney blocks which are 100% compatible with the new INNOREG shapes. All-in-all, with INNOREG, RHI Magnesita provides the most sophisticated glass furnace regenerator system available on the market

Worldwide

Innovative Prefabricated Ladle Bottoms Skyrocketing in Demand

With the introduction of innovative prefabricated ladle bottoms based on doloma-carbon bricks RHI Magnesita has met with strong demand on the market. Annual growth rates of 35% during the last years clearly indicate that an increasing number of steel mills appreciate the advantages of time and labour savings during installation and the significant improvement in steel yield of optimized designs compared to conventional linings. Prefabricated ladle bottoms are available in a wide range of refractory materials and are produced in tailor-made designs, based on computer simulations and customer requirements.

Worldwide

RHI Magnesita Awarded for Customer Focus

RHI Magnesita was awarded for its customer focus at the joint ceremony of the third edition of the Cemex's Integrate Innovation Program and the first global edition of Supplier of the Year Award. Cemex, a leading global building materials company and one of the world's top producers and traders of cement and clinker presented the awards at a ceremony on May 30, in Monterrey, Mexico. The award in the global category "Customer Focus" recognizes the excellent results and customer service obtained for the customer Cemex. RHI Magnesita's success is based on continuous and intensive cooperation with Cemex and seamless customer service over decades. The award also highlights the outstanding performance of the sales and technical service team and their accountability, reliability and flexibility in meeting customer requirements.

Austria

RHI Magnesita Receives Renowned Export Award from the Austrian Federal Economic Chamber

RHI Magnesita received the silver award for its foreign trade initiatives at the ceremony for the 2018 Export Awards. This year's Export Awards were presented by Margarete Schramböck, Austrian Federal Minister of Digital and Economic Affairs and the newly elected WKÖ President Dr. Harald Mahrer. The award in the category "industry" for RHI Magnesita underlines the success of the company's export strategies in the recent past.

Norway

Porsgrunn Plant Restart

The restart of the RHI Magnesita's fused magnesia facility in Porsgrunn (Norway) took place in January 2018. The decision is based on positive results of a test run in September 2017 and continued demand for high-quality magnesia. It is also a reaction to the still tense situation in China where stricter environmental requirements significantly affected market prices, availability, and the stability in the supply of fused magnesia. The fused magnesia facility restart in Porsgrunn marks a major step in the extension of RHI Magnesita's vertical integration of key raw materials and will further increase the company's supply security.

Worldwide

Five R&D Locations and the new Technical Advisory Committee to Further Drive Innovations Globally

In today's globalized and highly dynamic age, trends and innovations emerge anytime and all over the world. Thus, RHI Magnesita has both expanded global research network with a research centre in India and established a new Technical Advisory Committee consisting of renowned external scientists and internal R&D experts to further develop its technology leadership globally. Our mission "Taking innovation to 1200 °C and beyond" reflects our commitment to R&D and innovation. To keep its finger on the pulse of the local markets, RHI Magnesita operates decentralized research at

five locations including the strategically important growth markets in China, India and North America. Besides the research hubs in Leoben (Austria) and Contagem (Brazil), our research network consists of the research centers in York (USA), Dalian (China) and Bhiwadi/Visakhapatnam (India).

The key role of the new Technical Advisory Committee (TAC) is to bring in new perspectives and knowledge from outside and strengthen the ties to the external technology and research world. "The new Technical Advisory Committee brings together external scientists and researchers with internal specialists from R&D, business development and technical marketing. The keyword is Open Innovation. Our objective is to open up the innovation process by actively and strategically using the outside world in order to increase the innovation potential through knowledge transfer and thought-provoking impulses from outside", says Chief Technology Officer Luis Bittencourt.

Europe

Award for RHI Magnesita's Collaborative Employee App

In April 2018, RHI Magnesita was awarded second place for its innovative employee app "MyRHIMagnesita" at the renowned Intra.NET Awards in Berlin. In the category "Best Collaborative Tool". The employee app was launched in October 2017 in time for the merger of RHI and Magnesita and plays a key role in the change process and in the cultural transformation of the company.

"Our employee app has become the central information and communication platform for our 14,000 employees worldwide. It promotes direct communication, openness, interaction and collaboration and is thus an essential driver for cultural change." In addition to Corporate News, the content of the app includes a CEO channel with reports on business trips, local channels for all locations as well as useful information such as menus of the local canteens, press reviews, fact sheets on the company, various brochures, forms for event registrations, feedback and important guidelines.

RHI Magnesita Worldwide news (continued)

Worldwide

The new President of the World Refractories Association (WRA)

Stefan Borgas was elected new president of the World Refractories Association (WRA) and took office in January 2018. He will assume the presidency previously occupied by François Wanecq, former CEO of Vesuvius plc, for two years.

The RHI Magnesita delegation directed their gratitude to Mr. Wanecq for his work and dedication as inaugural president of the WRA and thanked the whole Vesuvius team for the seamless handover they facilitated together with the WRA secretariat. "It is a great honour and pleasure for me to chair our industry's global association. I will continue with my team to work hard to further promote the interests of the refractory industry worldwide and expand its global network", said Borgas.

Besides strengthening the role of the association founded in 2014 as a counterpart to other world industry and customers organizations such as the World Steel Association, We will strive to increase the number of WRA members to unite as many producers as possible. Among the obvious main issues, special focus will be placed on innovation, safety, safety data collection, and the tense global raw material situation driven by stricter environmental regulations in China as thematic priorities for the presidency in 2018.

For more information please visit www.worldrefractories.org

US

RHI Magnesita Named Finalist for the American Metal Market's Award for Steel Excellence

RHI Magnesita has been named a finalist for the renowned American Metal Market's Award for Steel Excellence in the category of Raw Materials/ Consumables Provider of the Year. The American Metal Market Award is one of the most prestigious awards programs for the global steel industry and recognizes world-class innovation and excellence in steel industry throughout the whole supply chain and by key partners to the industry. The nomination alone is recognition of the excellent results obtained in the Full Line Service work for Outokumpu Americas. The basis for this success is the long-term, constant and intensive cooperation with the customer by working hand-in-hand directly at the customer's plant to guarantee sustainable optimization of refractory material management and joint success.

For the past eight years, American Metal Market has presented the Awards for Steel Excellence, which is one of the most prestigious and recognizable awards programs for the global steel industry. The awards have recognized world-class innovation and excellence in steel and related industries for companies throughout the steel supply chain and by key partners to the industry.

Europe

Renowned Double Award for RHI Magnesita's new Brand and Visual Identity

The "Transform Awards Europe" has honoured brand development and rebranding projects for the past eight years rewarding excellence and innovation in branding across Europe. This year RHI Magnesita had two reasons to celebrate - the rebranded RHI Magnesita received the silver awards for "Best corporate rebranding following a merger" and in the industry category "Best visual identity from the engineering and manufacturing sector". The new logo and the visual system that has evolved from it consists of a horizontal eight, the symbol of infinity, and the shapes of refractory bricks. The brand is intended to mark the starting point of the business' cultural transformation and was created as the foundation upon which the new corporate culture can grow.



RHI MAGNESITA



RHI MAGNESITA

Operating worldwide



A letter from our editor



Research and Development is pivotal at RHI Magnesita, enabling innovative, reliable products and services to be tailored to our customers' requirements. Currently more than 270 employees comprise the research team at five locations in Leoben (Austria), Contagem (Brazil), York (USA), Dalian (China) and Bhiwadi/Visakhapatnam (India). Additionally, a newly established Technical Advisory Committee is providing further expertise to ensure we retain technology leadership and support the mission of having a best-in-class R&D organisation. For more information about these initiatives, please see the news item on [page 7](#).

Magnesite is an essential raw material for our industry and its mining and processing at RHI Magnesita dates back to 1881. Therefore, this edition opens with an overview of magnesite resources, the specific magnesia types used in refractory products, as well as our mines and production capabilities. In the second paper, the iron ore pellet induration process is described to highlight the tailored refractory lining solutions available for the grate and rotary kiln technologies. With a focus on cost-saving, the next article details the advantages of doloma magnesia bricks for the central burning zone in cement rotary kilns, which have the ability to withstand critical conditions resulting from alternative fuel firing.

The production of ferronickel results in large amounts of slag that is corrosive to the furnace lining. To improve refractory performance, microscopic investigations and thermodynamic calculations were performed and are presented in the fourth paper. This is followed by examples of laser scanning in an EAF and infrared shell temperature monitoring of a RH degasser and ladle furnace to demonstrate the value of condition monitoring for predictive maintenance, lifetime prognosis, and safe operations. In the sixth paper, development and implementation of slag modelling at a steelmaking plant in Brazil is presented that led to a sustainable improvement in ladle refractory life. The next article details an innovative modelling approach that considers the influence of joints on strains and stresses in equipment containing large numbers of bricks. To illustrate how the periodic linear homogenization technique can be applied, a complete steel ladle was examined. An additional article relating to the steel ladle describes a study using both numerical and physical simulations that shows how yield improvements could be achieved through a new well block design that minimizes slag carryover.

The last two papers in this edition focus on the tundish. The first is dedicated to the evolution of impact pots and RHI Magnesita's novel TUNFLOW HYBRID, a cost-effective design series that provides customer-specific solutions. In the concluding article, a study is presented showing how a coupled modelling approach was used to optimize the position and size of tundish furniture and improve mixing efficiency.

Finally, I would like to express my gratitude to all the authors and editorial team for their valued contributions and commitment. This Bulletin edition is particularly special, because it is the first occasion to publish papers that have been jointly written by colleagues who have combined their expertise as a result of last year's merger.

Yours sincerely

Stefan Schriebl

Corporate Research and Development
RHI Magnesita



“ This Bulletin edition is particularly special, because it is the first occasion to publish papers that have been jointly written by colleagues who have combined their expertise as a result of last year’s merger. ”



RHI MAGNESITA

Introducing...

The driving force of the refractory industry

RHI and Magnesita.
A new global leader in refractories.

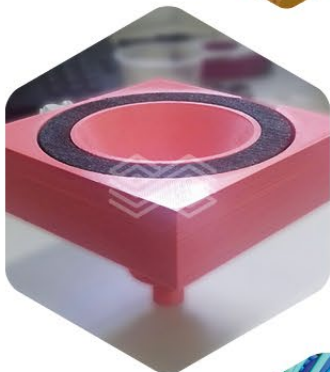
Find out more at
rhimagnesita.com

Contents



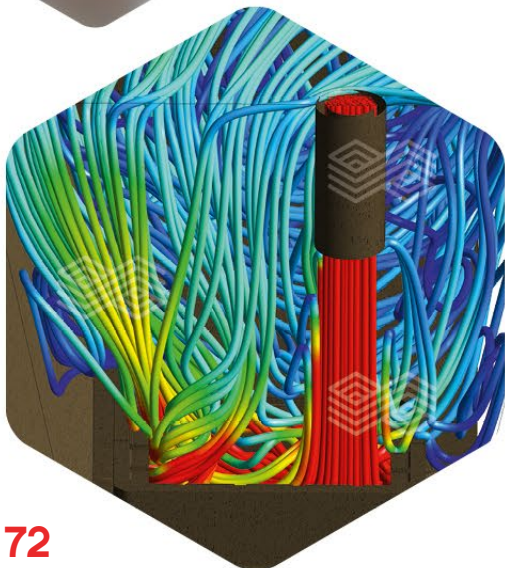
32

Benefits of Modern Doloma Magnesia Linings



58

Investigation of Ladle



72

Tundish Furniture Optimisation

- 14** **Overview of Magnesite**
- 24** **Refractory Concept for Grate Kiln Technology Induration Machines**
- 32** **Benefits of Modern Doloma Magnesia Linings in Modern Cement Kilns**
- 38** **Evaluation of High Temperature Refractory Corrosion by Liquid Ferronickel Slags**
- 42** **Refractory Condition Monitoring and Lifetime Prognosis**
- 48** **Development and Application of a Slag Model for Increasing Ladle Life at Integrated Steel Mill — Brazil**
- 54** **An Investigation on the Influence of Expansion Joints in the Mechanical Behaviour of Steel Ladles**
- 58** **Investigation of Ladle Yield Improvements Through New Well Block Design**
- 64** **Tundish Technology and Processes: Ladle to Mould Systems and Solutions (Part III)**
- 72** **Tundish Furniture Optimisation Through Mathematical Modelling**

Subscriptions service and contributions

We encourage you, our customers and interested readers, to relay your comments, feedback, and suggestions to improve the publication quality. Furthermore, to receive the Bulletin free of charge or contribute to future editions please e-mail your details (name, position, company name, and address) to the Subscription Service:

Email
bulletin@rhimagnesia.com

Phone
+43 50213 5323

Thomas L. Drnek, Matheus Naves Moraes and Paschoal Bonadia Neto

Overview of Magnesite

This article provides an overview of magnesite and magnesia. The various raw materials and production processes have been summarised. Specifically, the RHI Magnesita magnesite and magnesia production sites, focussing on those in Brazil, Brumado and Contagem. Worldwide magnesite production and consumption statistics have been summarised and analysed on the basis of various references [1–11], notably World Mining Data [5], the historical data series of the United States Geological Survey [6], and the Roskill study of magnesium compounds [11]. Future consumption trends were also analysed, with a specific focus on the steel industry, CO₂ emissions, recycling and finally the current magnesite production situation in China.

Summary

Magnesite is a magnesium carbonate with the chemical formula: MgCO₃. magnesite occurs in three types: sparry or macrocrystalline magnesite (also called type Veitsch), cryptocrystalline magnesite (also called type Kraubath), and the type Bela Stena (fluvial-limnic). The global magnesite resources are 13 Gt, that provides a static resource production ratio of approximately 500 years, however if the dissolved magnesium in seawater is added, the figure would be much higher.

Magnesite is converted into magnesia. Magnesia has three types: caustic calcined magnesia (CCM), sintered magnesia (also called dead burned magnesia, DBM), and fused magnesia (FM). CCM is very reactive and has many applications. The two other types (DBM and FM) are nearly solely used in refractory applications. The largest type is the DBM with an annual production of around 7.5 Mt, then the CCM follows with around 4 Mt and then the FM follows with around 2 Mt of production. The total magnesia market has a volume of approximately 13 Mt. The most important consumption region is Asia, followed by Europe, North and Latin America. The other regions play a minor role.

The specific consumption of refractories has shown a significant decrease since 1950, however this trend has changed, due rising steel production, the absolute consumption has increased.

Looking forward the following trends are most significant, the shift from primary to secondary steel production, the legal frame work for the CO₂ emissions trading (ETS), that will become more significant in Europe, the increased recycling of magnesia, and the situation in China.

Definition of Magnesite, Magnesium Salt and Magnesia Types

Magnesite

Magnesite is a magnesium carbonate with the chemical formula MgCO₃. It is an industrial mineral and forms deposits, occurring partly as rock forming resource. Three important deposits types are:

- sparry or macrocrystalline magnesite (also called type Veitsch).
- cryptocrystalline magnesite (also called type Kraubath).
- type Bela Stena (fluvial-limnic), Serbia.

The sparry magnesite displays macroscopic crystal habit and is very often iron-rich. The Fe₂O₃ content normally ranges of 1% and 8%. This type occurs often with dolomite and talc. Important occurrences are located in, Veitsch, Breitenau, Radenthein (Austria), Brumado (Brazil), Satka (Russia), and China (often partly with low Fe₂O₃ content).

The cryptocrystalline magnesite has no macroscopic structure. It forms from magnesium-rich rocks (mostly serpentine). The iron content is mostly very low with values below 1%. Important occurrences are in Kraubath (Austria), in Turkey and in Greece [1] The type Bela Stena is a cryptocrystalline special form and it occurs in fluvial or limnic sediments and is named from the type locality in Serbia [2].

Magnesite Resources

Generally, only minimal data exists on the extent of global magnesite resources. One relevant figure is from Ian Wilson, and is shown in Table I [3].

The total amount of magnesite resources is 13 Gt, the most important countries are: China, North Korea, and Russia, with each having approximately 20% of the global resources. Slovakia follows with 10% and Brazil with 7%. From this a static resource production ratio of approximately 500 years can be calculated [3].

Table I.
Global magnesite resources [3].

Country	[Mt]	[rel.%]
Australia	628	5
Brazil	862	7
China	3439	26
North Korea	3000	23
Russia	2745	21
Slovakia	1240	10
Others	1086	8
Total	13000	100

Magnesium Salt

The main salt consumed for magnesia production is magnesium chloride $MgCl_2$, however in some cases the magnesium ion can also be bonded with sulphate ($MgSO_4$)₆. These salts can form solid deposits (evaporite), but also occur as a water solution (brines and seawater). The mining method is solution mining (Netherlands), where water is pumped into the ground and the solution retrieved, or if it is already a liquid, the liquid is pumped up (similar to crude oil). Additionally, it can also be concentrated from the seawater.

Important occurrences are in Europe, in the Zechstein formation, Mexico and USA (near the Great Lakes), Moreover, magnesium salt can be found in solution in the Dead Sea (in a high concentration), and in all seawater.

The “Magnesia lifetime” (similar to resource production ratio) would be much higher if all the magnesium content of seawater was taken into consideration.

Magnesia Types

Magnesia

Magnesia is chemically pure magnesium oxide (MgO), also called periclase. The melting point of magnesia is 2800 °C, hence it is used in high temperature applications in the refractory industry (e.g., linings in the BOF vessel). Magnesia is used in the following types, dead burned magnesia (DBM, also called Sintermagnesia or sinter), fused magnesia (FM) and caustic calcined magnesia (CCM).

Caustic Calcined Magnesia

CCM is commonly decomposed magnesite or calcined magnesium hydroxide (it can also be established by burning magnesium metal). That means that the molecule loses the CO_2 or the water, and in these areas a porous structure remains. Therefore, the CCM has typically a very high specific surface area, resulting in a very reactive behaviour. This is the opposite of the DBM or the FM, which are densified and develop large periclase crystals due to the sintering or fusion process. CCM has no strength; it displays a soft-lumpy or a fine powder macro-structure. CCM has, due to the very high reactivity, numerous applications.

Dead Burned Magnesia

DBM, also called Sintermagnesia is produced by firing with a high temperature at around 1800–2300 °C. It has a cubic crystal system, and a bulk-density in the range of 3.00–3.45 g/cm³. The size of the crystals range from 50–200 µm. The main application is the refractory industry.

Fused Magnesia

FM is produced by melting in an electric arc furnace. The difference to the DBM is in the higher density (FM has typically a density in the range of 3.43–3.54 g/cm³) and the crystal size, that ranges from 200 up to more than 2000 µm. The main application of the FM is the refractory industry.

Production of Magnesia

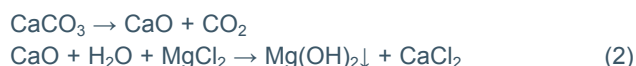
The production can be divided by the initial material:
Natural: magnesite ($MgCO_3$).
Synthetic: Magnesium salt ($MgCl_2$).

The reaction formula for the natural process – route is as follows:

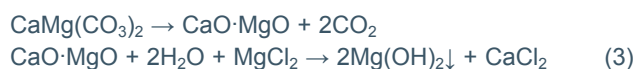


For production, magnesite is heated to approximately 1000 °C and the carbonate decomposes into CO_2 and is eliminated through the furnace exhaust gases, what remains is the magnesia (MgO). The further treatment in temperature and time defines if CCM, DBM or FM is produced and CCM in DBM are normally produced in shaft kiln or rotary kiln multiple hearth furnaces (MHF).

The synthetic process route to produce MgO is more complex. The common method uses the wet-chemical process route. That process is described as follows:



or



The lime (CaO) is produced by firing limestone ($CaCO_3$). In addition to the limestone, dolomite ($CaMg(CO_3)_2$) can also be used – then dolime is the product of the first step. In the wet-system the $Mg(OH)_2$ is removed, and the calcium is soluble and is dissolved as calcium chloride. The resulting magnesium hydroxide is then dried and calcined at around 1000 °C. CCM is established in this process and it can be further processed (by firing or melting) to DBM or FM.

RHI Magnesita NV's production of Magnesite and Magnesia

Figure 1 shows the RHI Magnesita NV magnesia production sites worldwide.

The largest MgO producer within RHI Magnesita is Brumado (Brazil), responsible for 370 Ktpy of DBM and 40 Ktpy of CCM, through a sparry magnesite processing.

Brumado's process starts with the mine operation, blasting the ore and transport to the primary crushing facility. There are two mines operating: Pedra Preta, responsible for the M10 DBM ore (94.5% DBM) and Pomba, responsible for the M30B DBM ore (98% DBM with Fe_2O_3 lower than 0.5%). Figure 2 shows the mines.

Both ores share the primary crushing facility, which is responsible for the reduction of the ore size from 900 mm to 300 mm and removal of hand size impurities by hand picking. The crushed ores follow different lines from this point, direct sintering for the M10 ore and mineral processing followed by double step firing for M30B ore.

The M10 ore is fed in eight vertical shaft kilns to produce the DBM. As this is a single step sintering, the ore is fed into the kiln and, calcined and sintered.

The M30B ore, in turn, has a more complex process, as the MgO content of the ore must be raised from 95% to 98% for the DBM production. In order to achieve such high purity, the crushed ore is sent to a mineral processing plant to remove silicates, the main impurity. In the processing plant, the ore is milled to release the silicates from the magnesite and then removed through a reverse flotation process.

The concentrated magnesite is then ready for densification. Firstly the purified magnesite is fed into a multiple hearth furnace to calcine the magnesite (magnesium carbonate), converting it into periclase (magnesium oxide). The calcined material follows a compaction process to produce briquettes with high strength and green density. The briquettes are then directed to the shaft kiln and sintered at temperatures

up to 2300 °C. The Brumado unit relies on four lines of MHF, briquetting, and shaft kilns for M30B production.

The DBM produced in Brumado is sent to different refractory plants for basic bricks and mixes production around the world, and for FM production in Contagem (Brazil).

The fusion plant in Contagem has 6 furnaces producing approximately 20 Ktpy of FM. The fusion plant can use crushed DBM or CCM briquettes as feedstock, depending on the furnace set-up. The melting process requires approximately 8 to 10 hours and the electric arc can generate temperatures in excess of 2800 °C. During the solidification process, different FM qualities develop throughout the ingot volume, especially with respect to the physical properties. The highest grade premium product is the large crystal material (LC) with a density of 3.54 g/cm³ and a crystal size larger than 2100 µm. Additionally, a high-grade FM with a density of 3.51 g/cm³ and a crystal size of approximately 1300 µm is also obtained.

Another DBM and FM production site is located in China. The site, located in Dashiqiao, has a similar process when compared to Brumado, relying on milling and reverse flotation to remove the impurities from the magnesite ore to obtain concentrates, with up to 98% MgO. The purified

Figure 1.

RHI Magnesita NV raw material production sites.



Figure 2.

Showing the Pedra Preta mine (a) and Pomba mine (b), in Brumado, Brazil.



(a)



(b)

magnesite is calcined in an MHF, briquetted, and then sintered in a shaft kiln. The main difference in this process, when compared to the operation in Brazil, is that the product is ground prior to briquetting, allowing the DBM to reach the targeted bulk density ($>3.35 \text{ g/cm}^3$). This facility also produces FM by melting briquetted CCM with 98% MgO.

The Austrian sites of RHI Magnesita NV produce approximately 300 Ktpy of magnesia. The mines in Breitenau, Hochfilzen, and Radenthein produce DBM from a sparry magnesite.

The mine in Breitenau operates a large underground mine and also an open pit. The mine operates two mining methods. In the upper section the so called post-pillar mining is used and in the deeper areas sublevel stopping with backfill is adopted. The ore is sintered in three rotary kilns to produce different DBM grades. The Z Sinter (Z for cement) is used for the production of refractory bricks for the cement industry. Moreover, different grades of DBM for the use in monolithics are produced. The main application in monolithics is for hearth ramming and hearth repair mixes for the electric arc furnaces in recycling steel production (ANKERHARTH, ANKERFRIT).

The mine in Hochfilzen operates a large open pit, that is situated at high altitude in the Alps, and is only operated in summer. The ore is sintered in a rotary kiln to produce DBM, used for monolithics, predominately hearth mixes, but also gunning, and tundish mixes.

The operation in Radenthein is an underground mine, that is situated on the Millstätteralpe. The ore is transported by cable car to the plant. There the magnesite is calcined, generating CCM, that is used in the construction industry and for agricultural purpose.

A different type of ore deposit is found in Eskişehir, Turkey, where a cryptocrystalline magnesite mine is operated by RHI Magnesita. In this case, the processing plant takes advantage of the host rock, a serpentinite, rich in magnetic minerals. Therefore, the process relies on subsequent magnetic separation stages combined with manual selection for the coarser fractions. This site has two rotary kilns and three shaft kilns to sinter to concentrated magnesite, fed

according to the particle size and quality of the material. More than 15 types of DBM can be produced, with varying MgO, CaO, and bulk density levels.

The seawater plant in Drogheda, around 50 km north of Dublin in Ireland, produces DBM and uses the synthetic process route, with limestone. The seawater is mixed with lime to produce the magnesium hydroxide, which is dried and calcined in an MHF. The CCM is then briquetted and sintered in a shaft kiln. The sinter is used for the production of refractory bricks.

The plant Porsgrunn in Norway, around 80 km southwest of Oslo, produces FM using CCM from the synthetic process route from seawater. The plant operates a rotary kiln for calcining the magnesium hydroxide and 10 electric arc furnaces for the production of FM.

To complete the description in Figure 1: The plants York, Chizou, Sinterco, and Belo Horizonte produce dolomite, and the plants Uberaba and Santa Luz produce synthetic bauxite and chromite, respectively.

The Worldwide Production of Magnesite and Magnesia

Figures 3 and 4 show the historical development of magnesite production on a global basis. The source of Figure 3 is [5], which shows only explicit magnesite production. It can be seen that in the 1980's global magnesite production was at approximately 15 Mt and then as a result of the collapse of the COMECON, fell to approximately 10 Mt. Production then rose slightly until 2002, whereupon the growth rate increased rapidly until production reach 25 Mt in 2010, since then production has remained in this range [5].

The comparison with the Figure 4, the source [6], shows a much longer timeline, starting in 1913, however, it shows all types of magnesium compounds, not only magnesite. It shows a production level below 5 Mt until 1960, it rose rapidly to 10 Mt and remained in this range until 1995, and increased to 30 Mt recently. The difference in the volume is because, dolomite and some other magnesium sources, are included. In general, both graphs (Figures 3 and 4) show a very similar trend.

Figure 3.

Global magnesite production 1981–2015 [5].

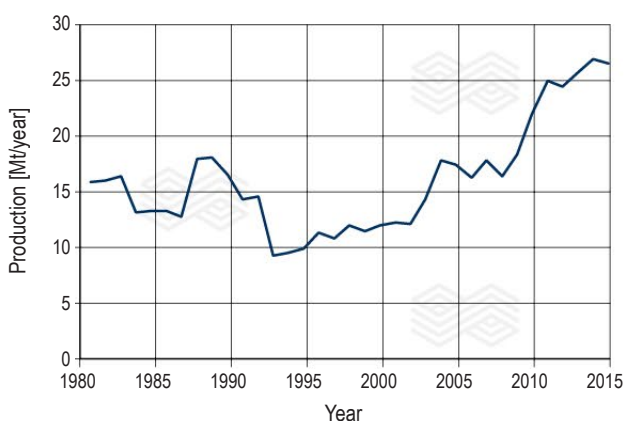


Figure 4.

Global magnesium compounds production 1913–2015 [6].

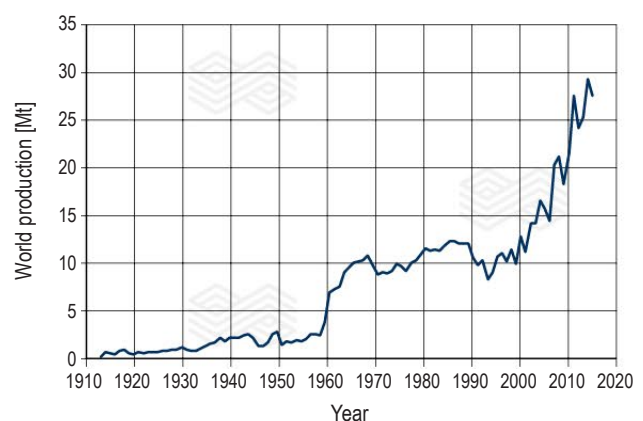


Figure 5 shows the distribution of the magnesite production in the year 2015 by country [6]. It is clear that China accounts for roughly two thirds of production and has by far the largest share. Then countries like Turkey, Russia, Slovakia, Austria, Australia, and Brazil follow. Austria has rank five and Brazil rank 7.

The market concentrations are measured by the Herfindahl Hirschmann Index (it is the square of the market share by countries), based on the World Mining Data [5]. The historical development shows a low to medium concentration until the year 2004, this was when the critical value of 2000 was passed, and since that time we have a concentrated market. The reason being the market entrance of China, currently the value of the Herfindahl Hirschmann Index ranges between 4000 and 5000. This means that the market is very strongly concentrated and is dominated by China (Figure 6).

The European Commission regularly conducts analysis on the market for raw materials. A result of the European Union – Raw Materials Initiative that was initiated 10 years ago. The commission analyses the criticality, that is based on two values: the supply risk (mainly market concentration / HHI) and the economic importance (mainly value of the downstream products). The result for the year 2014 shows magnesite as critical (Figure 7). However, the EU analysis of the year 2017 (with a very strongly modified methodology) changed the classification to not critical [7, 14].

The analysis of the different magnesia type shows the following situation (Figure 8). The majority of magnesite is transformed into DBM with a share of 63%, then it follows the CCM with a share of 29% and finally the FM with a share of 8%. The total production of natural magnesia was 10.7 Mt for the year 2010 [8].

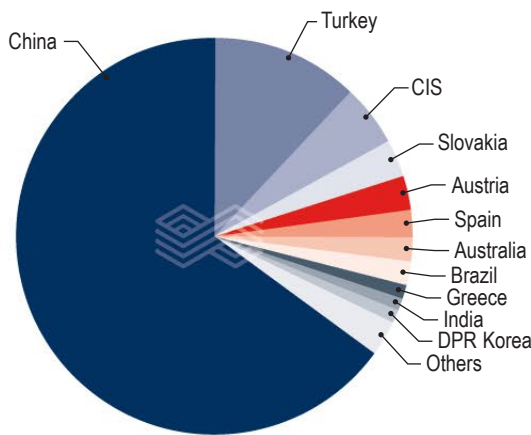


Figure 6.
The market concentration by countries of magnesite (HHI-WMD) [5].

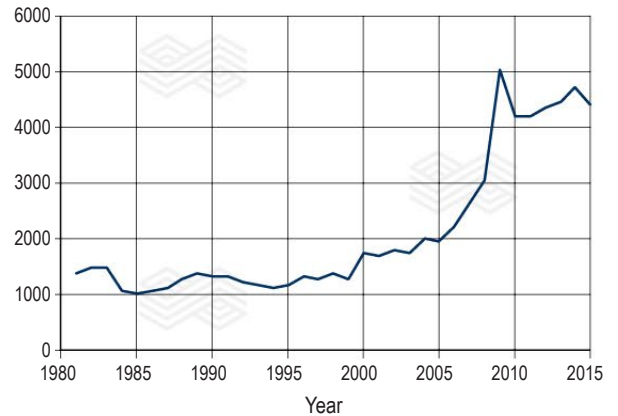


Figure 7.
The criticality analysis of raw materials of the EU Commission from the year 2014 [7].

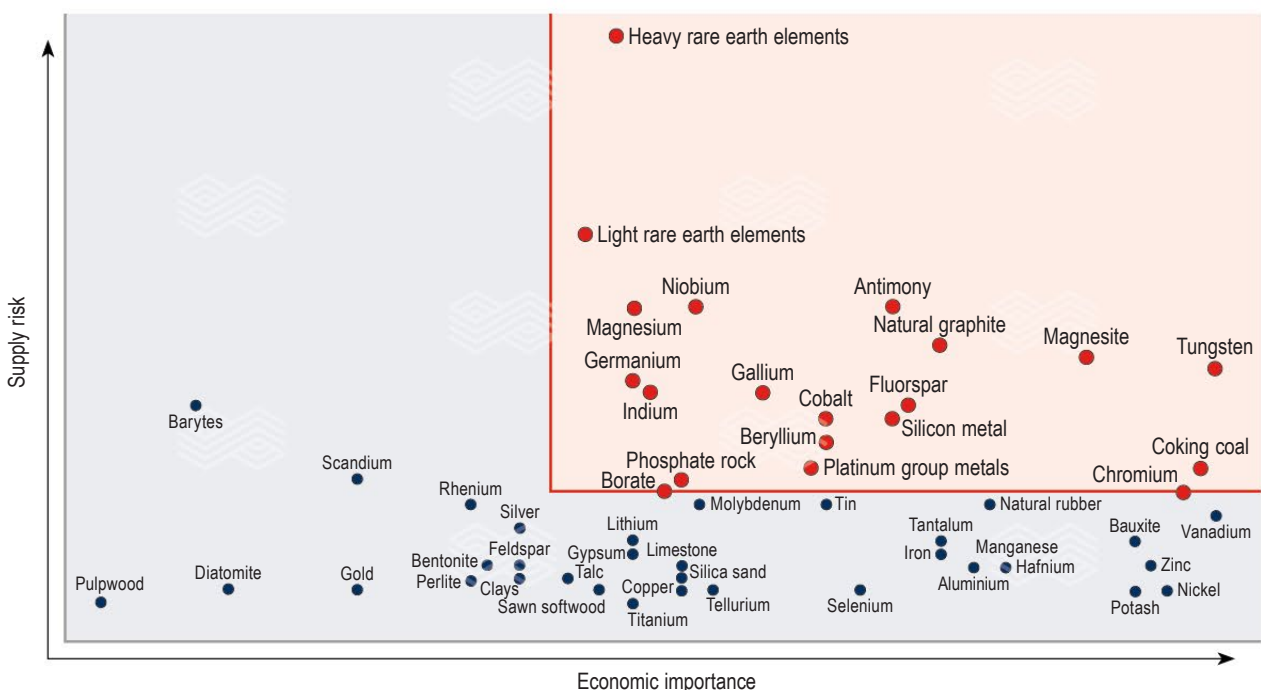


Table II.
Usage of magnesia by sector, type, and region (global, 2010).

Region in 1000 t	Refractories DBM	Refractories FM	Industrial CCM	Agricultural CCM	Others CCM	Total CCM	Total Magnesia
Asia	4200	1400	1800	70	200	2070	7670
Europe	2400	200	480	190	230	900	3500
N. America	400	100	170	80	90	340	840
S. America	350	40	40	50	20	110	500
Middle East	80	5	85	5	10	100	185
Oceania	60	15	70	20	10	100	175
Africa	30	10	35	5	10	50	90
Total	7520	1770	2680	420	570	3670	12960

Various statistics and information can be compared. The initial point is the global magnesite production shown in the World Mining Data (the quantity is 22.1 Mt for the year 2010) [5]. This quantity results in a theoretical magnesia quantity of approximately 11 Mt. This agrees with the 10.7 Mt value, it can be assumed that all magnesite is fired to magnesia as it is nearly the sole use of magnesite.

Roskill shows the total magnesia production (natural and synthetic) with around 13 Mt (year 2010) [10]. With this information the production of synthetic magnesia can be calculated at approximately 2.3 Mt (Figure 9).

Figure 8.
Production of natural magnesia type in the year 2010 [8].

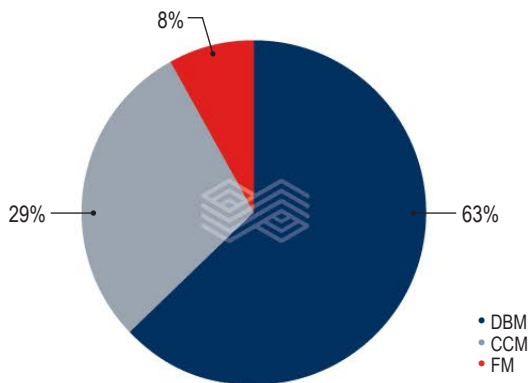
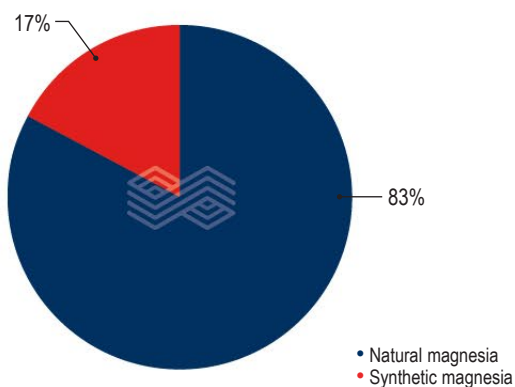


Figure 9.
Production of natural and synthetic magnesia (2010) [10].



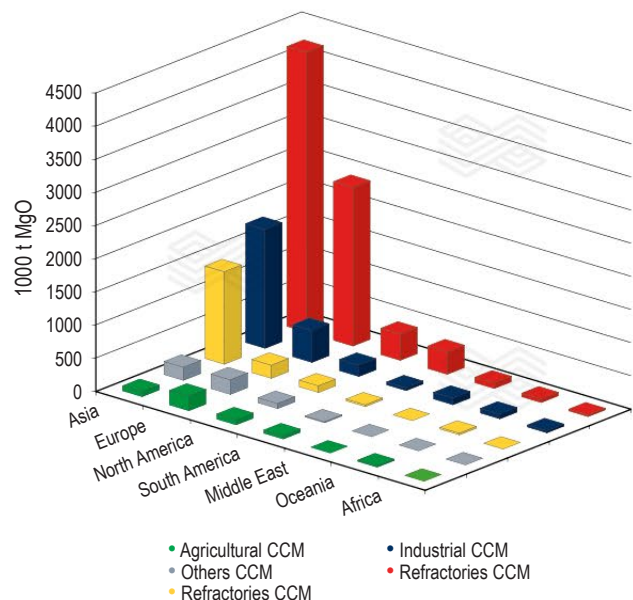
The Consumption of Magnesia

The consumption or usage of magnesia by sectors and the regional distribution show that the main quantity is used as DBM in the refractory industry. This application consumes around 7.5 Mt. It must also be taken into consideration that nearly all DBM is used in the refractory sector, with only a few other applications. The situation is similar with FM, but with one exemption, that is the application in heating elements.

The situation with the CCM is different, there are nearly 100 applications. The industry is by far the largest consumer, with 2.7 Mt, followed by the agricultural sector, with 0.4 Mt, and other applications with 0.6 Mt. In total the CCM has a market volume of 3.7 Mt.

The analysis of the regional distribution by continent shows the following, Asia consumes the majority with around 7.7 Mt followed by Europe with 3.5 Mt, North America with 0.8 Mt, Latin America with 0.5 Mt. The details are shown Table II and Figure 10.

Figure 10.
Usage of magnesia by sector, type and region (global, 2010).



By analysing the trend in the consumption of refractories over decades, the trend for the specific consumption, measured in kg refractories per tonne of steel, has significantly decreased, as shown in Figure 11. This trend is in the steel industry, but also in other consumption areas like the cement industry and glass production. This trend is common to all refractory products. Within the timeframe from 1950 to 2008 there has been a decreasing demand from 60 kg refractory/t steel to 15 kg refractory/t steel. This is a significant reduction of 75%, which is similar to the situation in the areas of cement and glass.

If the magnesia demand in the steel industry is analysed for the last 20 years the situation is as follows. In 1994 the specific demand was at around 5.5 kg MgO/t steel, then this figure came down to 4.5 kg in 2004, and since then the reduction slowed and in 2014 a demand of around 4.2 kg MgO / t steel was observed. If these figures (specific MgO consumption) are multiplied by the global steel production, the magnesia demand in the steel industry can be calculated. The demand in 1994 was approximately 4 Mt magnesia and in 2014 the demand was approximately 7 Mt magnesia.

This result fits to the consumption that was shown in the Roskill study and the general trend in the curve of the

Figure 11.

Development of the specific refractory consumptions by sectors from 1950–2008.

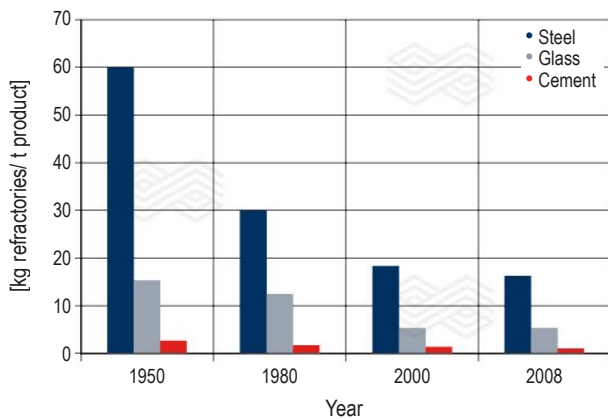
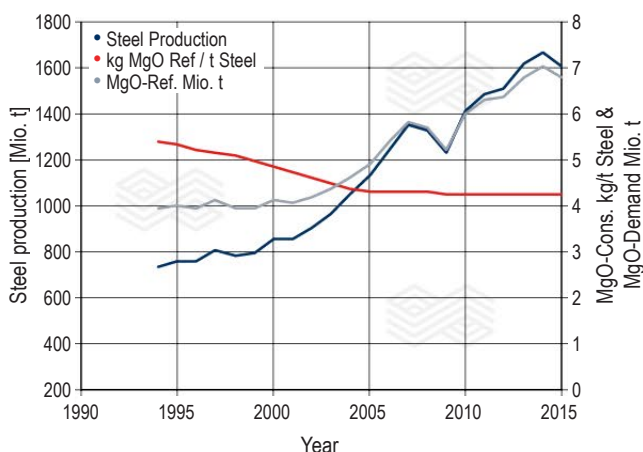


Figure 12.

MgO demand in the steel industry 1994–2015.



magnesia consumption in the steel industry fits well to the shape of the magnesite production based on the World Mining Data. The different data sources (World Mining Data and Roskill study), are in close agreement, with a quantity difference of 0.5 Mt or approximately 2%.

The trend of reduced specific consumption is currently very slow. Further significant reductions in the specific magnesia consumption are not expected. The magnesia demand (and as consequence the magnesite) is linearly linked with the strong increase in steel production (Figure 12).

Outlook

The outlook focuses on four different issues. The process routes of the steel industry, the CO₂ regulatory framework (Post Kyoto legislation), recycling of magnesia and the recent situation in China for the production of magnesia.

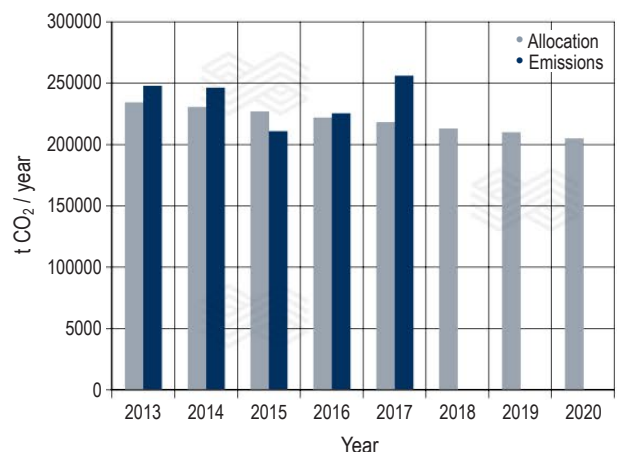
Currently, the steel production follows two main process routes. The primary route with using iron ore, a blast furnace, and a steel converter to produce steel. This route, represents approximately 70% of production. The secondary route, using steel scrap and melting in an electric arc furnace, has a market share of around 25%, and the other process routes can be classified as special processes. Due to an increase in the “production” of steel scrap, the amount of steel that is produced via the secondary process route will increase. Nevertheless, the primary route will also grow, driven by increasing steel demand. From this it follows that the demand for magnesia will also increase, because both process routes require magnesia in the refractory lining.

The CO₂ legislation or also called “Post Kyoto Legislation” plays an important role in the EU and in the associated countries. Starting with the “climate target”, a reduction of 20% of the CO₂ emissions, based on the year 1990. The EU adopted the so-called Emission Trading Scheme (ETS), which is valid for the industrial sector.

The production sector requires the so-called “allocations”, that allow the industry to emit CO₂. Theoretically, a site is not allowed to emit more CO₂ unless it can acquire new licenses (also called allowances). In the producing sector,

Figure 13.

Plant Breitenau CO₂ emissions and allocation.



and especially, the sectors that are a threat for “Carbon-Leakage”, when the burden reaches a defined limit, the sector can get up to 100% of free allocation.

Figure 13 shows the allocations for the Breitenau Plant for the current trading period (2013–2020). It can be seen that the current free allowances from the State are insufficient. Currently under discussion is the next ETS period (2021–2030) and it is expected the free allocation will be further reduced.

If the different process routes are now analysed, by process and region, it shows the following picture (Figure 14). All process routes and regions have a very similar amount of the so-called “process emissions”, that is the CO₂ that is a result of the decomposition process of the carbonates, magnesite, limestone, or dolomite. The specific amount is around 1 t CO₂/t MgO. The further CO₂ emissions come from the firing process. The difference in this field is a result of the process, the efficiency, and the type of fuel used.

When the fuel-related emissions between Breitenau and MAS are analysed, both plants use natural gas as fuel, MAS has a higher energy input, that is caused by differences in the chemical composition of the ore. MAS has a low-iron magnesite, while Breitenau, an iron-rich one. The iron aids in the sintering process, resulting in the difference. Breitenau has fuel related CO₂ emissions of around 0.3 t CO₂/t MgO and MAS has around 0.5 t CO₂/t MgO.

In contrast, the synthetic process route can be shown. In this case, three heat processes are needed (calcining the limestone or dolomite, calcining the magnesium hydroxide to CCM and then the final sintering process). This process has (by using only natural gas as a fuel) specific fuel-related emissions of around 0.8 t CO₂/t MgO.

The last alternative shows the case in China, where also the natural process route is in use, but the efficiency is not optimised and the fuel is coal. Therefore, the specific emissions in China are in total 2.2 t CO₂/t MgO.

Within this field, the significantly better emissions provide a real asset for the EU. A longer-term outlook in the field of Emission Trading, indicates that a global emissions regime is far from reality. However, in the meantime the EU will maintain and tighten the current regime. Details of the next period are not yet fixed, but the situation is not expected to become easier for producers. Which harms the competitiveness of European magnesia producers, when compared to producers outside the EU.

Another point in the outlook is recycling of magnesia. In many applications, especially of CCM in the agricultural sector, the direct recycling of magnesia is not possible, as it is consumed.

In the field of refractories, a large portion of the refractory material ends up in the slag, making the direct recycling of magnesia once more impossible. Nevertheless, the slag can be used as a construction material, but especially within Austria this approach is not possible, leading the slag to be

dumped and used as landfill. Definitely, these are wasted resources.

The recycling of the remaining refractory material in the plants after use, when they are broken out, is a possible way for recycling. Technically it is a challenge, because of different impurities from the production and/or the process. Nevertheless, significant efforts are ongoing to increase the share of this material used in refractories. In the future recycling will be a viable source of magnesia.

The last point in the outlook is the situation in China. The government has stopped nearly all production of magnesia via environmental restrictions at the end of 2017. The reason was the poor environmental situation, mainly the air quality, in large regions of China. The supply collapsed within China and because no magnesia was being produced, export was nearly impossible. The exact amount of the production restrictions cannot be provided currently, because no recent statistics have been published, if they exist. But, the situation is reflected in the price of magnesia for export. Figure 15 shows the development of the price for the quality DBM grade 94–95% MgO content. The price for the first half of 2017, was around 200 USD/t, the price then doubled to approximately 400 USD/t and at the end of first

Figure 14.

CO₂ emissions in different productions sites worldwide.

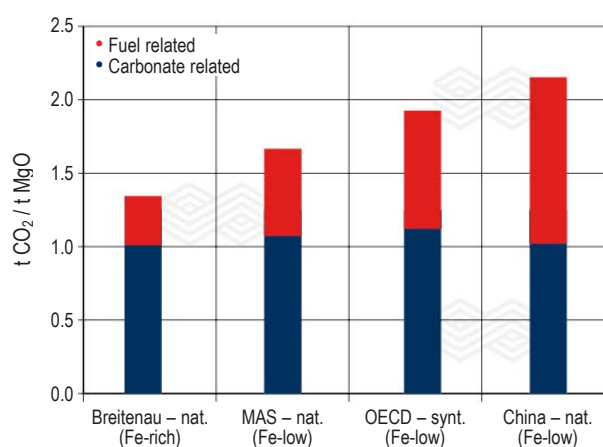
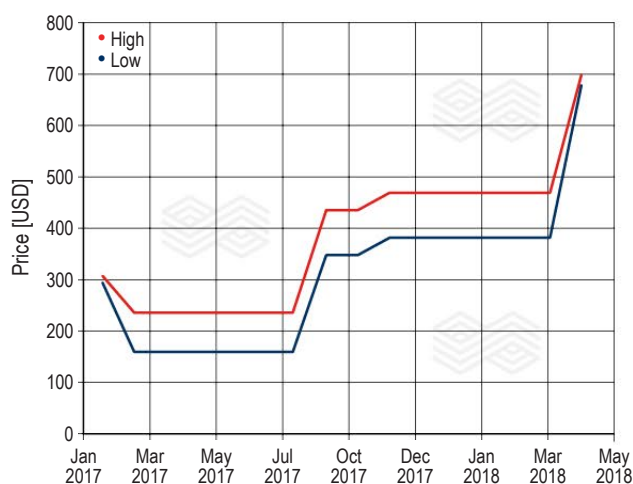


Figure 15.

Magnesia price development for the grade DBM 94-95, from Jan. 2017–Apr. 2018.



quarter of 2018, nearly doubled again to 700 USD/t. A further outlook is currently difficult to provide, but it is assumed, that production in China will resume at some point, under better environmental standards. However, a significant decrease in prices is not expected.

In summary, a further growth in the demand for magnesia is expected, which will result in further growth in magnesite production. This growth will be driven mainly by the steel industry, however growth is also expected in other applications. It is expected that there will only be incremental reductions in the specific consumption of magnesia within the steel industry. The role of CO₂ emission trading will continue to have an increasing influence on the production of magnesia within the EU. The impact of recycling is expected to grow across industry. The situation in China will change, however the process has just started.

References

- [1] Rösler, H. J. Lehrbuch der Mineralogie. Deutscher Verlag für Grundstoffindustrie, Leipzig. 1991. p. 700.
- [2] Pohl, W. L., W. und W.E. Petrascheck's Lagerstättenlehre. Mineralische und Energie-Rohstoffe. 5.Auflage. Stuttgart 2005, p. 268 ff.
- [3] Wilson, I. Magnesite – Global update and Chinese Situation. MagMin, 2012, Salzburg, p. 72.
- [4] Drnek, T. Die Sintermagnesita im Spannungsfeld von technologischen und wirtschaftlichen Veränderungen (Dissertation). Montanuniversität Leoben, 2002. p. 13.
- [5] Weber, L. und Reichl, C. World Mining Data. Jahrgänge 1981 bis 2017, International Organizing Committee for the World Mining Congresses, Wien.
- [6] NN, Historical Data Series, Magnesium Compounds, USGS, www.usgs.gov.
- [7] NN, Report on critical raw materials for the EU. Report of the Ad hoc Working Group on defining critical raw materials. 2014. European Commission, Brussels, 2014, p. 24.
- [8] see 3.
- [9] Reichl, C., M. Schatz, M. and Zsak, G. World Mining Data 2015. Heft 30, International Organizing Committee for the World Mining Congresses, BMWFW, Wien, 2015, p. 125.
- [10] NN: Magnesium Compounds and Chemicals: Global Industry Markets and Outlook. Twelfth Edition, 2013, Hrsg: Roskill, London, p. 28.
- [11] NN: Magnesium Compounds and Chemicals: Global Industry Markets and Outlook. Twelfth Edition, 2013, Hrsg: Roskill, London, p. 327.
- [12] Feytis, A. Between the linings. In: Industrial Minerals, June 2010, p. 46–51.
- [13] Drnek, T. Is the Current European Emissions Trading System a Suitable Means for Achieving Climate Protection Goals? In: RHI Bulletin, 1 – 2015, p. 44–50.
- [14] NN, Study on the review of the list of Critical Raw Materials. Criticality Assessments. Written by Deloitte Sustainability, British Geological Survey, Bureau de Recherches Géologiques et Minières Netherlands, Organisation for Applied Scientific Research. Hrsg: European Commission, June 2017, Brussels, p. 93.
- [15] Ghilotti, D. Magnesia: market tightness continues to bite. Industrial Minerals, April 2018, p. 29–31.

Authors

Thomas L. Drnek, RHI Magnesita, Breitenau, Austria.

Matheus Naves Moraes, RHI Magnesita, Contagem, Brazil.

Paschoal Bonadia Neto, RHI Magnesita, Contagem, Brazil.

Corresponding author: Thomas L. Drnek, thomas.drnek@rhimagnesita.com





RHI MAGNESITA

Taking
innovation
to 1200 °C
and beyond



Erick J. Estrada O., Gerald Hebenstreit, Christina Stimpfl and Cesar Nader

Refractory Concept for Grate Kiln Technology Induration Machines

Iron ore pellets have been from beginning last century one of the most desired feeds in iron making processes, with productions levels over 2000 million tonnes per year. The high Fe content and the capability for easy transport, makes them an ideal solution for direct reduction plants and blast furnaces. The technologies available for pellets production are wide, but the Grate kiln brings the most flexible of all systems. As high temperature and aggressive conditions are common in these processes, one of the main items to take in count is the refractory lining concept.

Introduction

Iron ores are natural state raw materials used for later induration processes. To obtain high purity levels of iron, initial procedures are needed, such as mining and beneficiation. These activities begin with the mineral extraction, crushing, and concentration. The resulting fine iron-rich ore material is then balled into pellets as shown in Figure 1.

The main components of iron ore are hematite and magnetite, however other components are also present, a sample composition determined by XRF analysis is shown in Table I.

The induration process begins by providing the iron ores a circular form, using binder products that help the enriched fines attach, this eases further processing and transport.

Currently, there are different technologies for obtaining high quality pellets that are used in direct reduction process and blast furnaces. One of the most widely known is the Grate

Table I.

Example of green pellet characterisation, values based on ignited sample at 1050 °C by XRF analysis (ISO 12677).

	[% Mass]
Na ₂ O	0.9
MgO	10.9
Al ₂ O ₃	2.5
SiO ₂	21.4
CaO	3.5
TiO ₂	1.6
MnO	0.6
Fe ₂ O ₃	56.2
ZnO	0.1
P ₂ O ₅	0.5
K ₂ O	0.2
V ₂ O ₅	1.6
Total	100.0

kiln technology, in which after balling, the iron ore fines into green pellets, they are then dried and pre-heated over a travelling grate. Then, the pellets are transported to a rotary kiln where induration occurs. Finally, the indurated pellets enter to a cooler, in order to provide the correct temperature decrease.

Despite of the used technology, all these processes requires specially selected and tailor-made high-quality refractory materials to ensure a safe and issue-free operation of the iron ore induration machines.

Figure 1.

Iron ore green pellets.



The refractory industry is continually changing, looking forward to develop the best custom-made solutions for all high temperature processes. A system which provides customer specific requirements offers a unique opportunity to optimise individual systems.

Iron Ore Induration Machines

Pelletizing is one of the preferred agglomeration processes for iron ore concentrate, as the chemical, physical, and metallurgical characteristics of pellets make them a more desirable feed for iron making processes [1].

Since 1950, iron ore induration machines have been increasing their importance and installed capacity all over the world. In 2017, worldwide iron ore production was approximately 2093 million tonnes [2].

Table II

Main differences between Grate kiln and Traveling grate technologies [3].

	Grate Kiln	Traveling Grate
Electrical Energy Consumption	-	+
Energy Efficiency	-	+
Fuel Choices	+	-
Fuel Consumption	+	-
Generation of Fines	+	-
Pellet Quality	+	-
Process Flexibility	+	-
Raw Material Choices	-	+
Refractory Maintenance Costs	+	-
Steel alloy needs for Construction	-	+

Different technologies are available to obtain high quality indurated pellets. One of the most well known processes is the Grate kiln technology. There are a number of advantages and disadvantages when compared with one of the other important process, the Traveling grate technology as shown in Table II.

Grate Kiln Technology

Iron ore pellets production began in the middle of the last century, the history of the process dates back to 1912, when the Swede A.G. Andersson developed the first pelletizing method [4].

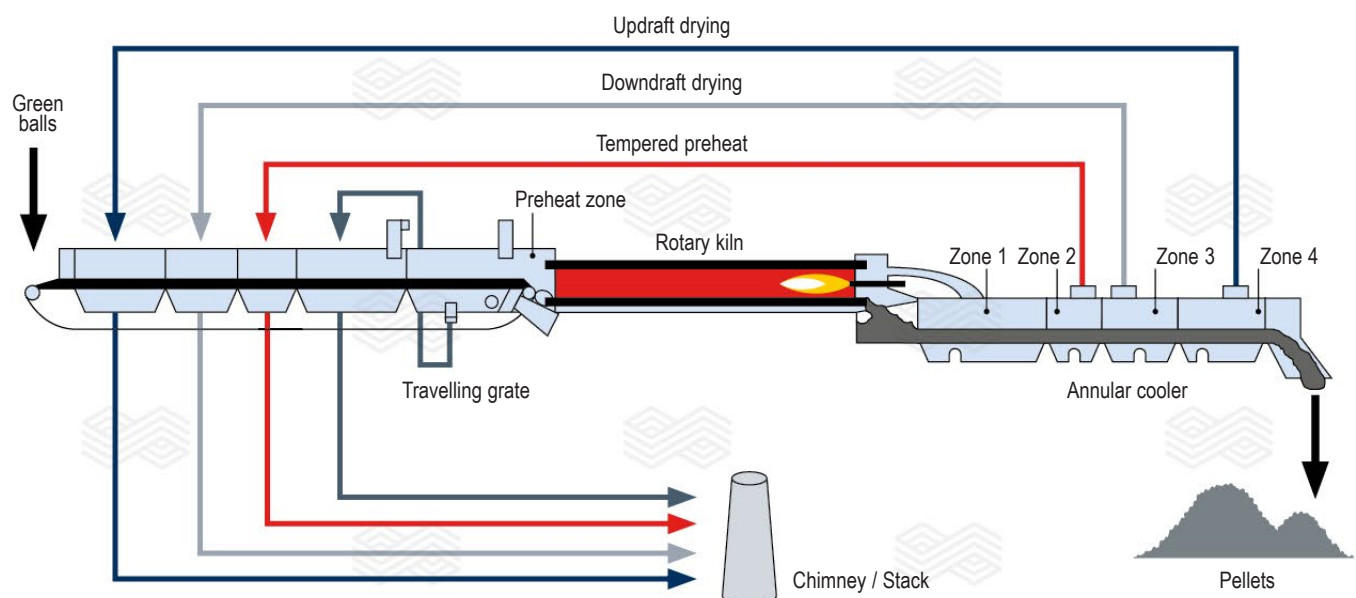
Since then, different technologies have emerged, improving the efficiency of the overall process, resulting in more productive and clean processes, allowing the use low grade iron ores and even different types of fuels.

First installed in 1960 and designed by Allis-Chalmers (now METSO), the Grate kiln technology has three main process stages: drying and pre-heating, induration, and cooling. These characteristics provide an incredible flexibility to the process, achieving a more consistent pellet quality with less electrical consumption [1].

In this technology, both the beginning and end of the process are based in grates, where pellets initiate the heating as well as the cool-down for stocking and delivery to end user. The grate uses pellets as beds where gases pass through and the refractory lining is not in direct contact. For drying purposes, temperatures inside the furnace are approximately 400 °C prior to the preheating of the green pellets. On the opposite side, at the end of the firing process, the pellets enter with a temperature of approximately 1000 °C until completely cooled (Figure 2).

Figure 2.

Modern Grate kiln system flowsheet [5].



The rotary kiln, located between the two grates, has a totally different condition for refractories, as the pellet goes up and down during the inclined rotation until the cooler is reached. In each revolution, the refractory lining can be exposed to different temperatures (Figure 3) [3].

Each step of the process has a single condition in which refractory materials are exposed. The dust agglomeration at the drying stages, mechanical stresses inside the rotary kiln, thermal shock, and abrasion during the cooling stages. These unique conditions demand specific materials selection. Knowledge and experience with these aspects are essential to achieve the best refractory solutions for this process.

Traveling Grate

After the iron ore is pelletized, the Traveling grate is the first step in the Grate kiln process.

The main objective is to dry and preheat the pellets before feeding the rotary kiln through several zones: updraft drying (UDD), downdraft drying (DDD), temperature pre-heat (TPH), and pre-heat (PH) [3].

The refractories are required from the beginning of the grate through all further stages.

Rotary Kiln

The second stage is where induration occurs. The rotary kiln is fed with pellets that already have sufficient mechanical properties to make the process possible [6]. With a burner located at the outlet of the kiln, the temperature is raised to 1300 °C during the process until the indurated pellets proceed to the cooler.

One of the main problems of rotary kilns in general, is the high thermomechanical stresses at the outlet. RHI Magnesita has developed the Thrust Lock System after years of investigations to solve this issue.

This system offers a variety of advantages:

- Lower mechanical stresses in load bearing bricks, retaining rings and outlet segments.
- Flexible inclination angle of the skew brick.
- High heat resistance.
- Possibility of using it at mid-kiln or outlet region.
- Can be used as single or multistep concept.
- Can be easily combined with any retaining design.
- Cost saver.
- Increases the availability of the kiln.
- Easy installation.
- Shorter shut-downs times.

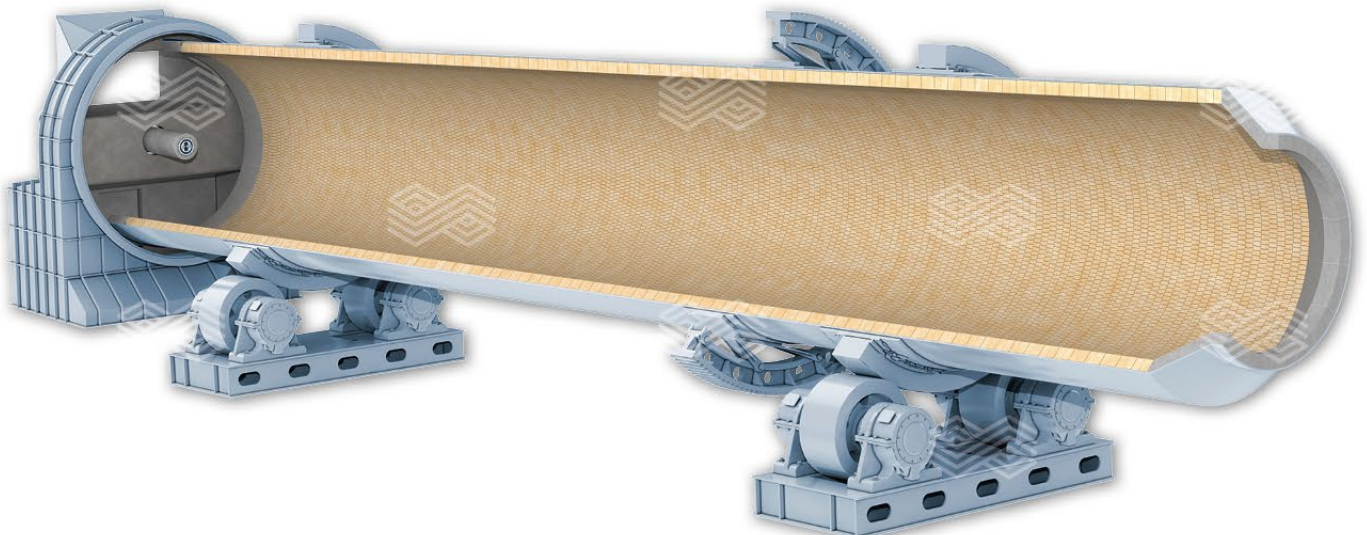
Combined with this state-of-the-art technology, the refractory lining inside the Rotary kiln require high alumina or alumina chromia bricks, to help resist the aggressive conditions. For inlet and outlets, the novel use of Sol-bonded mixes has provided clients great results in terms of performance and equipment availability.

Cooler

In this last stage of the process, the pellets are cool by zones in an annular grate (or straight grate), until discharging through the hopper [6].

Here, in the rotary lower sidewall, the refractory lining has one of the harshest conditions of thermal shock and dust abrasion as cooling gases pass through the pellet bed. An important step forward was to use COMPAC SOL brands on these walls, after several different trials and concepts were conducted. Achieving upgraded properties for this condition, as well as a rapid and easy installation and repair procedure (Figure 4).

Figure 3.
Rotary kiln refractory concept.



Refractory Lining

Every step of the Grate Kiln process has unique conditions and refractory arrangement. Mechanical and physical properties are very important in refractory selection. Additionally, other properties are desired in the overall refractory lining: high thermal shock resistance, high erosion and abrasion resistance, as well as chemical attack resistance.

In Summary, the refractory lining is based in high alumina and fireclay refractory bricks, insulating refractory castables and refractory concretes, among others. In the rotary kiln, as the temperature is higher and it has rotation, the refractory material needs upgraded properties to compensate for the additional mechanical stresses, abrasion, etc.

RHI Magnesita has developed refractory solutions for Grate kiln technology process that is unique in the use of Sol-bonded refractory concretes in all Grate kiln process stages.

As all are no-cement based materials, a mix with nano-colloidal silica component is required, making possible to obtain a refractory material with excellent advantages.

This state-of-the-art development using alumina based materials, which combine high performance properties, easy processing, and simpler heat-up requirements are available for casting, gunning, and shotcreting. The mixes known as COMPAC SOL and COMPAC SHOT have a wide range of available brands that can meet most custom requirement for all clients.

RHI Magnesita offers a wide capability of onsite attendance, local inspections, and technical discussions with all our clients. In addition, new developments and post-mortem analysis from internal specialists and R&D sites worldwide are available, making possible to build together with clients the best solutions for Grate kiln technology. Figure 5 shows an example of the refractory concepts while Table III shows the different refractory brands and zones of installation.

Table III.

RHI Magnesita refractory brands for grate kilns.

RHI Magnesita refractory brands for grate-kilns		Drying	Pre-firing	Firing	Cooling	Ducts
ALUKOR	High Alumina Brick			●		
CEKAST	Conventional Casting & Gunning	●	●		●	●
CERABOND	Mortar	●	●	●	●	●
COMPAC SOL	Sol-bonded Castable		●	●	●	
COMPRIT	Conventional Casting & Gunning	●	●		●	●
DIDOFLO	Free Flow Castable		●	●	●	
DIDOMUR	Mortar	●	●	●	●	●
DIDURIT	Conventional LCC		●	●	●	
LEGRIT	Conventional Casting & Gunning	●	●		●	●
PYROSTOP	Insulating	●	●		●	●
RESISTAL	High Alumina Brick			●		
TAFKAST	Premium Casting		●	●	●	

Figure 4.

Annular cooler rotary lower sidewall cast with RHI Magnesita COMPAC SOL technology mixes.



Figure 5.

Annular cooler refractory concepts.



RHI Magnesita Research and Development Centers have the capability to run the most important standardized tests according to the actual conditions of iron ore induration machines. Material characterisation, mineralogical investigations, corrosion tests, thermodynamic and thermomechanical simulations, are valued analysis that provides important information about how the refractory lining will behave in operating conditions.

Refractory selection has to consider the particularities of each plant location: range of temperatures in each zone, round per minute of the rotary kiln, chemistry of the green pellets and burner combustion fuel feeds. Also, all experiences of previous studies, common failures, new developments, and innovations lead to the design of a proper refractory solution. Additionally, parameters such as budget and time are decision making inputs during this task.

COMPAC SOL and COMPAC SHOT brands have been shown to be an excellent technological development, demonstrating that they are an easy to install no-cement material, shape flexible, safe, and fast heat-up capability used in a wide variety of applications, including the Grate kiln technology induration machine.

Figure 6.
COMPAC SOL B88 installed in the rotary kiln cones.



Sol Bonded castables have important advantages that make them suitable for this application:

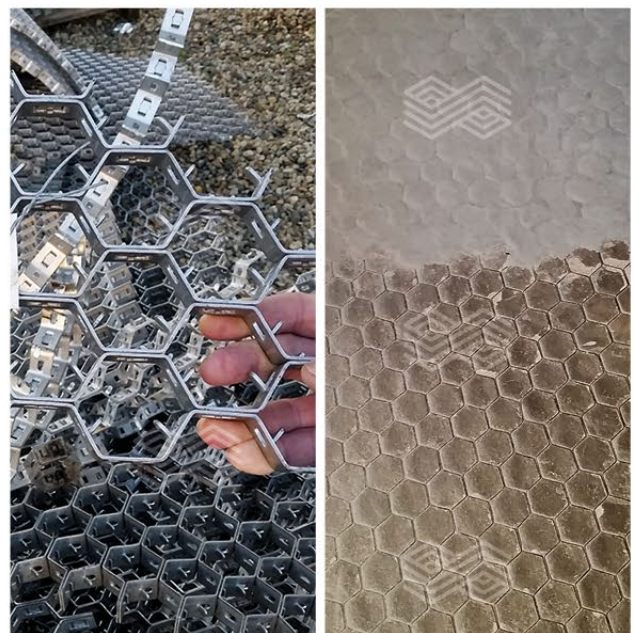
- Longer shelf life and storage.
- Lower impact of ambient conditions in setting behaviour.
- Shorter mixing times.
- Lower impact of inaccurate dosing in overall properties.
- Reduced drying time.
- Lower susceptibility to high steam pressures during heating.

The brands COMPAC SHOT SB F60-3, COMPAC SOL M64-6 and COMPAC SOL F53-6 are commonly recommended for use in the drying, preheating, and cooling stages. The properties desired in these regions are high mechanical resistance at low and high temperatures, thermal shock resistance, and wear resistance (abrasion and erosion predominantly). At the beginning of the Grate kiln process, the temperatures would increase by zones until reaching almost 1300 °C inside the rotary kiln. In the annular cooler, the opposite occurs, the temperature goes from 1300 °C to 100 °C in this circular or straight grate system. The mentioned brands have been developed to work in these aggressive conditions, providing clients excellent performing materials. The COMPAC SOL B88 brand is widely used for inlet and outlet cones inside the rotary kiln along with Trust Lock System for bricks (Figure 6).

In order to design the thickness and layer arrangement for each region, a thermal flow analysis is required, aiming to provide proper insulation and to protect the metallic shell.

Other region that has a unique condition is the dust hoppers, where the process has the highest abrasion condition that affects the refractory materials. HEXMESH is the best anchoring system for the low cement mixes that are installed here, providing an upgraded mechanical resistance to abrasion in low temperature conditions (Figure 7).

Figure 7.
Example of refractory cast material into a HEXMESH.



For all materials, the more useful analyses are the cup test and the rotary slag test. With them, it is possible to compare different brands in matters of chemical attack by green pellets in certain alkali and atmosphere conditions. As generally the client facilitates its own green pellets, it is possible to recreate similar process conditions for each kiln. Figure 8 shows examples of cup test with different refractory types.

Another important owned test is hot abrasion, which provides very important information related to Grate kiln process material behaviour as shown in Figure 9.

In addition, RHI Magnesita has available installation equipment such as the DAT rig. It provides clients an easy and faster way to install bricks inside a rotary kiln. Another important item is the Training Center for Installation Methods, providing a sound knowledge base to all client installation and technical teams.

Figure 8.

Cup test developed with green pellets using (a) COMPAC SOL F53-6 (b) RESISTAL RK10 (c) RESISTAL SK65IS and (d) RESISTAL SK65.

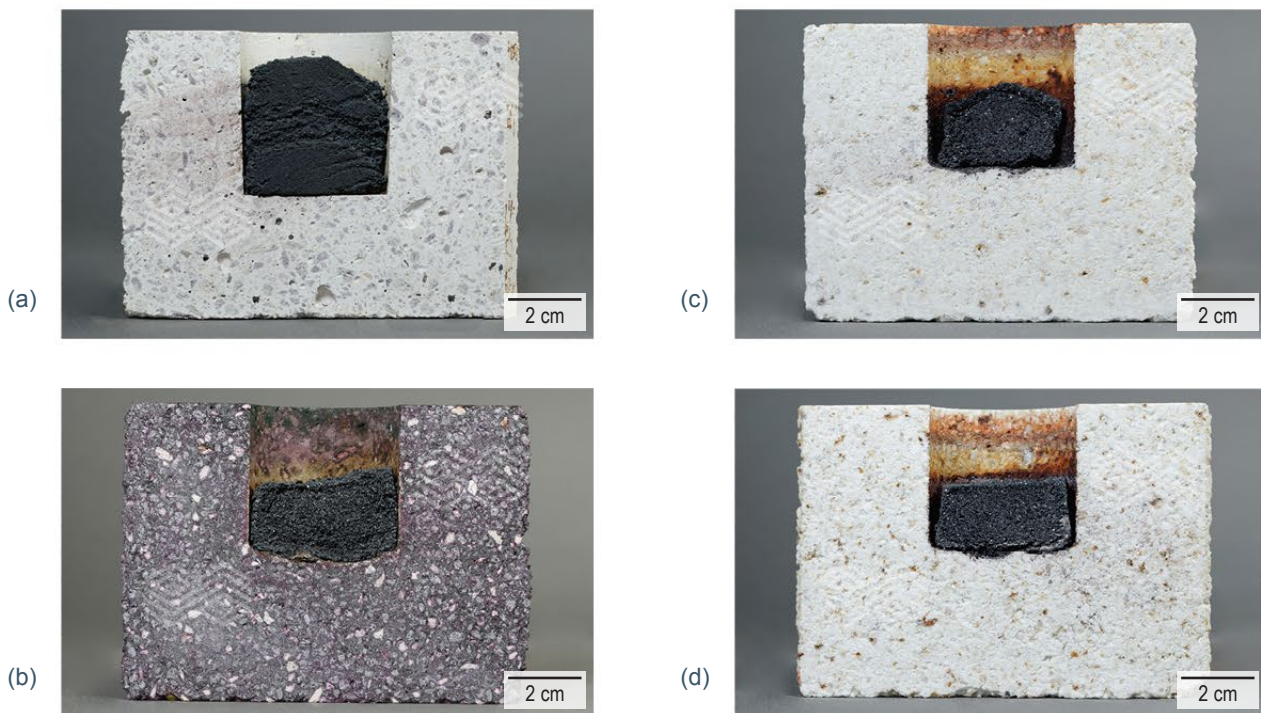
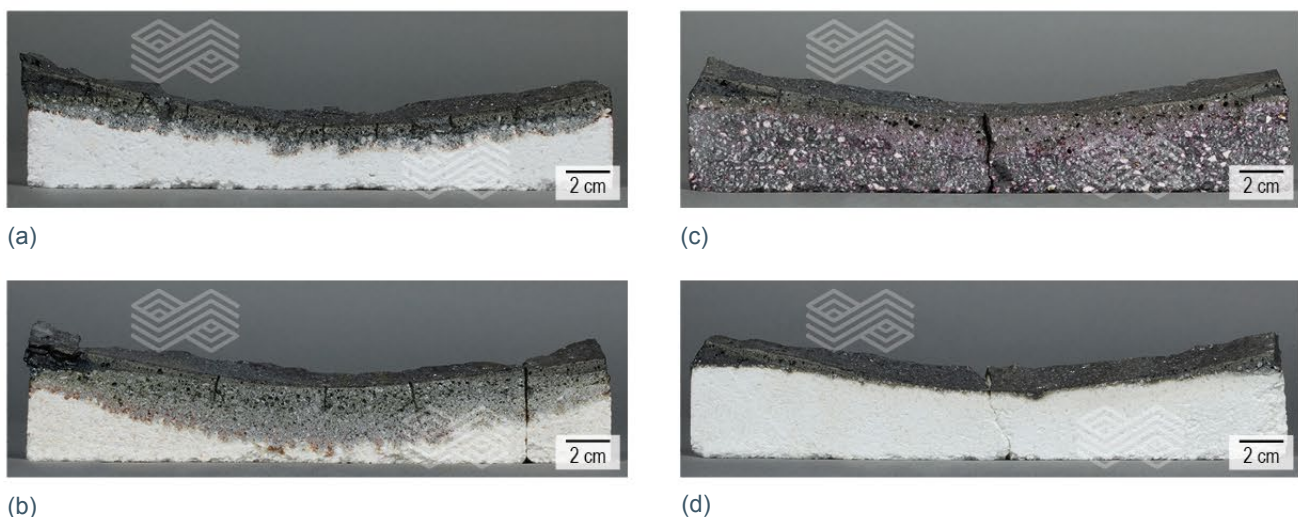


Figure 9.

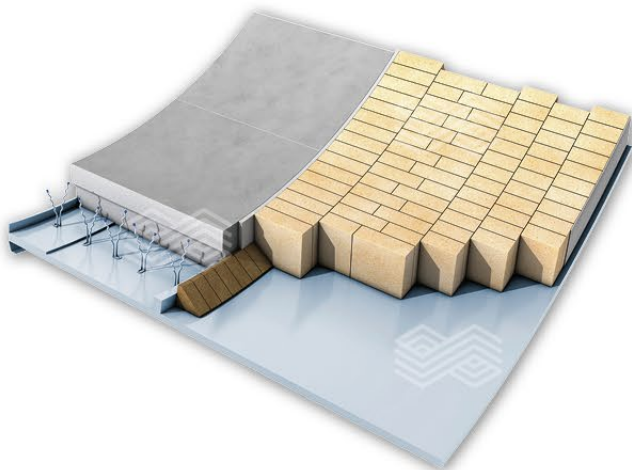
Customized test method at a temperature of 1700 °C with green pellets from customer using (a) DURITAL E90 (b) DURITAL AZ95 (c) RESISTAL RK10 and (d) RESISTAL KSP95-1.



Finally, the Thrust-Lock System brings the state-of-the-art design to avoid brick movements upon the outlet of the rotary kiln during operation as shown in Figure 10 [10]. Global technical assistance for custom made refractory solutions is also available for all clients.

Figure 10.

RHI Magnesita Thrust-Lock System [10].



Conclusion

Grate kiln iron ore induration process has a very complex condition in each region that generates important refractory needs.

RHI Magnesita has successfully implemented the use of Sol-bonded mixes with excellent results in the drying, preheating, rotary kiln and cooling stages.

R&D centers have the capability to recreate iron ore indurating conditions and run several standardized tests in order to obtain important information that technically enrich the selection of refractory brands for each application.

References

- [1] Mbele, P. Pelletizing of Sishen Concentrate. *The Journal of The Southern African Institute of Mining and Metallurgy*. March, 2012. pp. 221–228.
- [2] World Steel Association. *World Steel in Figures*. 2018. pp. 11.
- [3] Stjernberg, J., Isaksson, O. and Ion, J.C. The grate-kiln induration machine — history, advantages, and drawbacks, and outline for the future. *The Journal of The Southern African Institute of Mining and Metallurgy*. February 2015. pp. 137–144.
- [4] Yamaguchi, S., Fujii, T., Yamamoto, N. and Nomura, T. KOBELCO Pelletizing Process. *KOBELCO Technology Review*, No. 29, December 2010. pp. 58–68.
- [5] Metso Corporation. *Iron Ore Pelletizing. Grate-Kiln™ System*. USA. 2012.
- [6] Indian Bureau of Mines. *Iron & Steel Vision 2020*. Chapter 4, Agglomeration. pp. 84–97.
- [7] Nader, C., Athayde, M., Marschall, H.U., Hebenstreit, G. and Wilhelmi, B. Refractory Applications in Iron Ore Pelletizing Plants – Traveling Grate Furnaces. *RHI Bulletin*. No. 1. 2016. pp 20–27.
- [8] Blažs, M., von der Heyde, R., Fritsch, P. and Krischanitz, R. COMPAC SOL – The New Generation of Easy, Safe and Fast Heat-Up No Cement Castables. *RHI Bulletin*. No. 1. 2010. pp 13–17.
- [9] Wiry, A. and Marshall, H.U. RHI Thrust Lock System for Cement Rotary Kilns. *RHI Bulletin*. No. 2. 2013. pp. 17–19.
- [10] Patent applications and patents pending.

Authors

Erick J. Estrada O., RHI Magnesita, Sogamoso, Colombia.

Gerald Hebenstreit, RHI Magnesita, Vienna, Austria.

Christina Stimpfl, RHI Magnesita, Leoben, Austria.

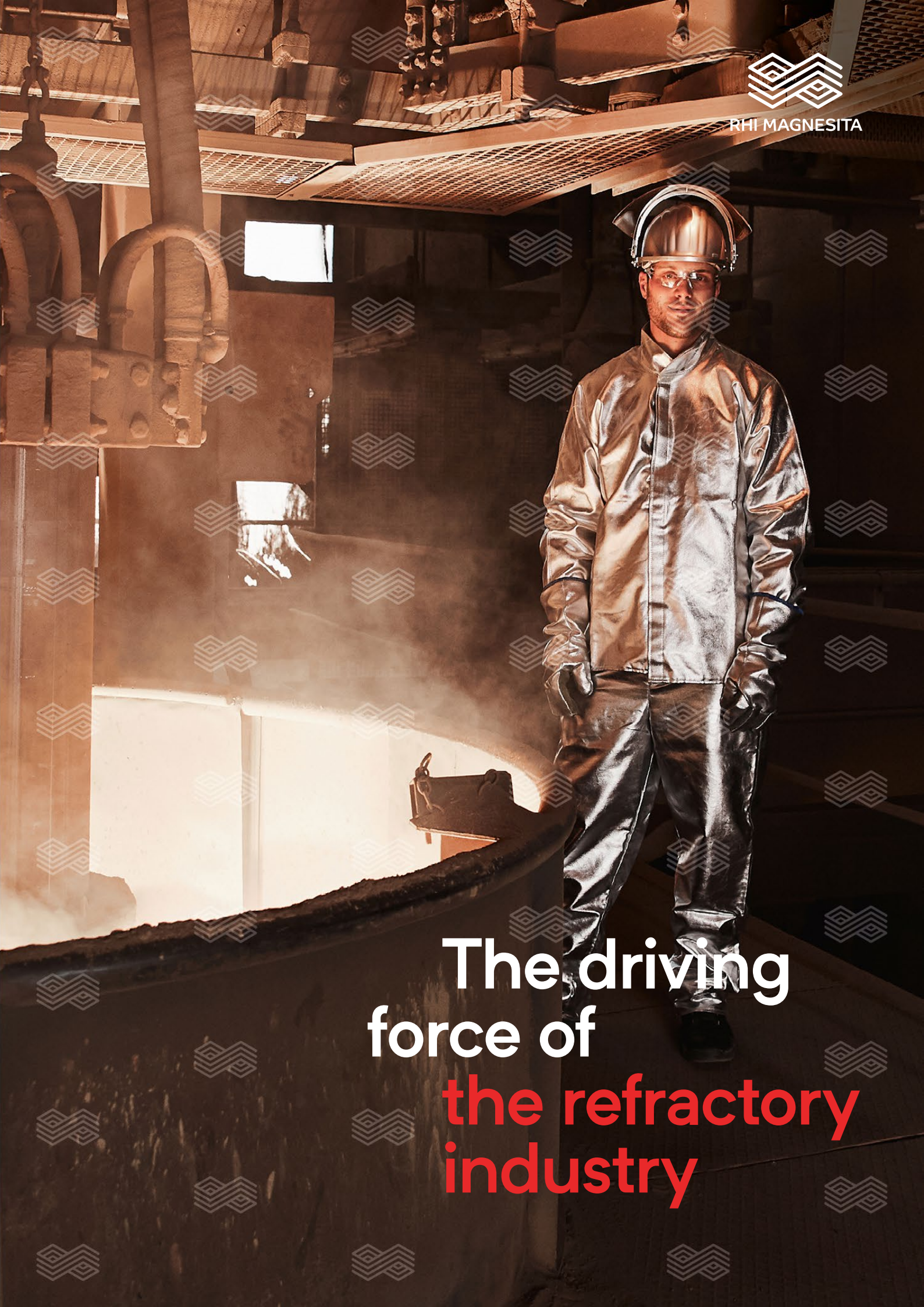
Cesar Nader, RHI Magnesita, Belo Horizonte, Brazil.

Corresponding author: Erick J. Estrada O., erick.ospino@rhimagnesita.com





RHI MAGNESITA



The driving
force of
**the refractory
industry**

Johannes Hartenstein and Roland Krischanitz

Benefits of Modern Doloma Magnesita Linings in Modern Cement Kilns

This paper addresses doloma technology which, if not deliberately followed may have faded out of prominence, especially for customers in cement industry. However, it is worth taking a closer look at this product segment since the technology has undergone a significant development, offering products able to cope with operation conditions of modern, alternative fuels fired cement rotary kilns. In light of, but not solely due to Chinese raw material crises, this alternative lining concept for the central burning zone becomes more interesting. However, doloma bricks are not only a solution for times of crises as shown by the North American market where doloma bricks are a common concept for burning zone linings offering technical benefits. Foremost doloma bricks stand out for the excellent ability to form a stable coating. A thicker and longer coated zone is formed reducing also energy losses.

Introduction

The worldwide refractory market has experienced strong and unforeseen changes within the last year since beginning of the Chinese magnesite crises. Now since more than one year the supply of dead burned magnesita (DBM) and fused magnesita has been impaired due to tightening and enforcing of environmental regulations in China, the world's biggest producer of magnesite based raw materials. Western suppliers were not able to completely compensate the severe reduction in supply, causing supply shortfalls and tremendous price increases. Despite being the most vertically integrated company in the market, even

RHI Magnesita has been challenged severely to fulfill customer demands, reflected in long delivery times throughout the year. Simply the availability of refractories has become the most important topic for the cement industry in the moment.

Even cost-efficient solutions for the central burning zone have become not only more expensive but also limited in availability, as the quantities do not countervail the shortages of raw material from China. Time to consider alternative solutions. But there is no need to look so far afield, an attractive alternative is close at hand – doloma bricks.

Development of Doloma Magnesita Refractories

Modern magnesita doloma bricks are a reasonable alternative. Not only for cases of magnesita supply shortfalls as is presently the case. With a market share of more than 40% in the burning zone of cement rotary kilns, the North American market shows that doloma bricks are a serious option. Some people might think that this is old fashioned technology but doloma bricks were also subject to significant development and improvement, so that state-of-the-art doloma bricks are able to withstand operation conditions of modern alternative fuel fired cement rotary kilns.

Reviewing the development of doloma bricks over the last decades, a significant progress has to be noticed. Doloma bricks of the 1st generation were made of pure doloma and high-grade magnesita, the ceramic matrix was also made from pure doloma and these bricks were fired at approximately 1500 °C. The lime part in these bricks supports an easy coating formation. They have a normal thermal shock resistance of about 30 cycles. They were in the 1970's and 1980's used as standard lining in European cement kilns in the burning zone and also in lower transition zones.

Figure 1.

Showing (a) schematic structure of a 1st generation standard doloma magnesita brick, (b) schematic structure of a 2nd generation doloma magnesita brick with zirconia addition and (c) the structure of a 3rd generation doloma magnesita brick with the corrosion resistant ceramic magnesita matrix.



(a)

(b)

(c)

The doloma magnesia brick of the 2nd generation are also manufactured from pure doloma and high-grade magnesia grains. The addition of zirconia grains improved the thermal shock resistance. They were successfully used in burning and transition zones in the 1980's and the early 1990's worldwide.

In 1990's a recession within Europe meant that the cement kilns were no longer fully loaded and nor were they operated with a full year campaign. As a result, the doloma bricks were subject to conditions which were far from ideal and had to be adapted to these new conditions, that included frequent thermal cycling and the significantly increased use of alternative fuels. To cope with these challenges the doloma magnesia bricks of the 3rd generation were developed. The pure doloma and high-grade magnesia grains remained unchanged, however the matrix which was subject to corrosion by the gases from the kiln atmosphere was improved. A special dense magnesia matrix formulation was achieved, resulting in low porosity and low permeability in order to improve the resistance to corrosive kiln atmospheres. The zirconia addition was optimised in order

to achieve a maximum thermal shock resistance, resulting in bricks which equal that of magnesia spinel bricks. The most recent product development based on 3rd generation is the addition of fused magnesia in the coarse grain which provides the bricks a further improved corrosion resistance.

Until now many successful linings have been installed. This new brick generation regained the desired campaign target life in Europe of 12 months—unless 100% alternate fuels are used through the main burner. Figure 1 shows the schematic structure of the different generations of doloma bricks, while Figure 2 shows the properties and raw materials of the 3rd generation doloma magnesia bricks. Table I shows the various properties of the different bricks.

Table I.
Characteristic properties of different doloma and doloma magnesia bricks.

Brick Grade		SINDOFORM K-DE K-FR	SINDOFORM Z40-EU	SINDOFORM Z5-EU	SINDOFORM Z60-EU	SINDOFORM Z60F-EU
Description of fired brick	Main raw material	Doloma	Doloma	Doloma	Doloma	Doloma
	Additives		Magnesia Zirconia	Magnesia Zirconia	Magnesia Zirconia	Fused magnesia Zirconia
Chemical composition						
MgO	% Mass	40.0	42.9	45.7	59.0	59.0
CaO		58.0	53.9	51.4	38.1	37.0
SiO ₂		0.8	0.8	0.7	0.7	0.8
Fe ₂ O ₃		0.6	0.6	0.5	0.5	0.6
Al ₂ O ₃		0.5	0.4	0.3	0.3	0.3
ZrO ₂			1.1	1.1	1.1	1.8
Physical Properties as received						
Bulk density	(g/cm ³)	2.85	2.90	2.91	2.92	2.92
Apparent porosity	(vol.%)	15.0	14.0	14.0	15.0	14.0
Permeability	(µm ²)	1.5	0.3	0.3	0.3	0.5
Cold crushing strength	(MPa)	70	30	40	50	45
Refractoriness under load T ₀₅	(°C)	1400	1420	1500	1570	1600
Thermal shock resistance		30	>100	>100	>100	>100
Thermal expansion (1000 °C)	(%)	1.3	1.3	1.3	1.3	1.3
Thermal conductivity (1000 °C)	(Wm ⁻¹ K ⁻¹)	2.6	2.4	3.0	3.0	3.0

Unique Advantages of Doloma Magnesia Refractories

Doloma magnesia bricks have a lot of unique advantages, one of them is the redox stability, which is important when the burner of the kiln has an incomplete combustion and an atmosphere with a high CO level present. Doloma magnesia bricks are very stable against such reducing conditions up to 1800 °C, which is based in the standard properties of their oxides (Figure 3).

The second advantage of modern doloma magnesia bricks is their good thermal shock resistance (TSR) which was improved within the last years to such a degree that it is nowadays comparable with those of magnesia spinel bricks. In beginning the TSR of ceramic bonded doloma bricks was poor. Trials with increased open porosity were not very successful because they were heavily infiltrated by condensing alkali salts which reduced the TSR further.

In the mid 1980's granular zirconia was introduced to doloma bricks and they became remarkably better in the TSR and also have a good infiltration resistance.

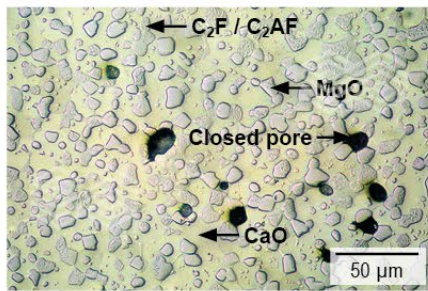
The 3rd generation showed again a considerable improvement, the TSR properties now match those of magnesia spinel refractories as shown in Figure 4.

The Coatability of Basic Refractories

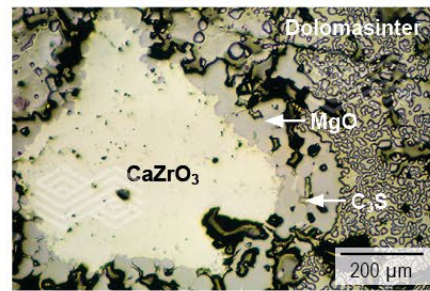
The biggest advantage of doloma magnesia refractories is their ability to promote coating, which is far better than that of any magnesia spinel brick, in the broadest sense, available on the market. A coating forms very easily on doloma magnesia bricks driven by the chemical affinity between clinker and doloma and the presence of lime (CaO). This lime reacts with di-calcium-silicate—C₂S of the clinker forming tri-calcium-silicate—C₃S as interface. We call this mechanism reaction coating bond. The adhered clinker coating forms an ideal insulation on the hot face of the refractory lining. The doloma magnesia refractories are protected thereby against high temperatures. There is no infiltration of liquid phases into the brick. The magnesia share in the brick grades controls the coating adherence with respect to the thickness of the coating. This reaction is stable up 2100 °C, which is decomposition point of the C₃S.

Figure 2.

Raw materials of a 3rd generation doloma magnesia brick and the properties.



Microstructure of doloma sinter CaO+MgO= 97.5% with minimal secondary phases



Microstructure of calcium zirconate CaO+ZrO₂= 98.5% with minimal secondary phases (C₃S)

MgO	CaO	SiO ₂	ZrO ₂	Fe ₂ O ₃	C/M ratio. molar	BD	AP	CCS	HMoR 1300 °C
[% mass]	[% mass]	[% mass]	[% mass]	[% mass]		[g/cm ³]	[vol.%]	[MPa]	
40.0	56.0	0.80	1.45	0.75	1.0	2.90	14.5	40	9.5

Figure 3.

Thermo dynamical stability of lime (CaO), magnesia (MgO), and zirconia (ZrO₂).

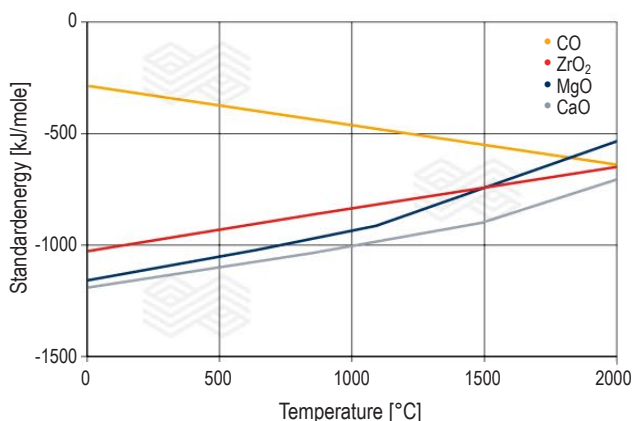
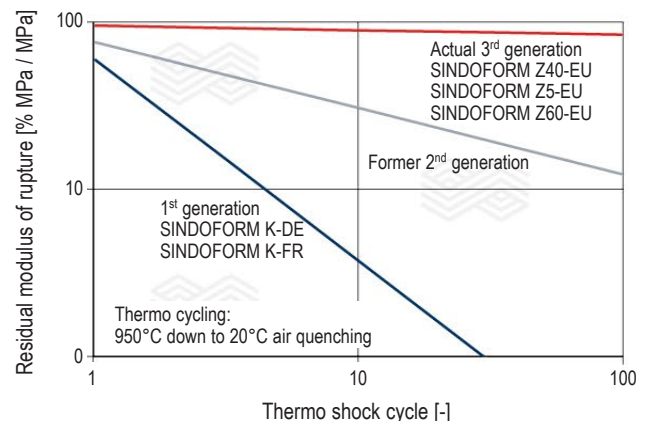


Figure 4.

Thermal shock resistance of the different generations doloma magnesia bricks.



The coating mechanism on magnesia spinel, magnesia hercynite, and also magnesia pleonaste refractories is quite different (Figure 5). Here the coating adherence is controlled only by the presence of liquid phases – $C_2(A,F)$ and the infiltration depth into the hot face of the brick. The percentage of adhered coating is controlled by the amount of impurities within the magnesia such as iron and manganese oxide and the share of spinel. Due to the far lower melting point of the liquid phases at 1450 °C the stability of the coating adherence is lower compared to doloma bricks as shown in Figure 6. Practical examples of the coating built-up in two kilns can be seen in Figure 7.

The best descriptions and tests for the coatability of refractory bricks have been made in the former “Holderbank Refractory Testing Laboratory”. In special furnace bricks were held for 3 hours at 1450 °C together with clinker, the mechanical loads on a coating in the kiln were simulated manually. The test procedure was completely standardised. The clinker used has had an unchanged composition for over 40 years. For this reason, the results of all tests are comparable.

Figure 5.

Showing (a) dense clinker coating on a pure doloma brick and (b) reactive coating bond on doloma magnesia bricks (schematic).

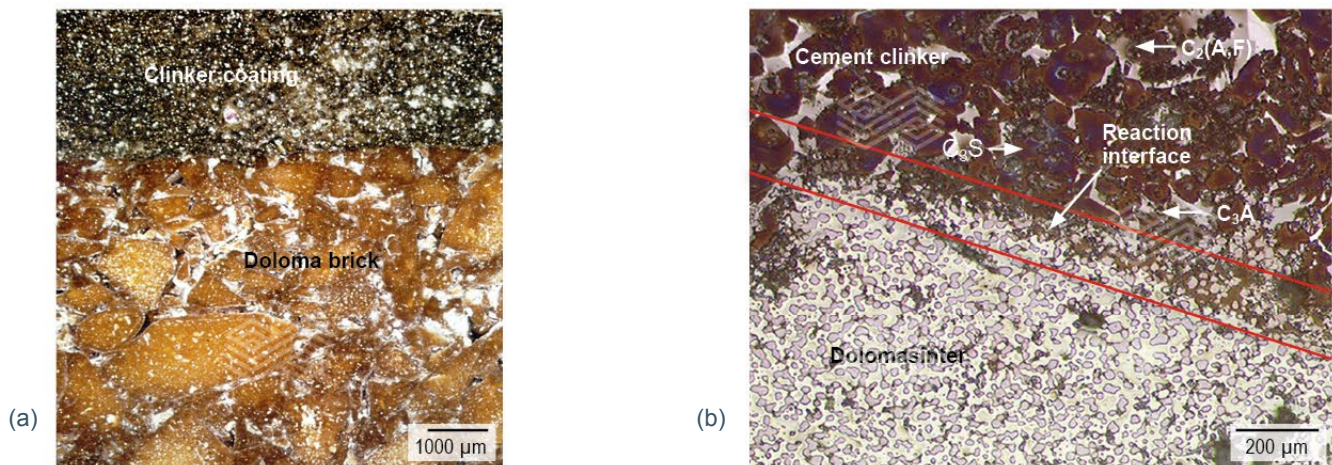


Figure 6.

Showing the schematic of (a) reactive coating bond on doloma magnesia bricks and (b) adhesive coating bond on magnesia spinel (hercynite) bricks.

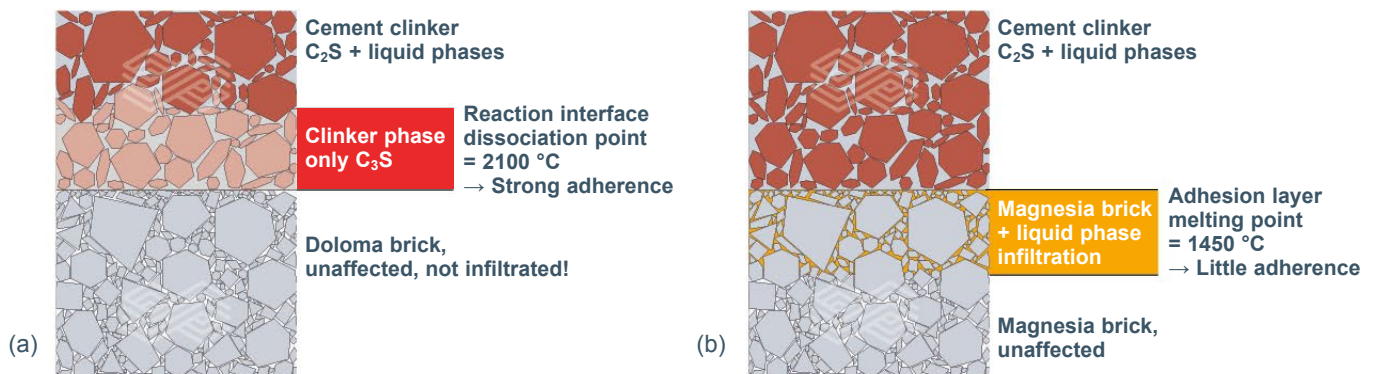


Figure 7.

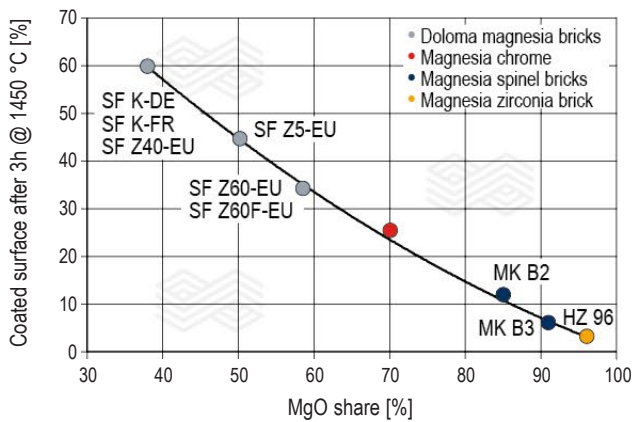
Showing (a) thick coating on doloma magnesia bricks – 5.0 m diameter precalciner kiln, 3500 tpd capacity and thin coating on magnesia spinel bricks – 5.0 m diameter precalciner kiln, 5000 tpd capacity.



In Figure 8 the results of the tests of doloma magnesia, magnesia spinel, and magnesia chrome refractories are compiled.

It can be clearly shown that the magnesia content of the refractories has an important influence on their coated surface. Pure doloma bricks create the largest coated surface of 60%. Doloma magnesia bricks show less coated surface but still keep more than 35% coated surface. Pure magnesia refractories reject the coating completely; only 3% surface is coated. With increasing spinel addition into magnesia bricks create up to 12% coated surface. Magnesia chrome refractories create a coated surface around 20 to 25%.

Figure 8.
Summary of Holderbank coating tests showing cement clinker adhesion on different refractory grades.



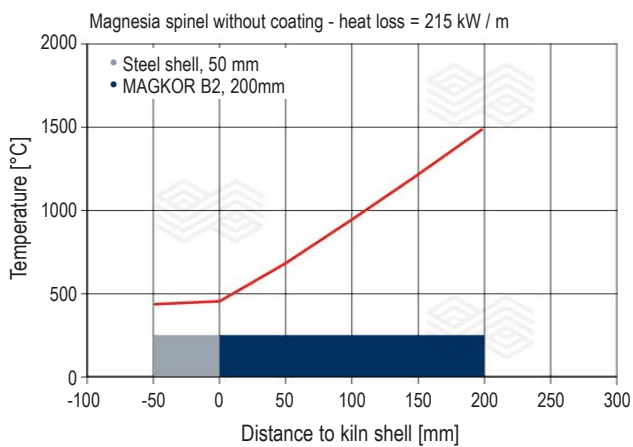
Doloma Magnesia bricks SF = SINDOFORM (K-DE, K-FR, Z40-EU, Z5-EU, Z60-EU, Z60F-EU)
Magnesia Spinel bricks MK = MAGKOR (B2; B3)
Magnesia Zirconia brick HZ96 = BASIMAG S1

Benefits of the Coating Adherence on Doloma Magnesia Refractories

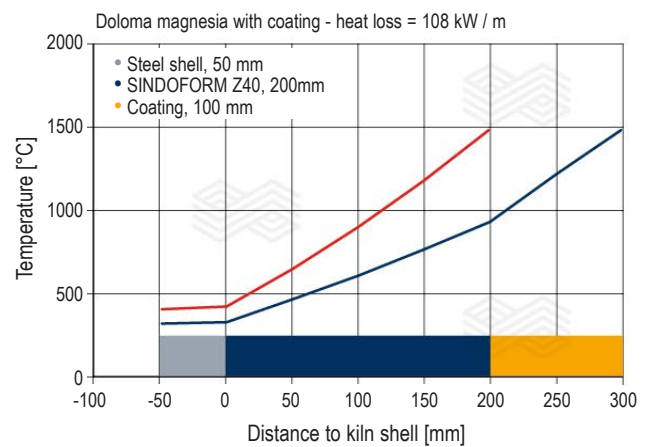
When it is possible to get a thicker coating on a refractory lining the thermal situation improves greatly. The thermal conductivity of clinker is quite low. According to composition, values from 0.8 up to 1.2 W m⁻¹ K⁻¹ can be measured with only little dependence on temperature. It should be noted that main constituents alite—C₃S and belite—C₂S are very stable because their decomposition points lie over 2100 °C. The next important fact is that the insulating layer is on the hot side, thus the refractories are protected against overheating, which can be clearly seen in Figure 9. The thermal calculations of interface temperature of the refractories show the drop from 1450 °C down to 935 °C. The heat loss can drop from 215 kW/m down to 108 kW/m with around 100 mm coating thickness (Figure 9).

Based on these facts a simulation with an “example kiln” was carried out in which a part of the magnesia lining of the 4.8 m precalciner kiln in burning and upper transition was replaced by a doloma magnesia lining of the same thickness and assuming a clinker coating of approximately 100 mm. It can be seen that the accumulated heat loss is reduced from 7.73 MW to 6.00 MW, which is 18.6% less or 2.4% less of the initial burner power. It is worth thinking about this difference. Over a 345 day campaign it accumulates to a saving of about 1200 tonnes of high grade coal or 1600 tonnes of a low grade coal (Figure 10).

Figure 9.
Showing (a) heat transfer through a magnesia spinel lining without coating in a 4.8m diameter kiln and (b) heat transfer through a doloma magnesia lining with coating in a 4.8m diameter kiln.



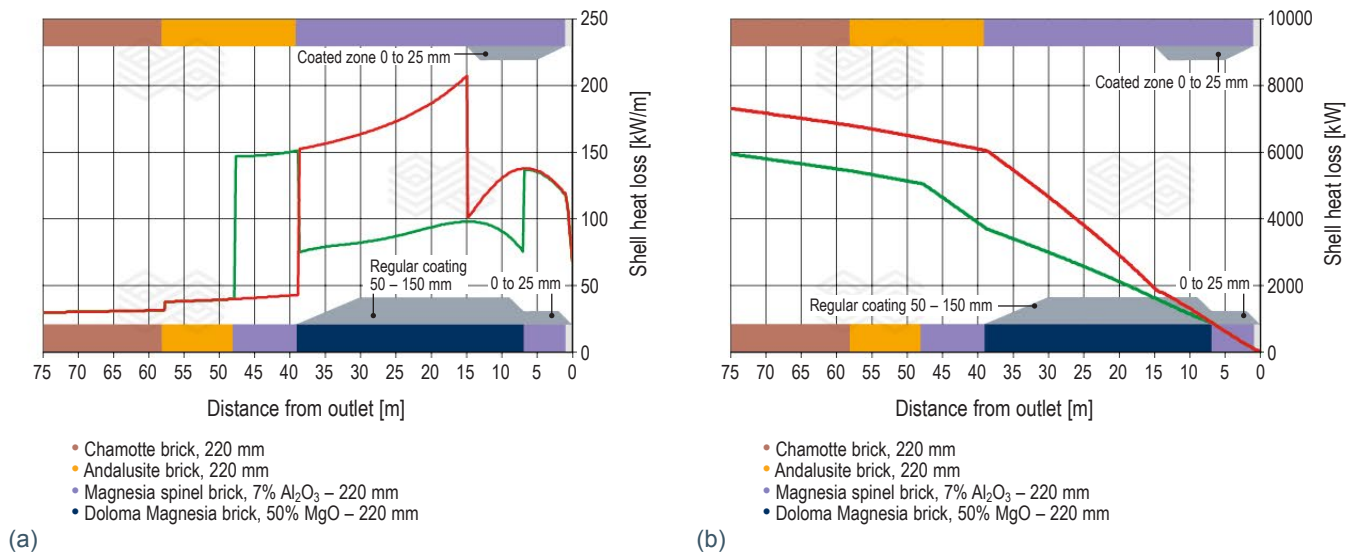
(a)



(b)

Figure 10.

Showing (a) heat loss profile in a precalciner kiln, improved (green) vs. typical (red) lining design; (4.8 m diameter; 75 m length; 5000 tpd capacity) and (b) accumulated heat loss in a precalciner kiln. Improved (green) vs. typical (red), lining design; (4.8 m diameter; 75 m length; 5000 tpd capacity).



Conclusions

State-of-the-art doloma products are a serious alternative for burning zone linings of cement rotary kilns. The latest generation of products offers properties able to withstand the critical conditions of modern alternative fuel fires kilns. Doloma bricks are not just a compromise in times of low availability of standard solutions, but offer reliable and safe performance and can also offer attractive benefits. The example based on the actual lining of a precalciner kiln and the thermal simulation of the impact of a different lining design show that the use of modern doloma bricks gives the cement manufacturer a possibility to save fuel costs when coating over a long part of the kiln can be created.

References

- [1] Miller, T., Griffin, D., Ishii, S. and Kunose, H. Development and use of Dolomite-Zirconia in Cement Rotary Kiln. Proceedings 2nd International Conference on Refractories, Tokyo, Japan, 1987, pp.609–622.
- [2] Yamaguchi, A. Dolomite Refractory and Atmosphere in the Burning Zone of Cement Kilns. *Journal of Technical Assn. of Refractories Vol. 9*, No. 4, 1989, pp 3–11.
- [3] Bongers, U., Hartenstein, J., Prange, R. and Stradtman, J. Use of Zircon dioxide to improve the Thermal Shock Resistance of Fired Basic Bricks for the Cement Rotary Kiln. Process Technology of Cement Manufacturing / VDZ-Congress '93, Wiesbaden, Germany 1994, pp. 389–393.
- [4] Bongers, U., Hartenstein, J., Prange, R. and Stradtman, J. Experience with a New Generation of Chrome free Magnesia Enriched Dolomite Bricks in Cement Kilns. Proceedings UNITCR' 97, New Orleans, Louisiana, USA, Vol.3, pp.1605–1611.
- [5] Thermal conductivities of Portland cement clinker. VDZ materials database. Düsseldorf, Germany.

Authors

Johannes Hartenstein, RHI Magnesita, Leoben, Austria
 Roland Krischanitz, RHI Magnesita, Vienna, Austria

Corresponding author: Johannes Hartenstein, johannes.hartenstein@rhimagnesita.com



Christoph Sagadin, Stefan Luidold, Christoph Wagner and Alfred Spanring

Evaluation of High Temperature Refractory Corrosion by Liquid Ferronickel Slags

The industrial manufacturing of ferronickel in electric furnaces produces large amounts of slag with a strong acidic character and high melting points, which places significant stresses on the furnace refractory lining in the slag areas. In this study corrosion mechanisms have been investigated between magnesia (MgO) refractory substrates and synthetic FeNi slags. The materials taken into consideration comprised a simple synthetically mixed slag with specific oxides of slags from a ferroalloy producer. The MgO refractory substrates with the slag specimens on it were heated in a hot stage microscope (HSM) to two different characteristic temperatures, 1350 °C and 1650 °C. The experiments proceeded under a controlled gas atmosphere that simulates the relevant process conditions. The corrosion mechanisms of each system were determined by SEM analyses. The obtained results showed that slag corrosion is dominating with a pronounced partial dissolution of refractory. It was also observed that iron oxide present in the slag diffused into the coarse refractory grains forming the relative low melting magnesia wuestite. Finally, the comparison of these findings with those predicted by thermodynamic calculation indicated the corrosion mechanisms and draw implications for improving the refractory performance.

Introduction

Ferronickel represents an irreplaceable alloying additive for stainless steels and plays an important role for other materials such as nickel-based and other steel alloys to improve cold formability and heat resistance [1]. The pyrometallurgical manufacturing of ferronickel in high temperature electric furnaces stresses the refractory linings by molten metal and/or slag. Chemical attack at high temperatures is the main factor for refractory corrosion. Reduced production efficiency and furnace shutdowns are the results of inferior refractory lifetime [1–4]. Therefore, the aim is to select adequate furnace linings for the individual processes to provide homogeneous abrasion and predictable refractory life for scheduled maintenance and high furnace availability. Taking these facts into account and in order to improve ferroalloy processes along the production route continuous optimisation of refractory materials, which represents a decisive factor for furnace performance, is inevitable. For the identification of corrosion mechanisms different laboratory scale experiments are used. Therefore, the slag was melted in a HSM under a defined CO/CO₂ gas mixture to mimic actual process conditions. Further, the examinations include investigations via scanning electron microscopy (SEM) for phase determination and thermodynamic calculation by using the software FactSage 7.1 [5]. The characterisation of the corrosion of refractories

by combining hot stage microscopy and SEM including energy dispersive x-ray spectroscopy (EDS) with thermodynamic calculations provides an important basis for the further development of the ferronickel process and therefore applied refractory [4–8].

Materials and Methods

Hot Stage Microscopy and Secondary Electron Microscope Analysis

Usually, a HSM is applied for investigations of the sintering and deformation temperature as well as the melting behaviour of different materials like slags, dusts, and ashes. In the current research, the HSM (EMI-201; Hesse Instruments Germany) served as melting and reaction device. The experiment was carried out by using the following procedure. A synthetic slag sample cylinder with 3 mm diameter and 3 mm in height was prepared, placed on a plate of MgO refractory substrate (14x14x2 mm) and horizontally inserted in the tube furnace. The heating rate of the furnace was fixed at 10 K/min to a temperature of 1350 °C or 1650 °C, which remained constant for 60 minutes. The higher value was defined by the maximum obtainable temperature of the HSM and the lower by the solidus temperature of the slag due to the assumption that the presence of any liquid phase will significantly enhance the chemical attack. To reflect process near conditions a mixture (Linde HiQ) of 60% CO and 40% CO₂ (corresponds to $p(\text{O}_2) = 1.94 \cdot 10^{-7}$ bar at 1650 °C) served as atmosphere. After this treatment the samples were cut in cross sections, embedded in a two-component resin and ground in several steps with different SiC foils (800, 1200, 2400 and 4000), to produce a metallographic specimen for the following analyses by scanning electron microscope. The microstructure of the slag/refractory interface was analysed by a SEM (JEOL JSM IT-300 LV) equipped with an EDS analyser.

Materials

Refractory Substrate

A high quality magnesium oxide plate (14x14x2 mm³) served as refractory. Its chemical analysis is shown in Table I.

Synthetically Produced Slag

The pure oxide mixtures for a synthetic slag similar to real ones (i.e., composed of 48% SiO₂, 28.8% Fe₂O₃, 19.2% MgO and 4% Al₂O₃) were homogenised in a swing mill and melted in a graphite crucible, whereas NiO was neglected due to its very low content. Afterwards the slag was solidified

Table I.

Chemical composition of the refractory magnesia substrate and the synthetically produced slag.

Chemical analysis	MgO [wt.%]	CaO [wt.%]	SiO ₂ [wt.%]	Fe ₂ O ₃ [wt.%]	Al ₂ O ₃ [wt.%]	BD [g/cm ³]	AP [wt.%]	CTE [10 ⁻⁶ /K]
Synthetical slag	19.2	-	48.0	28.8	4.0	-	-	-
Refractory substrate	>99.3	<0.35	<0.35	<0.12	<0.25	2.30	35.0	13.0

Chemical analysis - total Fe calculated as Fe₂O₃; non accredited laboratory procedure

BD bulk density; AP apparent porosity; CTE coefficient of thermal expansion

and grinded in the swing mill to achieve a homogenized powder. The composition of the synthetic slag is illustrated in the quaternary MgO-Fe₂O₃-SiO₂-Al₂O₃ system at 1650 °C in equilibrium with the CO/CO₂ gas mixture by Figure 1 which was compiled with FactSage. The chemical analysis of the slag is shown in Table I.

Corrosion Test and SEM/EDS Analysis

The corrosion test for the slag/refractory interface by combining HSM and SEM/EDS analyses are a main part of this research. The mineralogical investigation of the prepared samples was carried out by SEM/EDS in conjunction with thermodynamic calculations. This allows the determination of chemical reactions and diffusion sequences at the slag/refractory interface as well as an identification of new phases, resulting from slag and refractory interactions. The EDS mapping provided a good qualitative detection of the main elements close to the interface.

Slag/Refractory Interface at 1350 °C (SiO₂-MgO-FeO_x-Al₂O₃ System)

The thickness of the infiltration depth amounts to approximately 100–150 μm, which is about 100 μm less than at 1650 °C. The temperature was too low for a complete

melting of the slag. The interface between slag and refractory after the test at 1350 °C is shown in Figure 2. The associated spot analyses are shown in Table II and the distribution of the element close to the reaction zone is depicted in Figure 3.

An analysis of a series of spots (Figure 2) distributed over the infiltration area were additionally performed to identify the elements taking part in the reaction and diffusion events between synthetic slag and refractory at 1350 °C. The corresponding data of the spot investigation are summarised in Table II.

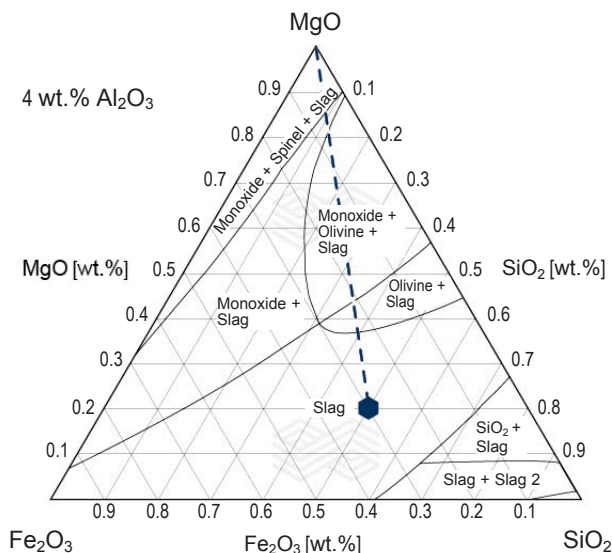
Table II.

Chemical analysis from spots of Figure 2.

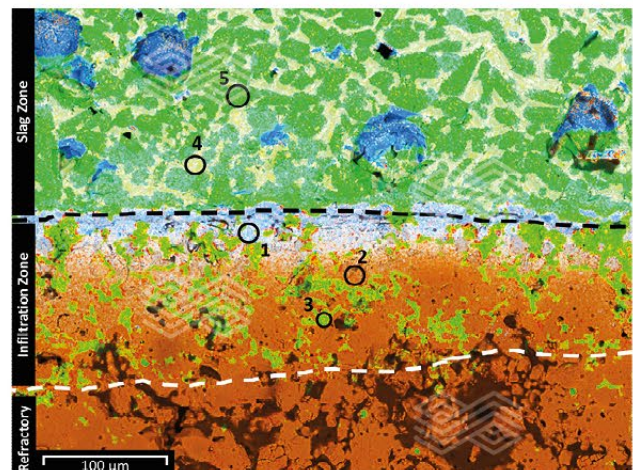
Element	EDX spot				
	1	2	3	4	5
Mg (mol.%)	82.6	88.8	62.6	12.3	32.1
Si (mol.%)	0.3	7.5	31.3	42.7	53.4
Fe (mol.%)	16.3	2.9	3.3	22.5	11.9
Al (mol.%)	0.8	0.8	1.8	9.0	2.6
(Mg, Fe)/Si ratio	329.6	12.6	1.9	0.81	0.82
Mg/Fe	5.1	30.6	18.9	0.55	2.69

Figure 1.

Quaternary MgO-Fe₂O₃-SiO₂-Al₂O₃ system at 1650 °C and a constant Al₂O₃ content of 4 wt.%, calculated for reducing atmosphere of 60% CO and 40% CO₂ the marker represents the slag composition and the line the varying mixtures of slag and refractory (MgO).

**Figure 2.**

SEM/EDS investigation from the cross section area of the infiltration and reaction zone between slag and refractory for 1350 °C including spot analyses of characteristic phases of this zone.



Slag/Refractory Interface at 1650 °C (SiO₂–MgO–FeO_x–Al₂O₃ System)

The influenced zone in this refractory is approximately 200 to 250 µm deep. However, depending on the open porosity of substrate the infiltration depth can vary. Figure 4 illustrates the interface between slag and refractory, which shows the infiltration of the slag into the refractory. The EDS spot analyses are shown in Table III and the slag/refractory interface mapping comprising the distribution of each element is illustrated in Figure 5.

Thermodynamic Calculations

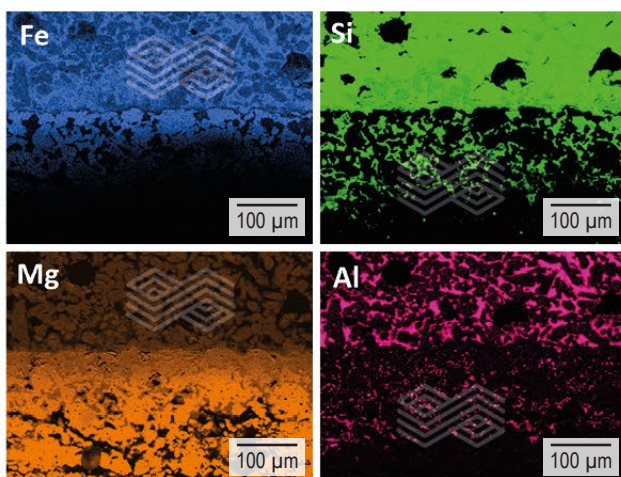
Thermodynamic calculations were carried out with the software FactSage 7.1 to understand the sequence of interaction between synthetic FeNi slag and magnesia refractory. The calculations were performed by using the same reducing atmosphere as for the HSM investigation test. Figure 6 shows the slag refractory phase diagram with varying portions of synthetic ferronickel slag (SiO₂–MgO–Fe₂O₃–Al₂O₃ system) and the pure refractory (MgO). The pure slag exhibits a liquidus temperature of approximately 1410 °C, which increases with rising refractory content in the slag. At approximately 17.5% refractory the first solid phase olivine becomes stable for a constant temperature of 1650 °C. When the refractory content reaches about 29%, the next phase monoxide appears. This stability area containing slag, olivine and monoxide extends to 83% refractory where the solidus temperature is reached.

Results and Discussion

The results of the melting trials regarding the slag/refractory interface show good agreement with thermodynamic calculations. The matrix consists of slag and refractory, where the slag fills up the pores of the refractory. Large MgO particles of the substrate within the infiltrated layer are not dissolved. The slag first infiltrates along any available pores in the refractory and then reacts with MgO. One newly formed phase is olivine, which emerges in the pores of the MgO substrate.

Figure 3.

SEM/EDS mapping, distribution of the elements at the slag/refractory interface from Figure 2.



Spot 1 (1350 °C) and 8, 9 (1650 °C) represent different MgO grains which comprise increased contents of Fe. Silicon and aluminium exhibit low concentrations, therefore these spot analyses represent Mg wustite ((Mg, Fe)O). A high iron oxide content in the slag causes an increase of Fe oxide in the MgO grains which reaches a Mg/Fe ratio of 6.4 in spot 8. This Mg

Table III.

Chemical analysis from spots of Figure 4.

Element	EDS spot							
	6	7	8	9	10	11	12	
Mg (mol.%)	62.6	65.1	85.3	90.1	95.3	29.1	41.7	
Si (mol.%)	32.3	31.0	-	-	-	0.7	-	
Fe (mol.%)	5.1	3.9	13.4	8.6	3.7	7.4	57.5	
Al (mol.%)	-	-	1.3	1.3	1.0	62.8	0.8	
(Mg, Fe)/Si ratio	2.1	2.1	-	-	-	52.1	-	
Mg/Fe	12.3	21.8	6.4	10.4	25.7	3.9	0.7	

Figure 4.

SEM/EDS investigation from the cross-section area of the infiltration and reaction zone between slag and refractory for 1650 °C including spot analyses of characteristic phases of this zone.

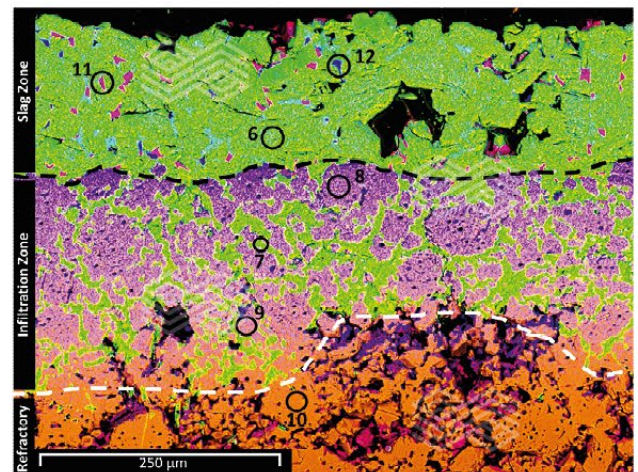
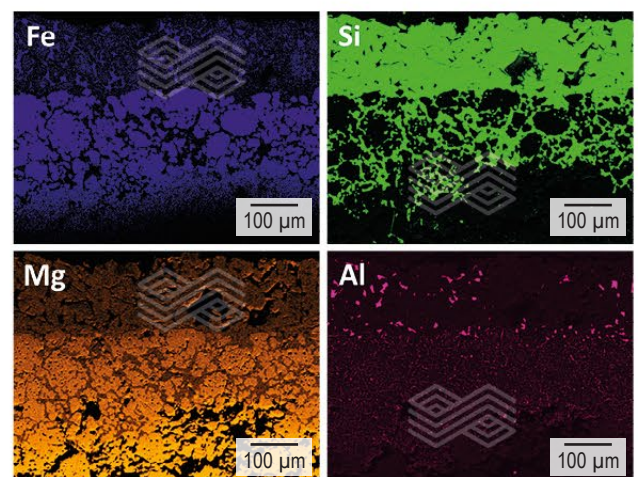


Figure 5.

SEM/EDS mapping, distribution of the elements at the slag/refractory interface from Figure 4.



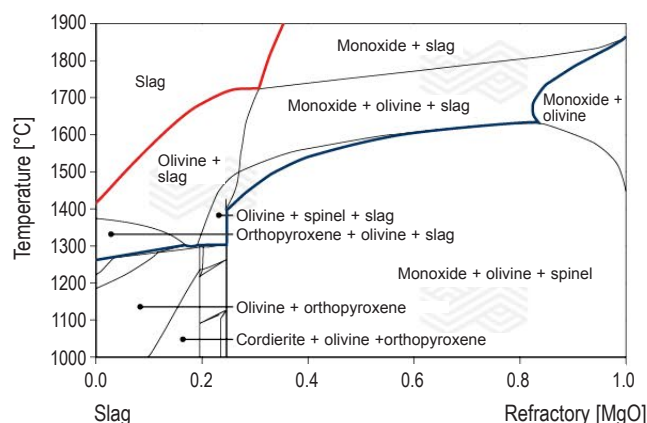
wustite phase corresponds to the phase monoxide (Figure 6) of the thermodynamic FactSage database FToxid. Deeper in the refractory the Fe content in the MgO grains decreases as indicated by spots 10 and 2. The mappings of synthetic slag visualizes different element concentrations: areas mainly composed of Mg (yellow), Si (green), Fe (blue) and Al (pink). At 1650 °C the effect of Mg wustite formation can be seen in Figure 5 because of the enrichment of blue Fe in MgO grains. Figure 3 and Figure 5 identify high Si concentrations in the slag and between large MgO grains. The spot analyses of 6 and 7 exhibit (Mg, Fe)/Si ratios of approximately 2 that coincides with the stoichiometry of olivine. Also spot 3 shows olivine phases in a deeper refractory zone at 1350 °C. The theoretical calculation also confirms the formation of olivine. In Spot 11 increased contents of Al could be localized. The

Al/Mg ratio of approximately 2 indicate MA spinel (MgAl_2O_4), which also emerges in the FactSage calculation at MgO enriched slags. In addition, Fe and Mg rich zones (Spot 12) appeared in the slag which can be interpreted as Mg wustite.

The mapping at 1350 °C shows the occurrence of similar phases as at 1650 °C. The Fe content in the slag is high and the Mg wustite starts to form from MgO, which can be seen in spot 4. With decreasing Fe content and rising Mg as well as Si contents spot 5 indicate that an olivine phase was formed.

Figure 6.

Phase diagram of the stable phases predicted by thermodynamic calculation as a function of refractory/slag ratio and temperature in a 60% CO and 40% CO₂ atmosphere.



References

- [1] Gasik, M. (Ed) *Handbook of Ferroalloys*. Butterworth-Heinemann: Oxford, 2013.
- [2] Gregurek, G., Ressler, A., Reiter, V., Franzkowiak, A., Spanring, A. and Prietl, T. Refractory Wear Mechanisms in the Nonferrous Metal Industry: Testing and Modeling Results. *JOM*. 2013; Vol. 65, Issue 11. 1622–1630.
- [3] Harders, F. and Kienow, S. *Feuerfestkunde: Herstellung, Eigenschaften und Verwendung feuerfester Baustoffe*. Springer: Heidelberg/Berlin, 1960, pp. 150–159.
- [4] Wagner, C., Wenzl, C., Gregurek, D., Kreuzer, D., Luidold, S. and Schnideritsch, H. Thermodynamic and Experimental Investigations of High-Temperature Refractory Corrosion by Molten Slags. *Metall. Mater. Trans. B*. 2017; Vol 48, Issue 1, 119–13.
- [5] C.W. Bale, E. Belicle, P. Chartrand, S.A. Deckerov, G. Eriksoon, K. Hack, I.-H. Jung, Y.-B. Kang, J. Melancon, A.D. Pelton, C. Robelin, and S. Petersen, FactSage thermochemical software and databases — recent developments. *CALPHAD Comput. Coupling Ph. Diagr. Thermochem.* 2009; Vol 33, Issue 2, 295–311.
- [6] Sagadin, C., Luidold, S., Wenzl, C. and Wagner, C. Evaluation of High Temperature Refractory Corrosion by Liquid Al_2O_3 - Fe_2O_3 - MgO - SiO_2 . Presented at TMS 2017. 8th International Symposium on High-Temperature Metallurgical Processing, San Diego, USA, Feb, 26– Mar, 2, 2017; 161–168.
- [7] Hu, D., Liu, P.X. and Chu, S.J. Study on Slag Resistance of Refractories in Submerged Arc Furnaces Melting Ferronickel. Presented at INFACON XIV 2015. Fourteenth International Ferroalloys Congress, Kiev, Ukraine, May 31-June 4, 2015; 115–121.
- [8] Luidold, S., Wenzl, C., Wagner, C. and Sagadin, C. High Temperature Corrosion Mechanisms of Refractories and Ferro-Alloy Slags. Presented at MOLTEN16. Proceedings of 10th International Conference on Molten Slags, Fluxes and Salts, Seattle, USA, May 22-25, 2016; 53–61.

This is a post-peer-review, pre-copyedit version of an article published in 8th International Symposium on High-Temperature Metallurgical Processing. The final version is available online at https://doi.org/10.1007/978-3-319-51340-9_16.

Authors

Christoph Sagadin, CD – Laboratory for Extractive Metallurgy of Technological Metals, Montanuniversität, Leoben, Austria.

Stefan Luidold, CD – Laboratory for Extractive Metallurgy of Technological Metals, Montanuniversität, Leoben, Austria.

Christoph Wagner, RHI Magnesita, Vienna, Austria.

Alfred Spanring, RHI Magnesita, Vienna, Austria.

Corresponding author: Christoph Wagner, christoph.wagner@rhimagnesita.com

Conclusion

To achieve an understanding how the corrosion mechanisms at the slag/refractory interface act in ferronickel manufacturing, an analysis of the microstructure is unavoidable and constitutes the main topic of this work. The thermodynamic calculations were carried out for the main oxides (MgO , SiO_2 , Al_2O_3 and FeO_x) dependent on the temperature. The practical corrosion tests investigate the penetration of the molten slag and interaction with the refractory substrate under formation of new stable phases. The combination of theoretical and experimental investigation methods, namely hot-stage microscopy inclusive SEM/EDX analysis and thermodynamic FactSage calculations, provides excellent results. The thermodynamic calculations are a suitable tool for predicting the sequence of phase transformations in equilibrium and are, therefore, useful for supporting experimental investigations.

Acknowledgment

The financial support by the Austrian Federal Ministry of Digital, Business and Enterprise and the National Foundation for Research, Technology and Development is gratefully acknowledged.



Andreas Viertauer, Gregor Lammer and Patrik Bloemer

Refractory Condition Monitoring and Lifetime Prognosis

Condition monitoring is very well known for mechanical components in the industry and mainly used for predictive maintenance. The paper describes the use of a laser scanner to determine the residual lining thickness and the use of infrared cameras (IR) to monitor the shell temperature of metallurgical vessels. Both methods are linked for further analysis. Examples will be presented in the paper. The 1st example is an electric arc furnace (EAF) application with discontinuous data from laser measurement data to predict the wear lining focusing to optimize the gunning maintenance and life time prognosis. The examples are descriptions for a Ruhrstahl-Heraeus (RH) degasser and ladle furnace (LF) applications. Data from IR which are continuously recording the shell temperature used on one hand as hot spot detection to avoid any unplanned vessel shut down. On the other hand, the IR data are linked with process data for condition monitoring as tool for preventive maintenance. In general, the data for both cases are essential inputs to generate algorithms as prognosis tool to reduce unplanned down time which leads to a higher availability at lower operational expenditure (OPEX) and gives indication for operation improvement. Finally, an outlook will be given how such an intelligent system can be used as self-learning instrument that will take the decision on how to proceed.

condition (e.g., vibration, temperature, pressure etc.), to identify a significant change which in turn is indicative of a developing fault. It is a major component of predictive maintenance. The use of condition monitoring allows for scheduling of maintenance or other actions to be taken to prevent failure and avoid its consequences. Condition monitoring is uniquely beneficial to detect conditions that would shorten standard lifetime and to address issues before they develop into major unexpected failures. Condition monitoring techniques are normally used on rotating equipment and other machinery (e.g., pumps, electric motors, internal combustion engines, and presses), while periodic inspection using nondestructive testing techniques and fit-for-service evaluation is used for stationary plant equipment such as steam boilers, piping, and heat exchangers. Currently, decisions of process adaptations are predominately made by humans based on experience. This is also valid for refractories [4]. In the future, the decision process will be increasingly assisted by self-optimizing and knowledgeable manufacturing systems. In this paper, we discuss methods of condition monitoring for different metallurgical vessels where we apply image processing and analysis algorithms to support the decision base for the current status and refractory maintenance scheduling.

Introduction

The numbers of measurement systems are growing in the metallurgical industry [1, 2]. Traditional measurements related to process tracking and follow-up, such as temperature measurement, steel and slag samples for chemical analysis, are still crucial and remain the back-bone in industrial production, to ensure a high process performance [3]. Based on the definition, condition monitoring is the process of monitoring a parameter or

Discussion

During the last decades, the increasing need for repeatable and stable operations in metallurgical production has put even higher requirements on equipment performance. Costly down-times and damages due to failures must be avoided. Consequently, refractory related measurement systems have been developed to monitor critical equipment and vessel functions which, in principle, can be divided into two different groups based on the frequency and condition of measurement. The status of the vessels under load and in

Table 1. Possible measuring methods for hot metal, primary, and secondary metallurgical process steps.

Measuring system	Shell temperature	Residual lining thickness	Hot metal		Primary metallurgy		Secondary metallurgy						
			Torpedo	HM Ladle	BOF	EAF	Ladle LF/LT	VD	RH	AOD			
			ON	OFF	ON	OFF	ON	OFF	ON	OFF	ON	OFF	
Thermocouple	●		●	●	●	●	●	●	●	●	●	●	●
Laser ¹		●	●	●	●	●	●	●	●	●	●	●	●
Infrared ²	●		●	●	●	●	●	●	●	●	●	●	●

¹ Laser couter measurement
² Infrared thermal imaging

ON – online – permanent monitoring
 OFF – offline – discontinuos – vessel is empty – no production
 ● state of art
 ● possible, not common
 ● not applicable for daily operations

steel making mode is called online. In contrast, offline means the steel making plant/vessel is empty, and measurement is performed during downtime (e.g., maintenance or idle time). Table I provides an overview on different measurement methods and their applications. At the end of the day, the purpose of different groups of measurement systems for metallurgical plant/vessels is similar, namely to generate an accurate database for decision making.

In the 1980's thermocouples were introduced and are still used today to monitor the vessel shell temperature. Later in the 1990's laser-based contour measurement systems, e.g., EAF bottom steel as an example for offline measurement systems, entered the market to determine the residual lining thickness. A major inherent disadvantage of this measurement method is that, for basic oxygen furnace (BOF) or EAF, the vessels are not in service for steel production during measurement (i.e., in the offline state) and recording of valuable data describing the vessel behaviour is therefore not possible.

Intermittent or Offline Measurements

Intermittent measurements are taken outside steel making operation time, e.g., laser contour scanning of the refractory profile for example during idle time. The outcome is a snapshot of the residual thickness and presents the current status of the wear lining. This should be remembered when discussing system purpose.

Continuous Measurement or Online Measurements

Continuous measurement means a permanent ongoing 24/7 monitoring. These systems allow for safety-oriented workflow. The most common example of which is the continuous temperature scanning of vessel shells for hot spot detection [5]. Infrared (IR) supervision of metallurgical vessels can be done both online and offline (during operation and also during idle times). Often, IR systems are used to detect hot spots, mainly on transport vessels like torpedo, hot metal or steel teeming ladles which is a useful tool for steel plant operation, as it provides easy and comprehensible information, especially regarding go/stop/inspect decision [6, 7, 8, 9].

IR detection systems are the typical decision base for the onsite operator of the specific vessel to take immediate action. When combined with process data, the measurement data is crucial as an additional input for condition monitoring. Processing this complete data set would provide valuable input to plant operators and managers. Especially when the output of such systems could be the current refractory status as a function of the shell temperature, which could include the lining lifetime forecast and finally reducing unplanned downtime.

In most cases, the online and offline systems are complementary, and most value is generated when combining them.

Recent trends aim at producing more intelligent evaluations of measured data and results, thus taking benefit of relevant process data, which will increase the value-in-use.

These additional input values in addition to the process data enables algorithms to find trends which will be described for EAF, RH degasser and ladle furnace (LF) in detail.

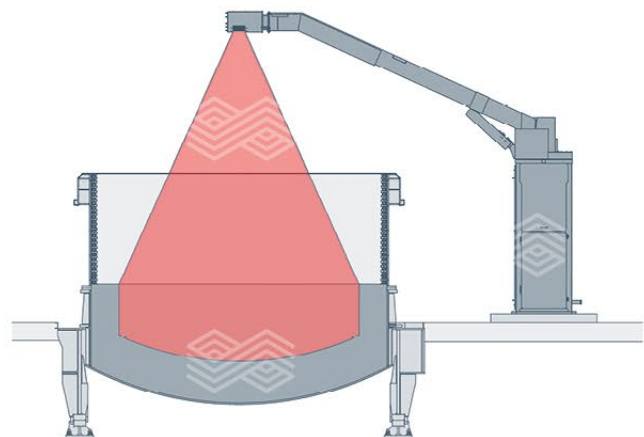
Example EAF Condition Monitoring and Lifetime Prognosis with Laser

As described in Table I, laser contour measurement systems to determine the residual lining thickness are already well established in the steel industry. Before being able to take laser measurements, the roof of the EAF must first be opened and the vessel bottom must be completely empty. This means the measurement can be only taken during idle time as the depicted in Figure 1. The manipulator arm with the mounted laser measurement head is moved into measuring position. The measurement itself takes less than 20 seconds [10, 11]. The result provides a snapshot of the current status of residual working lining thickness.

When combining laser measuring data with analyses of more than 140 process parameters such as power on time, data from electrode control system, slag chemistry, and refractory maintenance (e.g., amount and frequency of hot bank repair or gunning areas) just to name some parameters machine learning systems can generate a refractory model which is describing the refractory behaviour. All the residual lining thickness measurements during the campaign are used as a training target for such algorithms. The number of base points for the regression model depends on the measurement frequency, and thus a high number of laser measurements have a beneficial impact on the model accuracy. Usually one measurement per day is a sufficient input for model calculation.

Such machine learning systems, e.g., automated process optimization (APO) [12] can also provide refractory wear prediction to provide information on the future refractory wear behaviour. As an example, Figure 2 shows the residual lining thickness for a specific area both as historical data as well as prediction over lifetime as calculated by APO. The vertical blue line represents dates of actual laser measurements. In this example, the measured refractory wear (blue dotted line) is in the upper light blue area.

Figure 1.
Laser measurement of EAF using a manipulator.



The upper (light blue-gray) area of the window indicates that refractory wear is in accordance with planning if refractory maintenance is continued at the same level. The lower (darker) section indicates that more refractory maintenance is required to reach the lifetime target. The blue line indicates the future lining thickness as predicted by APO. Such tools deliver accurate information about remaining lifetime and give valuable input into operation scheduling.

Two Examples for hot Spot Detection, Condition Monitoring, and Lifetime Prognosis with IR System

As opposed to the offline measurement systems described above, online measurement systems provide a continuous data stream independent of the process steps such as idle, under load or maintenance. IR systems monitor the vessel shell thermal status with a sufficient resolution to detect developing hot spots and shows the operator the current state e.g., go/no-go/inspect.

Figure 3 shows an example of how to monitor the shell temperature distribution online for defined shell areas.

Figure 2.

Residual wear lining thickness over life time for a specific area [13, 14].

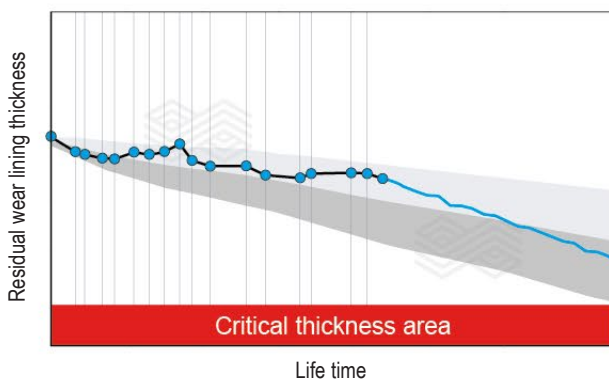


Figure 4.

Showing (a) ladle break out in the slag line, and (b) LF in operation, the ladle side wall temperature will be online monitored with IR system.



For the RH degasser in general, the most critical area besides the snorkel, is the conjunction between the bottom and wall up to the level of the alloying chute. The snorkels are immersed into the steel during the treatment and therefore not suited for online detection. Direct output of such a setup on the shop floor level is a monitoring and alarming system for immediate action.

Figure 4 (a) shows a break out in the slag line area of a steel teeming ladle. The shell temperature of a steel teeming ladle can reach up to a red spot or finally to a break out if heating without sufficient purging performance combined with extremely extended steel and slag contact time, high amount of carry over slag, and finally high refractory life time during LF operations occur. Figure 4 (b) describes the online ladle shell temperature measurement during LF treatment. The shell temperature and distribution online process data

Figure 3.

Deskulling, preheating of an RH vessel, the shell temperatures will be online monitored with IR system.

(e.g., steel and slag contact time, purging details like line and back pressure, flow rate, power-on time) are processed in an algorithm to monitor the operation conditions. This allows prevention of hot spots, to create maintenance plans for gunning and purging plug [15] and to predict the ladle lifetime.

The influence of the different steps of the metallurgical process on the temperature can clearly be distinguished in the data stream as shown in Figure 5. The temperature peaks (rising and dropping of mean temperature for a defined area) follow certain rules in a defined range corresponding to steel contact time. A temperature increase beyond a certain limit can indicate a unique event (e.g., deskulung with oxygen lance or extended preheating for a RH degasser).

Figure 5.
Temperature trend of a selected area in the side wall of a RH degasser.



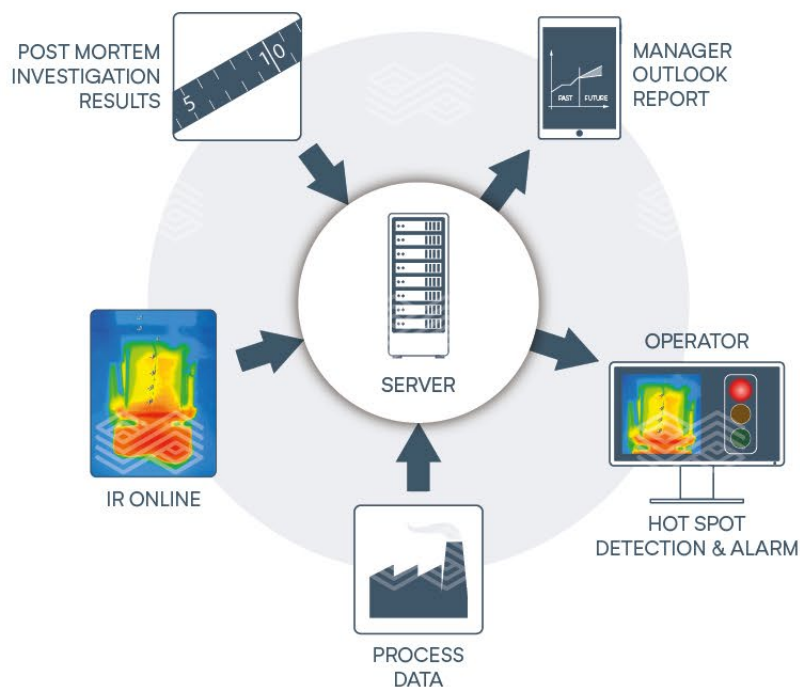
Correlating temperature profile with process data can be used as a refractory wear indication. In addition to process data, post mortem results should also be included in the data set for a holistic analysis approach described in Figure 6. One key task of successful modelling is to calculate main influencing parameters for in-depth impact analysis of process events on refractory performance. Given the high number of process parameters (more than 200), the modelling itself is a complex task. Modern machine learning methods can autonomously identify, select, and validate the input parameters according to their influence on the target value (i.e., refractory wear).

Figure 6 describes the vision of the interaction of closed control loops. All production key components, e.g., cyclic online process and IR data together with offline data (post mortem and laser measuring results) are condition monitored in real time. All module data, current plant set up, maintenance schedule, operating times, and statuses are then visualized on intuitive human machine interfaces (HMIs). The outlook report for the manager is based on the model and gives a prediction of the future plant availability.

Conclusions

Figure 7 finally describes the interaction of plant/machine as the source of online (cyclic) and offline data. Online cyclic data (Level 2) is related to the steel making process (e.g., treatment duration, oxygen consumption or shell temperature). Cyclic data is defined as recurring events with time stamps. Offline data (e.g., residual lining thickness measurements, post mortem refractory reports, and gunning consumption) is the second class of input. Combining both groups of data with the production plan and processing it using a self-learning algorithm gives two major output streams. The first stream provides an ad-hoc status

Figure 6.
Interaction of closed control loops.

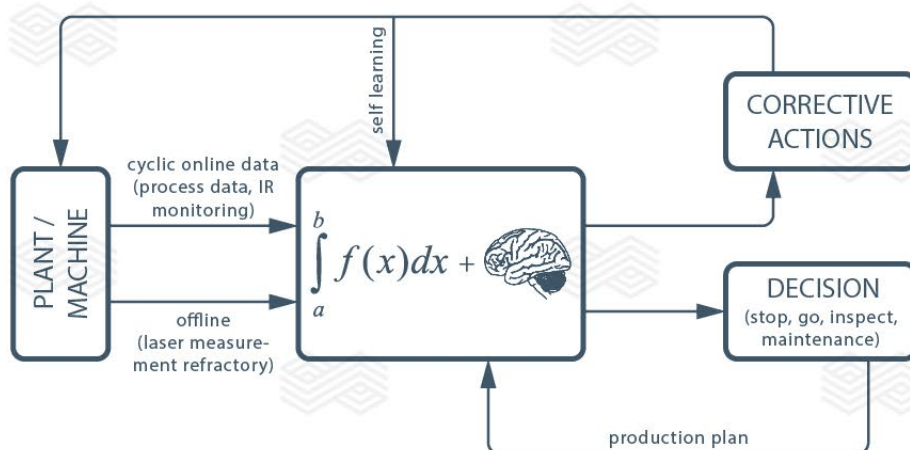


(go/no go/inspect), predicts remaining lining lifetime, schedules maintenance, and interacts seamlessly with production planning. The second stream indicates corrective actions to be taken to ensure best plant/machine performance in a self-optimizing loop if there is a difference between the behaviour of the digital twin (the digital representation of physical system) and the vessel itself as retraining of the model is triggered [16].

Following the trend of digital manufacturing, this cyber physical model contributes to the vision of decision making without human influence [17]. We continue to focus on this issue and optimize the processes for safe operation at longest possible lifetime in order to achieve best cost/performance level and high productivity with decreased downtimes of the vessels.

Figure 7.

Holistic interaction.



References

- [1] Herzog, K., Winter, G., Kurka, G., Ankermann, K., Binder, R., Ringhofer, M. and Maierhofer, A. The Digital Transformation of Steel Production, AISTech, 2017, Conference proceedings, pp. 504–513.
- [2] Ringhofer, M., Wimmer, G., Plaul, J.-F., Tatschl-Unterberger, E. and Herzog, K. Digitalization in the Metals Industry. *Stahl und Eisen*, 2017, Vol. 137, No. 5, pp. 45–51.
- [3] Hecht, M. Industry 4.0 – the Dillinger way. *Stahl und Eisen*, 2017, Vol. 137, No. 4, pp. 61–69.
- [4] Steiner, R., Lammer, G., Spiel, C. and Jandl, C. Refractories 4.0, *BHM*, 2017, Vol. 162, No. 11, pp. 514–520.
- [5] Görnerup, M. Thermal Imaging in Metals Production. Metsol, white paper, www.metsol.se.
- [6] VISIR- Torpedo Safe, Agellis, Data sheet, www.agellis.com.
- [7] VISIR- Ladle Safe, Agellis, Data sheet, www.agellis.com.
- [8] Sarfels, J and Wandelt, M. *Infrarotbildverarbeitung zur Gießpfannenüberwachung*. *Stahl und Eisen*, 2010, Vol. 130, No. 4, pp. 100–102.
- [9] Viertauer, A., Trummer, B., Dott, K.-H., Spiess, B., Hackl, G., Skala, K. and Pellegrino, M. Efficient Hot Metal Desulphurization Ladle. UNITECR, 2017, 15th Biennial Worldwide Congress, Conference Proceedings, pp. 345–347.
- [10] Lamm, R. and Kirchhoff, S. Optimization of ladle refractory lining gap crack detection lining surface temperature sand-filling of the ladle tap hole by means of a 3D-Laserprofile-measurement system that is immersed into a hot ladle to evaluate the entire condition. UNITECR, 2017, 15th Biennial Worldwide Congress, Conference Proceedings, pp. 604–607.
- [11] Laser Contouring System for Ladle Lining Thickness Monitoring. Process Metrix, Presentation, www.processmetrix.com.
- [12] Patent applications and patents pending.
- [13] Razza, P., Yaseen, A., Lammer, G., Rom, A and Hanna, A. Statistical Data Analysis for Process Improvements at Emirates Steel Abu Dhabi. AISTech 2015, Conference Proceedings, pp. 3994–4002.
- [14] Lammer, G., Lanzenberger, R., Rom, A., Hanna, A., Forrer, M., Feuerstein, M., Pernkopf, F. and Mutsam, N. Advanced data mining for process optimizations and use of A.I. to predict refractory wear and to analyze refractory behaviour. AISTech 2017, Conference proceedings, pp.1195–1207.
- [15] Viertauer, A., Trummer, B., Kneis, L., Spiess, B., Pellegrino, M., Ehrenguber, R. and Hackl, G. Holistic Approach for Gas Stirring Technology in a Steel Teeming Ladle. *RHI Magnesita Bulletin* No. 1, 2017, pp 31–36.
- [16] Kurka, G. and Hohenbichler, G. TPQC- Through- Process Quality Control. 9th Int. Steel Congress, May 2016, Beijing, China, Conference Proceedings.
- [17] The future of metals- the outlook for the metals industry in the decades to come. *Metals Magazine*, 2/2016. www.primetals.com, pp. 22–35.

Paper presented at 7th International Congress on Science and Technology of Steelmaking - The challenge of industry 4.0 - ICS 2018, Venice 13-15 June 2018, organized by AIM.

Authors

Andreas Viertauer, RHI Magnesita, Vienna, Austria

Gregor Lammer, RHI Magnesita, Vienna, Austria

Patrik Bloemer, Agellis AB, Lund, Sweden

Corresponding author: Andreas Viertauer, andreas.viertauer@rhimaginesita.com





RHI MAGNESITA



The
global leader
in refractories

Francisco Jose López Gonzalez, Paulo Souza, Mateus Garzon, Dickson de Souza and Robson Dettogne

Development and Application of a Slag Model for Increasing Ladle Life at Integrated Steel Mill — Brazil

The use of phase diagrams for simulating and understanding steelmaking slags is possible and feasible, enabling computer programming for creating a user-friendly spreadsheet interface to the shop-floor operator. This paper describes the real case creation of a tailor-made tool for a steelmaking plant in Brazil, which led to a meaningful and sustainable improvement of ladle refractory life.

Introduction

A slag modelling for heats, going through the ladle furnace (LF), was initiated in August 2011 at Plant A, using the mass balance developed by Eugene Pretorius (SlagBal V3-5). This task went through different stages: initial diagnosis, collection and processing of process data, room training for operators of secondary metallurgy process, design of a tailor-made model using Visual Basic programming and EXCEL macros, initial set-up of the tailored model, field validation of it and personalized training of the secondary metallurgy operators with real heats. The full use of the model started on March 2012. It was necessary to proceed with minor adjustments in order to better reflect what was happening in the reality. The net result of the model application was an increase of ladle life from 95 heats initially to 128 currently, without slag line replacement. It is important to mention that the SlagBal V3-5 is available and used sporadically by several steelmakers, but this is the first time that the model is used as a permanent tool for adjusting ladle slags on a heat-per-heat basis.

Description of the Facilities

Plant A is an integrated steel mill located in Brazil. It produces 4 million tons per year (mtpy) of steel. The different production routes after BOF tapping are shown in Figure 1.

The steel grades produced are silicon-killed (SK), aluminium killed (AK) and silicon aluminium killed (SAK), for a total of approximately 1085 different qualities, with the percentage distribution shown in Figure 2.

All grades are processed on the same type of ladle lining, which is basically an Al₂O₃-MgO-Carbon (AMC) brick for the bottom, MgO-Al₂O₃-Carbon (MAC) for the barrel and MgO-Carbon for the slag line, as shown in Figure 3.

Figure 2. Percentage distribution of different steel grades produced.

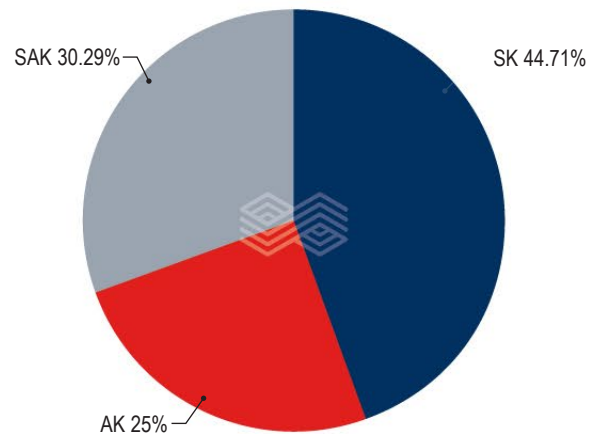
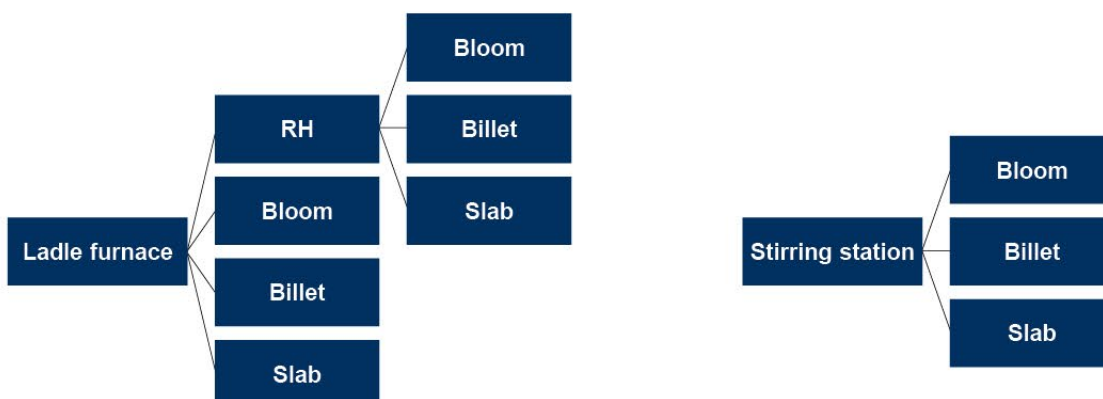


Figure 1. Flowchart of heats after BOF tapping.



Traditional Standard Operation Practices (SOP) at LF

The traditional standard operating practice (SOP) at LF consisted of making additions of fluxes according to fixed and generic guidelines for each type or family of steel. The consequences were mostly, crusty slags, poor sulphur capacity (Cs), due to a low amount of CaO dissolved in the liquid fraction of the slag [1], noisy LF operations, and a significant use of fluorspar for heats leaving the LF to the RH, in order to ensure a fluid slag [2]. The determination of the slag adjustments during the LF process was either done visually or based on predefined recipes that did not consider the specific slag, thus leading to errors, including the absence of coating formation on the ladle barrel and low performance of ladle refractories.

Figure 3.

Refractory configuration of ladle at Plant A.

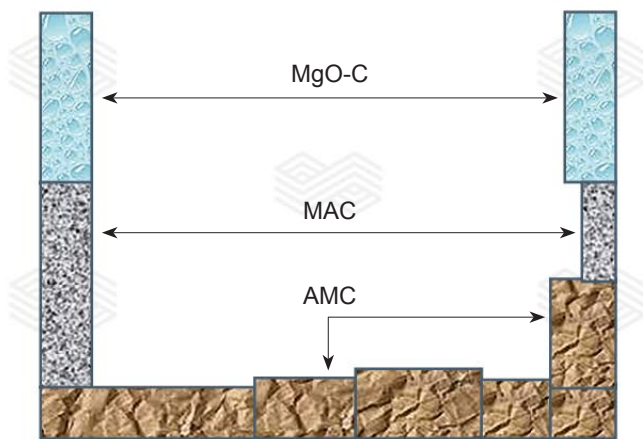


Figure 4.

Plan for improvement the LF-SOP at Plant A.

Sampling and analyses of slags and fluxes
Training of LF & RH operators about slag fundamentals
Definition of slag mass and important input for the model
Application of SlagBal V3-5 single heats
Construction of encrypted program for the operators
Training of operators using the program with real heats

Table I. Electrical parameters of LF 2.

TAP	Current curve	Power factor	Tension (V)		Power (MW)		Current (I) KA	Arc length mm
			Secondary	Arc	Active	Arc		
5	8	0.67	346	232	15.44	14.15	38.20	88.30
6	8	0.67	365	245	17.11	15.68	40.30	94.80
8	10	0.69	386	266	19.06	17.56	41.20	106.90
11	10	0.69	425	293	22.90	21.10	45.20	120.80
13	10	0.69	450	311	25.51	23.50	47.70	129.20

Plan for Improvement

The plan for improvement involved a multilateral reassessment of operations and is outlined in Figure 4.

Definition of the Slag Mass

The initial approach was to calculate the arc length on both LF, in order to define the slag mass required for the longest arc length. The worst case was LF 2, where 5 different tap positions were used, as shown on the Table I.

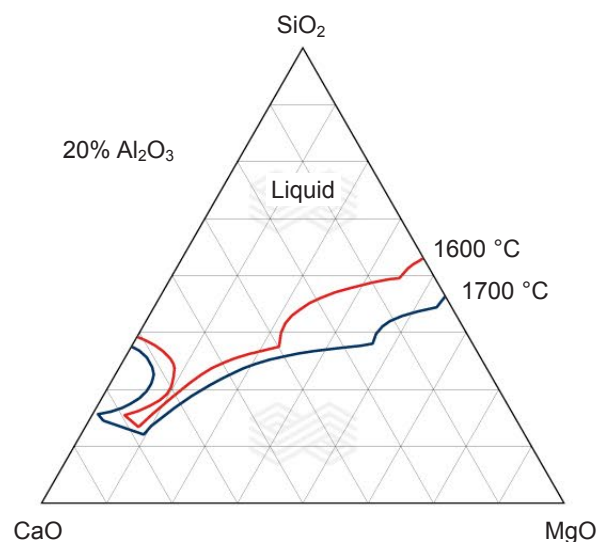
The last two TAP positions (11 and 13) were seldom used (only in emergency situations). Therefore, the maximum arc length was defined as 106.9 mm, which corresponds roughly to a mass of 3045 Kg, considering an internal diameter of the ladle of 3.78 m (for covering all possibilities, when the residual thickness was 40 mm). This slag mass became one of the targets of convergence for the model.

Theoretical Background

The whole development of the model looks for the optimum saturation point on the liquidus line of a quaternary diagram defined by the calculations done on the program SlagBal V3-5, aiming for a fluid slag at the temperature of the final LF process, as shown on Figure 5, for a CaO-MgO-SiO₂ (CMS) system at 20% Al₂O₃ [3].

Figure 5.

Quaternary CMSA diagram at 20% Al₂O₃.



Alloy Recovery

As the amount of steel qualities were so high (1085), it was necessary to create a simple spreadsheet to calculate the alloy recovery, because, depending on that, varying amounts of oxides were formed to the slag. The basic guidelines for this spreadsheet were that only the alloys which contain Si and Al were considered, because they form the most stable oxides under steelmaking conditions, according to the Ellingham Diagrams and only the alloys added during tapping were considered for slag formation, because that is when the oxygen potential is the highest and most of the oxides are formed [4]. Trimming additions at the LF were not considered, because the formation of oxides was minimal, having almost no impact in the slag formation, due to the high recovery of the alloys at this stage.

An example of the recovery calculation spreadsheet is shown on Table II.

Construction of the Model

The philosophy of the model was to be as follows, to be as user-friendly as possible, to offer an easy interface for the operator. It was to eliminate any calculation for the operator. The only task the operator should perform is to input a basic data for each heat arriving at the LF and then click on the CALCULATE key. The basic engines of the model are shown in the matrix, with the result on the centre (Figure 6).

Table II. Spreadsheet for calculation of alloy recovery.

Heat size	t	224	
Tapping additions (Kg)			
	Alloy	Pure-Si	Pure-Al
FeSi	295	221,25	
FeSiMn	4057	649,12	
Total pure-Si		870,37	
Al	21		21

LF initial analyses (%)	Dissolved		Recovery	Oxides formed (Kg)		
	Kg	%S	%S	ilicaA	lumina	Total
Si	0,150	336,00	38,60	1143,55	31,22	1174,77
Al	0,002	4,48	21,33			

The sequence operates as shown in Figure 7 and follows the input of the tapping alloy addition, initial percent of Si and Al at the LF, the temperature of the LF at the end of process, which defines the target liquidus temperature of the slag, tapping flux additions, and an estimation of slag mass after tapping.

The initial information is input to the SlagBal V3-5 model and the tapping alloy additions and initial percent of Si and Al are added to the alloy recovery calculation spreadsheet. The calculated alloy recovery of Si and Al feeds was also included in the corresponding fields of the SlagBal V3-5 model. The input of fluxes added during tapping plus the calculation of oxides formed on the alloy recovery spreadsheet are subtracted from the estimation of slag mass after tapping, in order to calculate the slag carryover from the BOF.

The calculated slag carryover from the BOF feeds also the corresponds to the field on the SlagBal V3-5 model. It should be mentioned that the chemistry of the BOF slag depends on the tapping carbon and is constantly updated in order to better reflect the period of operation. The impact of this variation on the MnO is important for the adjustment of the model, which affects significantly the slag corrections.

Figure 6. Basic engines for the calculation of flux additions at the LF.

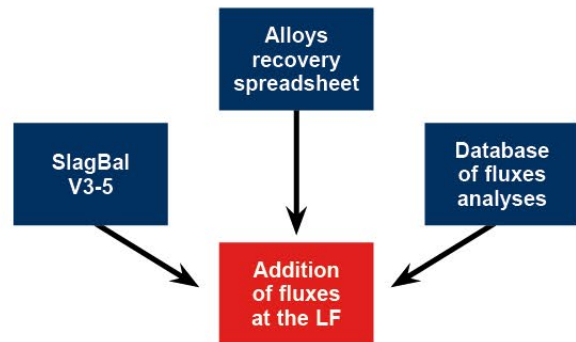


Figure 7. Flow of calculation of the model.



The operator’s interface has the following features (Figure 8):

- Yellow coded fields for inputs.
- A key to execute the calculations: CALCULATE.
- A key for erasing previous calculation: NEW HEAT, in order to clean all the fields and leave the spreadsheet ready for new calculations.

Results

The model was put into operation in March 2012. Since then, ladle life has been gradually increasing until obtaining the current level of 128 heats, as shown on Figure 9.

In addition, the use of fluorspar itself was eliminated on the LF process completely, especially the significant amounts for the heats which go through the LF-RH route.

Ongoing Developments

The model went through a streamlining process between 2016 and 2017 in the programming architecture. This included the creation of an abstraction layer in calculation routines, so that raw materials were selected from a dropdown list, which comes from pre-filled tables of raw material and its correlated chemistries. The creation of general use functions. The creation of global constants, to enable future customization for other customers and easier maintenance. Many of the links between the interface and SlagBal V3-5 were replaced by custom functions and built in codes, in order to centralise calculations. SlagBal V3-5 was customised to allow more fluxes and alloys to be added and

there was a new design of the input layout in the operator’s interface, which included assumptions and alloy recovery calculation sheets. Additional streamlining included, the definition of upper and lower bounds for slag weight after additions to the ladle, allowing the selection of an arbitrary number of alloys (up to 10) and fluxes (up to 5) and providing an expected final chemistry of the slag in the ladle to the operator. As well as many other streamlining functions. Further developments and customisations are continuously under consideration.

Figure 9. Evolution of ladle life at Plant A from 2012 (shown by month) then annually to 2017.

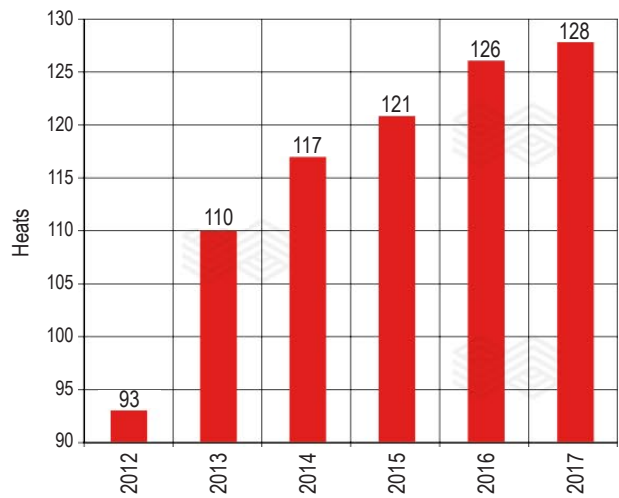


Figure 8. Showing the operator interface.



**SLAG MODEL
FLUX ADDITIONS CALCULATOR**

HEAT		DEGASSER?		SKIMMER (S/N)		SLAG WEIGHT AFTER SKIMMER	
Fe-ALLOY ADDITIONS (kg)		SLAG FORMING ADDITIONS		CHEM ANALYSIS L1 (points)		SLAG DEOXIDANTS (kg)	
FeSi		Cal		Si		CaC2	
FeSiMn		ESC 224		ALS		LMF DEOXIDANT	
Al		MgO	195	CHEM ANALYSIS END-BLOW		SiC	
		ESC DES BAG		C			
RELEASE TEMPERATURE		TAPPING SLAG WEIGHT (KG)		SYNTHETIC SLAG TYPE	ESCÓRIA 224		
		CALCULATE		NEW HEAT			
LADLE TREATMENT ADDITIONS							
Lime	MgO	ESC 224	ESC DES BAG	ESC DES SILO	CaC2	SiC	
0	0	0	0	0	0	0	
NEW SLAG HEIGHT (cm)						CARRYOVER SLAG BOF (KG)	0

Conclusion

It is possible to transfer the theory of thermodynamic models to the day-to-day routine of a shop floor in a steel mill, using the right approach, through the understanding of the customer operation and the help of the high-end computer technology, in order to obtain tangible, consistent and measurable, improvements in the performance of ladle refractories.

Acknowledgments

The authors would like to thank Eugene Pretorius, who was the precursor of this type of approach in South America in the mid-nineties.

Also, many thanks to the technical personnel of Plant A, whose commitment to this project made possible to obtain meaningful results.

The invaluable assistance of INDG for the development of the VBA macros should also be acknowledged.

References

- [1] Oltmann, H.G. Desulphurization by Slag Treatment; Baker Refractories, 2000.
- [2] Pretorius, E. The Effect of Fluorspar in Steelmaking Slags; Baker Refractories, 2000.
- [3] Pretorius, E. Utilizing Phase Diagrams to Demonstrate Slag Principles; Baker Refractories, 2001.
- [4] Pretorius, E. Introduction to Slag Fundamentals; Baker Refractories, 2001.

Originally presented at AISTECH 2016; 16–19 May; David L. Lawrence Convention Center, Pittsburgh, Pennsylvania, USA. Reprinted with permission from the Association for Iron and Steel Technology (AIST).

Authors

Francisco Jose López Gonzalez, RHI Magnesita, Contagem, Brazil.

Paulo Souza, RHI Magnesita, Contagem, Brazil.

Mateus Garzon, RHI Magnesita, Rotterdam, Netherlands.

Dickson de Souza, RHI Magnesita, Contagem, Brazil.

Robson Dettogne, RHI Magnesita, Contagem, Brazil

Corresponding author: Francisco Jose López Gonzalez, Francisco.Gonzalez@rhimagnesita.com





RHI MAGNESITA



**We take
leadership
seriously**

An Investigation on the Influence of Expansion Joints in the Mechanical Behaviour of Steel Ladles

The correct determination of strains and stresses in the refractory bricks of a metallurgical vessel's lining represents a complex problem. From a computational point of view, the proper consideration of the bricks/joints subsystem imposes considerable problems due to the large amount of interfaces between them. In this work, a complete steel ladle masonry with dry joints was modelled by a homogeneous equivalent material that considers the possibility of joint closure. The thermo-mechanical properties of this equivalent material were determined using a periodic homogenisation method. The model demonstrates the influence of joints, when present, and thickness of joints. This study helps in the design of refractory linings and provides a better estimation of the applicability of a given lining to the loads imposed in operational conditions.

Introduction

A suitable refractory lining design represents an important aspect in the assurance of an appropriate lifespan of metallurgical vessels in steelmaking, cement, petrochemical and other industries that require the manipulation of molten metal. In addition to the economic gains obtained with the reduction of production's breaks due to refractory wear or mechanical failure, safety and environmental issues are constant concerns of refractory producers and plant managers.

Choosing the best combination of bricks' shapes, materials and joint's thicknesses, considering the uniqueness of each process and each vessel, is a complex task that has been addressed for years, initially making use of simplified analytical calculations [1] and more recently applying the finite element method (FEM) for the numerical simulation of more complex geometries [2,3]. Although great improvement has been made, two main problems are still under constant investigation [4]:

- The consideration of the dry joints in the calculation of strains and stresses in equipment containing large assemblies of bricks, such as a steel ladle.
- The high non-linearity of the refractory materials' thermo-mechanical behaviour.

Both problems are, of course, connected. The more accurate estimation of the stress reduction due to the presence of initial dry joints is dependent on the material's constitutive law, i.e., the nonlinear thermo-mechanical law governing the stress increase due to a strain or force increment.

Regarding the first point highlighted above, the main difficulty is the high computational cost involved in the discretization of the bricks/joints subsystem, in addition to the considerable increase in the simulation's nonlinearity degree due to the use of several contact elements between the bricks.

In this paper, an innovative technique was used to substitute this complex subsystem, from a discretization point of view, by a simpler, energetically equivalent, homogenised lining, in a first moment considered to have linear elastic material's behaviour.

Periodic Linear Homogenisation Technique

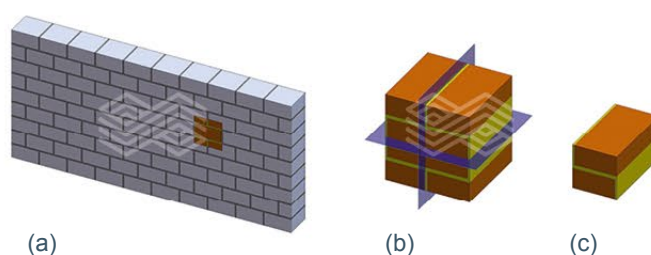
The basic idea of the linear homogenisation technique is to substitute the complex geometry of the bricks/joints subsystem with a homogenised, simpler geometry, with equivalent material properties, that can reproduce the same mechanical behaviour. This can be done due to the periodicity of the general refractory linings, i.e., the existence of a periodic cell that, if reproduced continuously through the domain, will result in the original geometry, as illustrated in Figure 1.

The determination of the equivalent mechanical properties is closely related to the masonry joints' states, shown in Figure 2. These states are:

- State 1: All joints are open. Although the bricks can be in contact, due to their surface roughness and shape defaults there is a dry joint, which is responsible for a decrease in the stresses observed in the refractory lining [5].
- State 2: Horizontal joints are closed; vertical joints are open.
- State 3: Vertical joints are closed; horizontal joints are open.
- State 4: All joints are closed.

Figure 1.

Periodic linear homogenisation scales. Showing (a) complete masonry, (b) periodic cell, and (c) domain of calculation.



It is clear that, although the refractory bricks are considered to be isotropic in this application, the behaviour of the masonry is, in general, orthotropic. For example, in State 2 the masonry assumes the same mechanical response as the bricks when a horizontal load is applied, because the joints are closed in this direction, and also in the thickness direction. Nevertheless, considering that the joints in the vertical direction are open, there is not initial stiffness in this direction, until the point when those joints also close, and the masonry enters in State 4.

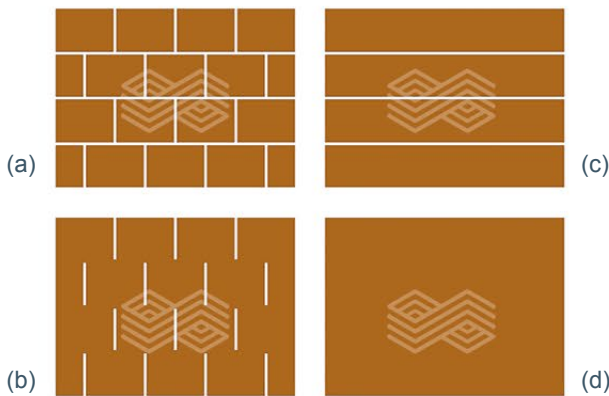
The relation between the equivalent and brick's materials' properties is straightforward for States 1, 2 and 4, and is summarized in Table I [6].

Table I. Elastic orthotropic parameters of the homogeneous equivalent material (E_b , ν_b and G_b are the brick's elastic isotropic properties).

	E_1	E_2	E_3	ν_{12}	ν_{13}	ν_{23}	G_{12}	G_{13}	G_{23}
State 1	0	0	E_b	0	0	0	0	G_b	G_b
State 2	E_b	0	E_b	0	ν_b	0	0	G_b	G_b
State 4	E_b	E_b	E_b	ν_b	ν_b	ν_b	G_b	G_b	G_b

Figure 2.

Masonry joints' states. (a) State 1 – All joints are open. (b) State 2 – Horizontal joints are closed; vertical joints are open. (c) State 3 – Vertical joints are closed; horizontal joints are open. (d) State 4 – All joints are closed.



For State 3 this relation is not so obvious. To guarantee that the mechanical response of the homogenised masonry will be an accurate approximation of the original geometry, it is important to have a strain energy equivalence between both. This can only be obtained by calculating equivalent mechanical properties in a specific domain using a finite element model (Figure 1-c) [7].

Once the equivalent material's properties are defined, another important aspect of the periodic linear homogenisation technique is to define a joint's closure criterion, i.e., based on the primary variables obtained through a finite element simulation, the deformations, characterise criteria that monitor if the concerned assembly of bricks has changed state. Figure 3 shows the two main criteria used in the method, the transverse brick's deformation and the normal brick's deformation coupled with brick's sliding.

Simulation of a Steel Ladle

To illustrate how the periodic linear homogenisation technique works, a complete steel ladle was modelled. This ladle corresponds to a generic design, used here only for exposition of the technique. The ladle is composed of a working layer, a backfill and two safety layers. A ramming mix with approximated material properties was considered to fill the empty spaces. The refractories of the working layer in bottom and in the cylindrical wall were homogenised. The general dimensions of the steel ladle are presented in Figure 4.

Figure 3.

Joint's closure criteria. Showing (a) transverse deformation and (b) normal deformation and sliding.

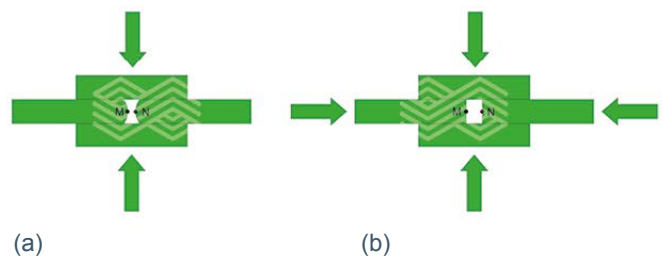
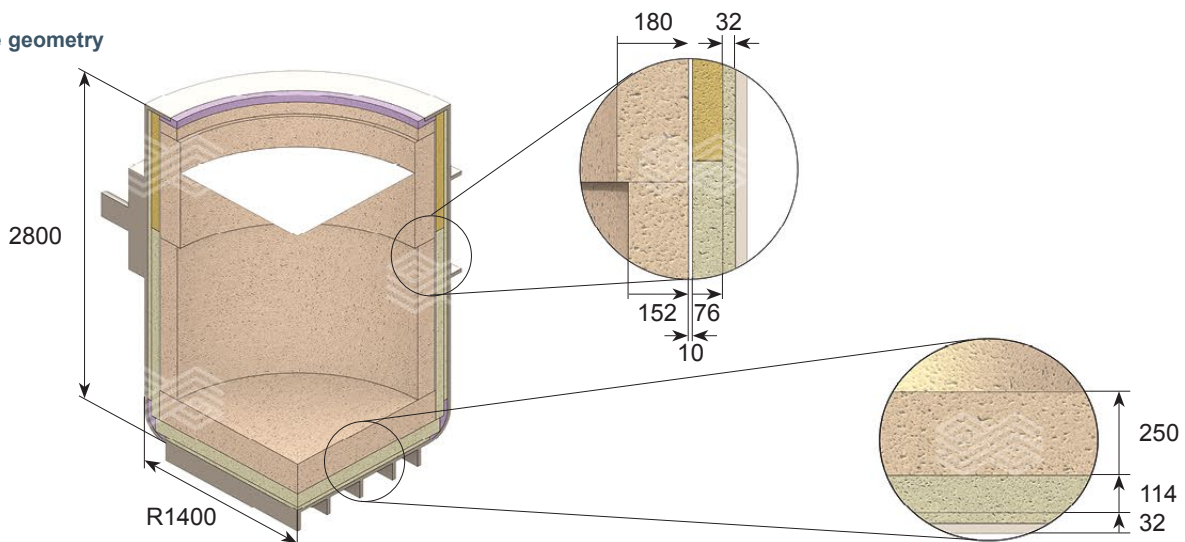


Figure 4.

Steel ladle geometry



The ladle was considered to be held by the trunnions, and the steady state thermal load shown in Figure 5 was imposed. The molten steel temperature was considered to be 1600 °C, and a temperature varying convection coefficient together with a radiation to ambient were used.

To evaluate the effect of the joints' thickness, four different situations were modelled, first considering isotropic linear elastic behaviour (no joints), and after considering the joints' thickness to be equal to 0.1 mm, 0.3 mm and 0.5 mm. It should be clear that the joint's thickness is not a design variable, meaning that it cannot be changed in practice, but is the result of a given refractory lining. Therefore, the consideration of different values in this study serves as a theoretical analysis.

Results

Figure 6 shows the progressive joints' closure due to the thermal loading. It is possible to observe that the joints effectively start to close in the refractory bottom after 25% of the applied thermal loading. This important expansion allowance effect is not taken into consideration when an isotropic material's properties are considered throughout the entire geometry, resulting in erroneous prediction of the strains and stresses. It is also possible to see that, even after 100% of loading, not all the joints are completely closed, because elements in State 2 can be observed in the region close to the junction between the bottom and the cylindrical wall, and elements with all joints open (State 1) can be observed near the slag line.

It is important to mention that the selection of bricks shapes and materials is always a compromise between the reduction of the stresses and strains in the refractory lining and the guarantee to have all joints closed when the molten steel comes in contact with the equipment. It is particularly important to have a design that, during thermal unloading due to the ladle cycle, does not become loose, ensuring the lining stability.

Figure 7 shows how the circumferential stresses are affected by the joints' size. Clearly, the region affected by compressive stresses above -40 MPa decreases as the joints' thickness increases. Although this was expected, it is important to have such a tool to quantify this effect and test different scenarios, depending also on the operational conditions.

Finally, the periodic linear homogenisation technique can also be used to predict more accurately the equivalent stresses in the steel shell, and the effect that a change in the refractory lining can have in the equipment's mechanical construction. Figure 8 shows that, an isotropic material's properties for the working lining results in a stress level above 500 MPa for the region close to the bottom. This value decreases substantially, reaching approximately 250 MPa if 0.5 mm joints are considered.

Figure 5.
Steady state thermal load

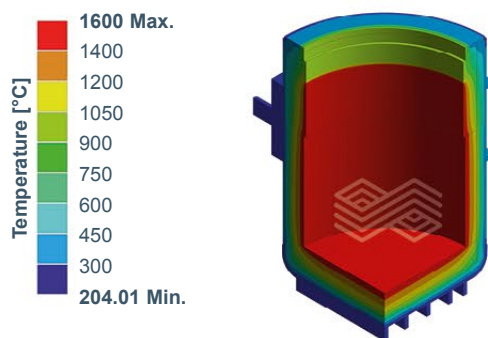


Figure 7.
Circumferential stresses in the refractory wall. Showing (a) 0.1 mm joints and (b) 0.5 mm joints.

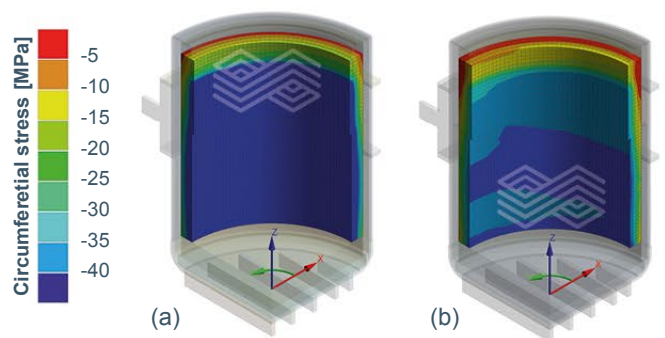


Figure 6.
Closure of joints during the thermal loading.

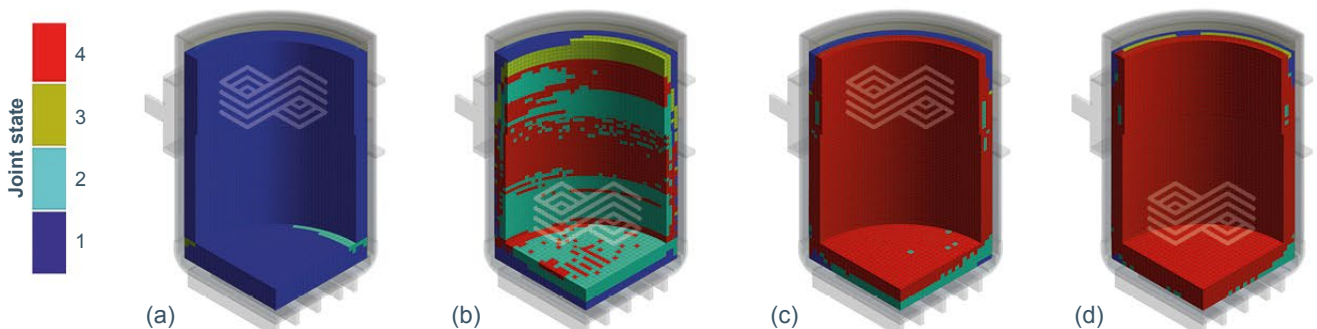
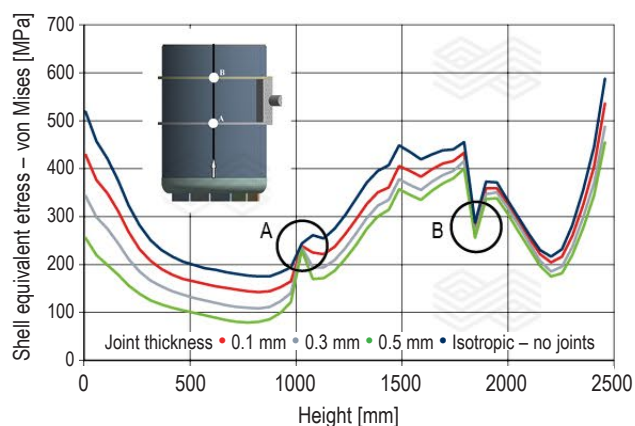


Figure 8.

Equivalent stresses in the steel shell, for different joint sizes.



Conclusions

The thermo-mechanical numerical simulation of complete metallurgical vessels, such as the steel ladle, represents a challenging task, but with valuable results, such as a more accurate prediction of strains and stresses in the refractory lining and the mechanical construction.

This paper shows how RHI Magnesita and the University of Orléans are developing new technologies to continuously improve the quality of the calculations. Further works aim to include in the framework of the periodic homogenisation the nonlinear behaviour of the refractory materials.

References

- [1] Schacht, C. Refractory Linings – Thermomechanical Design and Applications. Marcel Dekker. New York; 1995.
- [2] Poirier, J., Gasser, A. and Boisse, P. Thermo-Mechanical Modelling of Steel Ladle Refractory Structures. *Inter-ceram*, Vol 54, 2005, p. 182–189.
- [3] Russel, R., Hallum, G. and Chen E. Thermomechanical Studies of Obround Ladles During Preheating and Use. *Iron & Steelmaking*, 1993, p. 37–43.
- [4] Teixeira, L., Gasser, A. and Rekik, A. Thermo-Mechanical Study of a Steel Ladle Considering the Effect of Joints Using the Linear Homogenization Technique. 59th Aachen Refractories Colloquium. 2016.
- [5] Gasser, A., Terny-Rebeyrotte, K. and Boisse, P. Modelling of joint effects on refractory lining behaviour. Proceedings of the Institution of Mechanical Engineers, Part L: *Journal of Materials: Design and Applications*. 2015.
- [6] Gasser, A., Blond, E., Yahmi, N., Teixeira, L. and Sinnema, S. Thermo-mechanical modelling of a steel ladle using periodical homogenisation for the refractory masonries. Refractories Worldforum. 2017.
- [7] Nguyen, T. M. H., Blond, E., Gasser, A. and Prietl, T. Mechanical homogenisation of masonry wall without mortar. *European Journal of Mechanics A/Solids*. 2009.

“Reprinted with permission from the Latin American Refractory Producers Association (ALAFAR); UNITECR 2017, September 26-29, 2017”

Authors

Lucas Breder Teixeira, University of Orléans, Orléans, France.

Alain Gasser, University of Orléans, Orléans, France.

João Pedro Chaib, RHI Magnesita, Contagem, Brazil.

Rubens Alves Freire, RHI Magnesita, Contagem, Brazil

Corresponding author: João Pedro Chaib, Joao.Chaib@rhimagnesita.com



Paulo Vinícius Souza da Conceição, Carlos Antônio da Silva, João Victor Gomes Guimarães Ananias, Alexandre Dolabella Resende, Marcelo Borges dos Santos and Adi Mehmedovic

Investigation of Ladle Yield Improvements Through New Well Block Design

The effect of different well block design on the steel ladle draining operation has been studied using numerical and physical simulation. The results from a standard block design have been compared to those from a modified block design. The modified well block design showed lower critical height for drain sink formation (H_C) in most of the cases when compared with the standard design. Air injection increased significantly the H_C value. The numerical model was validated using the water model with good agreement.

Introduction

A number of studies [1–3] have shown that by the end of a ladle draining operation a structure called vortex or drain sink forms at the top surface of the liquid steel allowing slag carry over from the ladle to the tundish. This happens because, as the liquid steel level becomes low, the steel flow through the nozzle bore is higher than the steel flow into the nozzle bore, causing the surface to collapse. The result is slag entrainment. Emulsified slag in the liquid steel will likely be carried to the mould and cause steel quality issues as surface defects. Depending on the slag, reoxidation of Al, Si, and Mn can take place in the tundish causing a down grading of the steel. Additionally, depending on the amount of slag added heat by heat into the tundish the refractory lining will suffer a significant wear caused by chemical corrosion that can cause an early tundish fly or even the end of the casting sequence.

Steelmakers employ a number of devices to minimize slag carry over from ladle to tundish such as slag detector systems [4] but the most common systems still remain human dependent and will only detect the slag after it enters the tundish and floats to the surface.

A few methods are employed in some steel shops in order to increase the metallic yield. The most common is to brick the well block lower than the remaining of the ladle bottom [5]. This will not affect the drain sink formation height but as the bottom is in an upper position less steel will remain in the ladle before slag entrapment. However, as the refractory wears the whole bottom becomes worn and this type of construction will lose effect. Also, depending on the bottom construction (impact pads, well block, and plug block positions) it can be very hard or more expensive to brick such solution. Thus, it would be beneficial to develop a tailor-made device that minimizes the steel remaining when a vortex starts to form. It should be noted that every 1 cm height in a 4 m diameter ladle retains almost 1 tonne of steel. Postponing the start of vortex/drain sink formation will allow steelmakers to cast more steel without compromising steel quality.

Mathematical studies have been conducted in order to explain and predict the funnel formation [6] and it is well established that two different mechanisms can lead to the collapse of the top surface of a draining liquid: vortex sink or drain sink. Vortex sink is a phenomenon described by few authors as a funnel formed when a high tangential speed at the vicinity of the nozzle bore is present. Mazzaferro [7] has studied the influence of the well block location on the drainage of cylindrical ladles tangentially filled. They found that as the block moves towards the ladle wall less vortex sink is observed. Considering the industrial practices, they conclude that no vortex sink should be observed on draining ladles.

At the late drainage stage, when the radial liquid flow towards the nozzle bore is lower than the maximum flow allowed by the nozzle the top surface of the liquid collapses forming the drain sink. The formation does not depend on a prior vortex existence. Drain sink is reported to be the main source of ladle to tundish slag carryover [7] and as such is widely discussed for either explaining and predicting the appearance or developing a way to reduce its formation height (H_C).

The drain sink formation height was reported to be of the same order of magnitude of the nozzle bore size [8]. The H_C was found not to be dependent on nozzle position, vessel diameter, or the shape of vessel [7–8]. Hammerschmid [1] stated that the larger the resting time before draining start the smaller the H_C . They also found that gas injection on the bottom of the ladle decreases H_C . The same was observed by other authors [9] after injection of gas at the four corners of the well block during the ladle draining. In a previous study [5] H_C was reduced by introducing physical obstacles to postpone drain sink formation. In the same study it was reported that the larger the flow rate the larger the H_C . Morales and Davila [10] have developed a mathematical model that considers thermal losses and the influence on the flow pattern and the drain sink formation.

Isothermal water modelling has been used to investigate drain sink formation with two different well block designs and with/without air injection. Numerical modelling was created to mimic the physical trials and to become a new tool, to develop more quickly and cost effectively, customer specific enhanced yield well block designs. Air injection was introduced in order to reduce H_C .

Methodology

A cylindrical model following a 1:6.5 scale of an industrial ladle was made of acrylic, with inner diameter of 380 mm and 690 mm height. Since draining a ladle is gravity

dominated the Froude number, $Fr = V^2/Lg$ (where: V is the fluid velocity (m/s) L is the characteristic length and g is the gravity constant), has been used as a primary similarity criterion. A changeable bottom plate allowed the simulation of two different well block geometries. From the dashed line down both the well blocks are identical as shown in Figure 1. The total height is also the same. A circular porous element assembled at the top of the modified well block was used for air injection during the draining process. Inside the block a photoelectric sensor as well as a light source were placed in order to detect the passage of the fluids.

A continuous capture of the electric magnetic field (e.m.f) signal generated by the light impinging on photoelectrical sensor was made by a data collector. During the experiments the light passing through the water provides a certain value of e.m.f. When drain sinks occur the air funnel formed inside the well block disturbs the light passage and a different value of e.m.f emerges. The draining process was interrupted at the onset of this change, the remaining water was collected and weighed and the H_c is then estimated. Each experiment was performed 10 times and the lowest and

highest values were not considered. Table I shows the experimental conditions.

Figure 2 shows on the left the sliding gate refractories set and on the right the 3D printed modified well block with a refractory porous ring. The draining was performed with no air injection, 2 l/min and 5 l/min and stalled at predetermined liquid levels. All the other variables were kept constant.

Table I.
Experimental conditions.

Well Block	Physical Model	
	Standard	Modified
Filling	*T/**V	T/V
Height (cm)	10 and 20	10 and 20
Resting Time (min)	0 and 10	0 and 10
Flow Rate (L/min)	5, 7, 9	5, 7, 9
Air Injection (L/min)	No	2, 5
* Tangential, ** Vertical		

Figure 1.
Showing (a) the standard well block design and (b) new well block design.

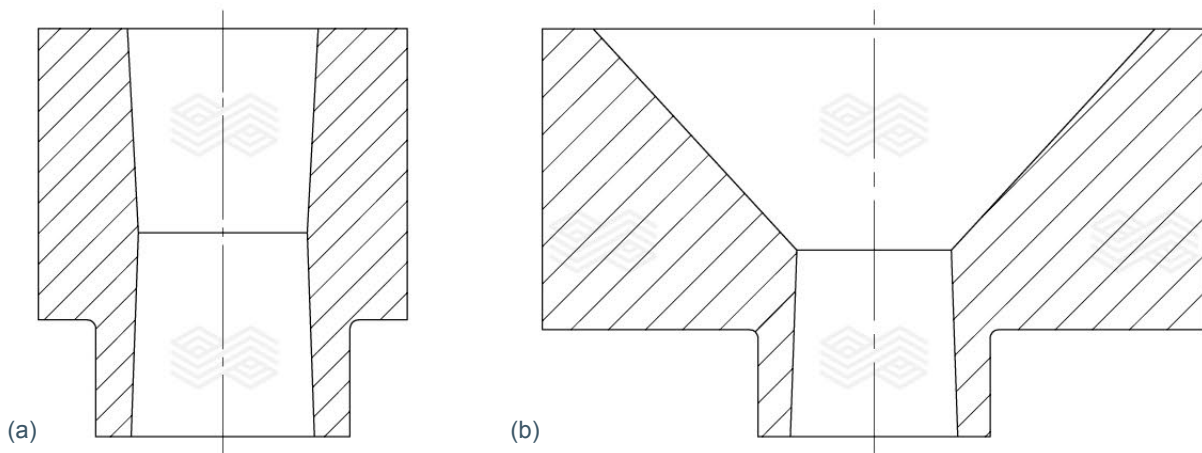
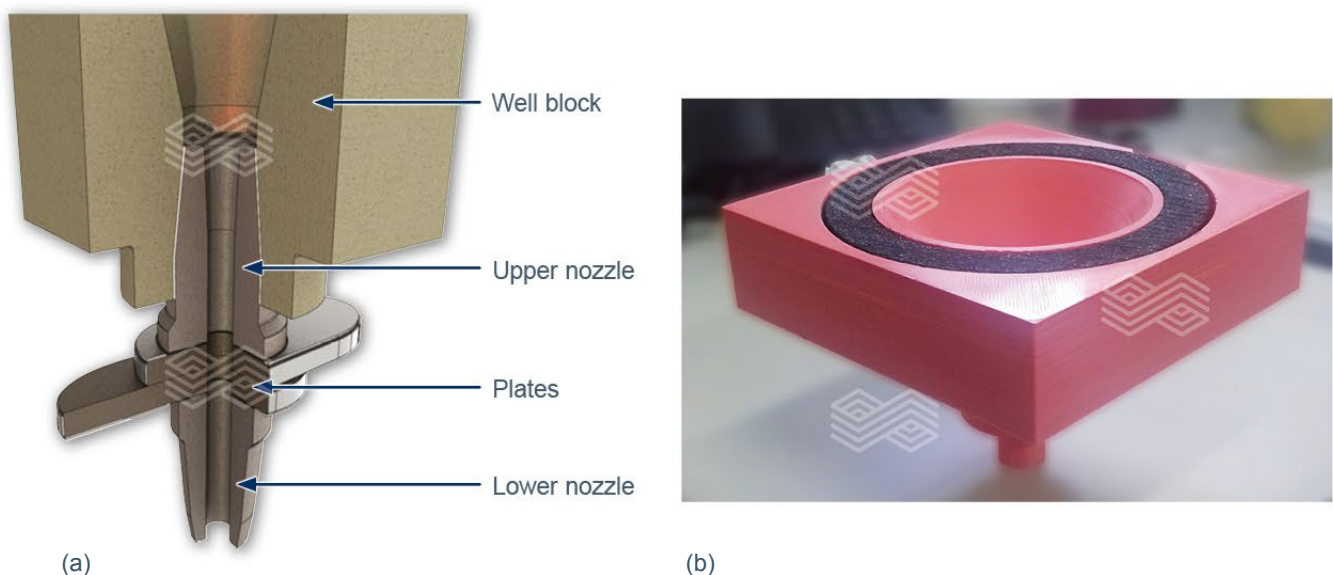


Figure 2.
Showing (a) sliding gate refractory set and (b) photo of the 3D printed modified well block assembled with refractory porous ring.



Numerical Simulation

Mathematical modelling was performed using Ansys – CFX [11-12]. Turbulence was modelled through the k-epsilon model. Therefore, the fluid flow equations which govern the phenomena for isothermal flow conditions are the continuity equation (Equation 1) and the momentum equation (Equation 2):

$$\frac{\partial \rho}{\partial t} + \frac{\partial}{\partial x_j} (\rho U_j) = 0 \quad (1)$$

$$\frac{\partial \rho U_i}{\partial t} + \frac{\partial}{\partial x_j} (\rho U_i U_j) = -\frac{\partial P}{\partial x_i} + \frac{\partial}{\partial x_j} \left[\mu_{eff} \left(\frac{\partial U_i}{\partial x_j} + \frac{\partial U_j}{\partial x_i} \right) \right] + S_M \quad (2)$$

Where ρ is the fluid's density, t is the time, x_j is the coordinate in the j-direction, U_j is the velocity component in the j-direction, P is the pressure field, S_M is the sum of the body forces and μ_{eff} is the effective viscosity accounting for turbulence, given by Equation 3:

$$\mu_{eff} = \mu + C_\mu \rho \frac{k^2}{\varepsilon} \quad (3)$$

Where μ is the fluid's molecular viscosity, C_μ is a constant, k is the turbulent kinetic energy and ε is the dissipation rate of turbulence.

Equations (4) and (5) represent the transport equations for turbulent kinetic energy and dissipation rate of turbulence:

$$\frac{\partial \rho k}{\partial t} + \frac{\partial}{\partial x_j} (\rho U_j k) = \frac{\partial}{\partial x_j} \left[\left(\mu + \frac{\mu_t}{\sigma_k} \right) \frac{\partial k}{\partial x_j} \right] + P_k - \rho \varepsilon \quad (4)$$

$$\frac{\partial \rho \varepsilon}{\partial t} + \frac{\partial}{\partial x_j} (\rho U_j \varepsilon) = \frac{\partial}{\partial x_j} \left[\left(\mu + \frac{\mu_t}{\sigma_\varepsilon} \right) \frac{\partial \varepsilon}{\partial x_j} \right] + \frac{\varepsilon}{k} \left(C_{\varepsilon 1} P_k - C_{\varepsilon 2} \rho \varepsilon \right) \quad (5)$$

Where: σ_k = Prandtl number for turbulent kinetic energy, σ_ε = Prandtl number for dissipation rate of turbulent kinetic energy, P_k = Production of turbulent kinetic energy, μ_t = Eddy Viscosity, $C_{\varepsilon 1}$ and $C_{\varepsilon 2}$ = Calibration constants of the turbulence model.

The equations above were solved for an Eulerian-Eulerian homogeneous multiphase model which uses a volume of fluid approach to track the interface, as the position of the free surface between the fluids at the moment of air aspiration is the main objective of the model. To properly describe the multiphase flow field, Equations 3–7 must be solved for the bulk flow, assuming all fluids share a common flow field [11–12]. For the calculation of the bulk flow, the density and viscosity values from Equations 1–5 must be replaced by the equivalent mixture quantities, given by:

$$\rho = r_{air} \rho_{air} + r_{water} \rho_{water} \quad (6)$$

$$\mu = r_{air} \mu_{air} + r_{water} \mu_{water} \quad (7)$$

Where r is the volume fraction of a given phase at each cell and μ the viscosity. For a two-phase model consisting of air and water:

$$r_{air} + r_{water} = 1 \quad (8)$$

The mathematical simulations were performed in a 1:6.5 scale isothermal water model. The H_C value has been evaluated taking into consideration the elapsed time when a significant drop on the mass flow rate takes place, which can be related to a second phase (gas) drawn into the nozzle bore. The boundary condition at the outlet is the velocity calculated to match the volumetric flow rate of the experiments, which did not vary significantly during the teeming process. As the outlet has a prescribed velocity, any change in the density of the incoming fluid will be detected as a variation of the mass flow through the nozzle. Table II shows the fluids properties for this simulation.

Table II.

Fluid properties for the draining simulations.

Property	Water	Air
Density (kg/m ³)	997	1.185
Dynamic Viscosity (Pa.s)	8.89 x 10 ⁻⁴	1.831 x 10 ⁻⁵

The top surface was regarded as an opening at the atmospheric pressure, to allow air to enter the domain as the water level becomes lower. No-slip boundary conditions were applied at the ladle walls.

Results and Discussion

The relationship between the water flow rate and H_C was studied and as can be seen in Figure 3a and in accordance with the literature the larger the water flow rate, the larger the H_C value. This can be observed in all 4 situations (standard and modified well block - vertical and tangential filling). Comparison involving different filling patterns shows a higher H_C value with tangential filling, that agrees with previous work as seen in Figure 3b [5].

Comparison of different well block designs, shown in Figure 3b suggests that the new design was able to significantly reduce the H_C for all flow rates. In addition, these differences increase as the flow rate increases. This is because in the new design H_C is much less affected by the flow rate compared with the standard design. A further observation was that the maximum flow rate possible (100% open) was greater for the modified well block when we compared with the standard design.

Air injection did not decrease the H_C ; quite the contrary air injection did increase significantly the value, despite other findings [5,9]. There was no observed a correlation between the air flow rate and the H_C value. Figure 4 shows the results and a photo of the experiments. Air bubbles were homogeneously distributed throughout the porous ring. No air entrapment was observed during the ladle draining.

Numerical Model

The numerical model is in good agreement with the physical model as it can be seen in Table III. Figure 5 shows the second phase distribution (in this case air) when the liquid level is just approaching H_C . As it can be seen the H_C value is significantly smaller if the new block design is adopted.

Table III.

Physical and numerical results.

H_C (Flow Rate = 8.1 L/min)	Physical [mm]	Numerical [mm]
Standard	5.3	6
Modified	2.2	2

Figure 3.

Showing (a) H_C values as a function of flow rates for a vertical filling and tangential filling – standard well block configuration, and (b) comparison between standard and modified well block – different flow rates; after 10 minutes of resting time.

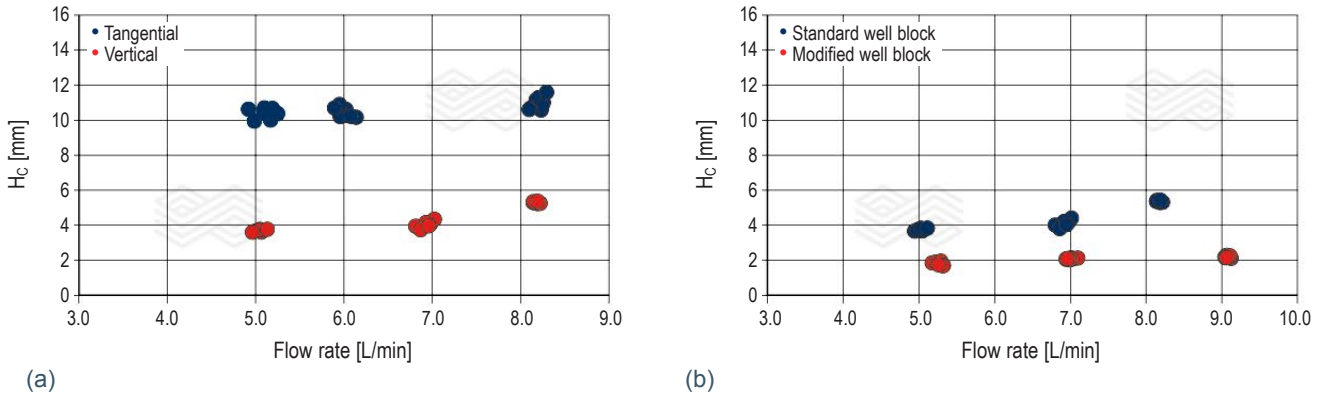


Figure 4.

Showing (a) relative H_C vs. air flow rate on the modified well block system, and (b) photo of the physical simulation for water flow rate of 8 L/min.

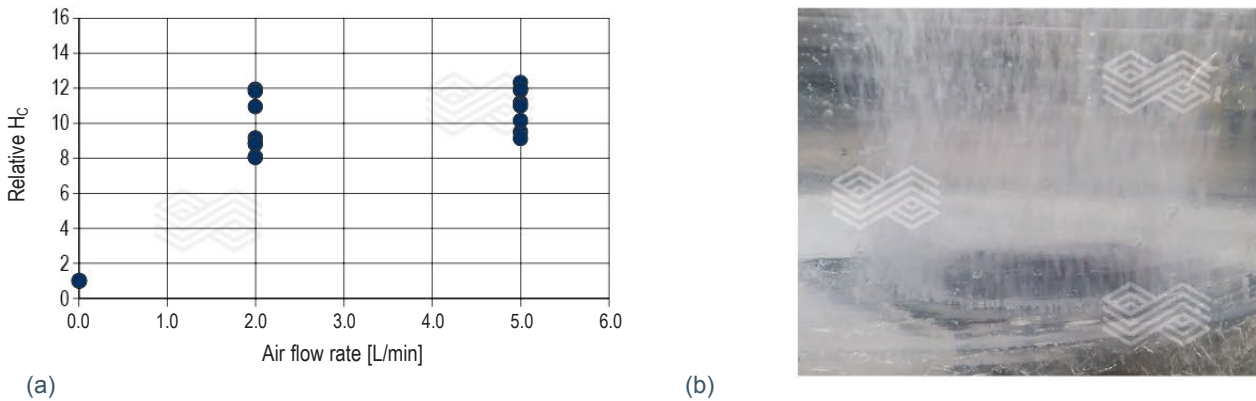
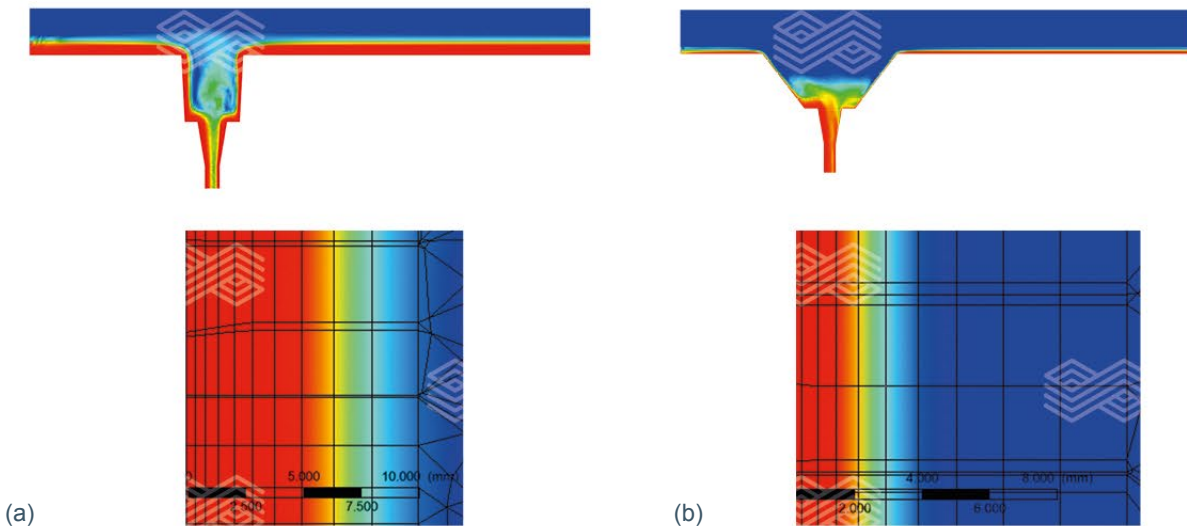


Figure 5.

Showing (a) the standard system and (b) the modified system, at the liquid level at the onset of drain sink formation.



The mass flow rate curve at onset of drain sink formation is steeper in case of the modified well block as shown in Figure 6. This behaviour would be related to a lesser degree of second phase entrainment.

In order to explain these differences a pressure distribution towards the well block for three different water levels was simulated: 17 mm, 10 mm and 5 mm from the bottom of the ladle. It is quite clear that as the water level decreases, the new well block design can provide a higher-pressure condition at the centre of the nozzle bore preventing for a longer time the axial pressure collapse that allows second phase entrapment as shown in Figure 7.

Figure 6.

Mass flow rate versus teeming time.

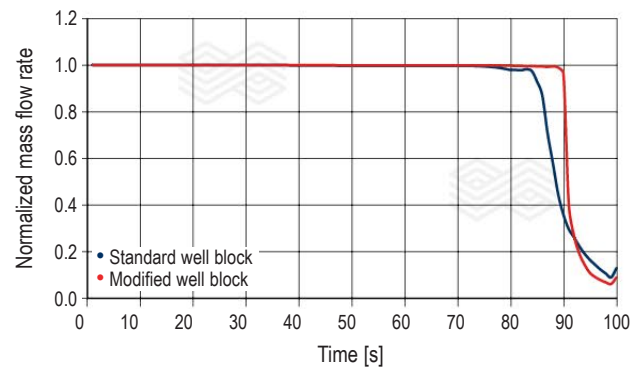
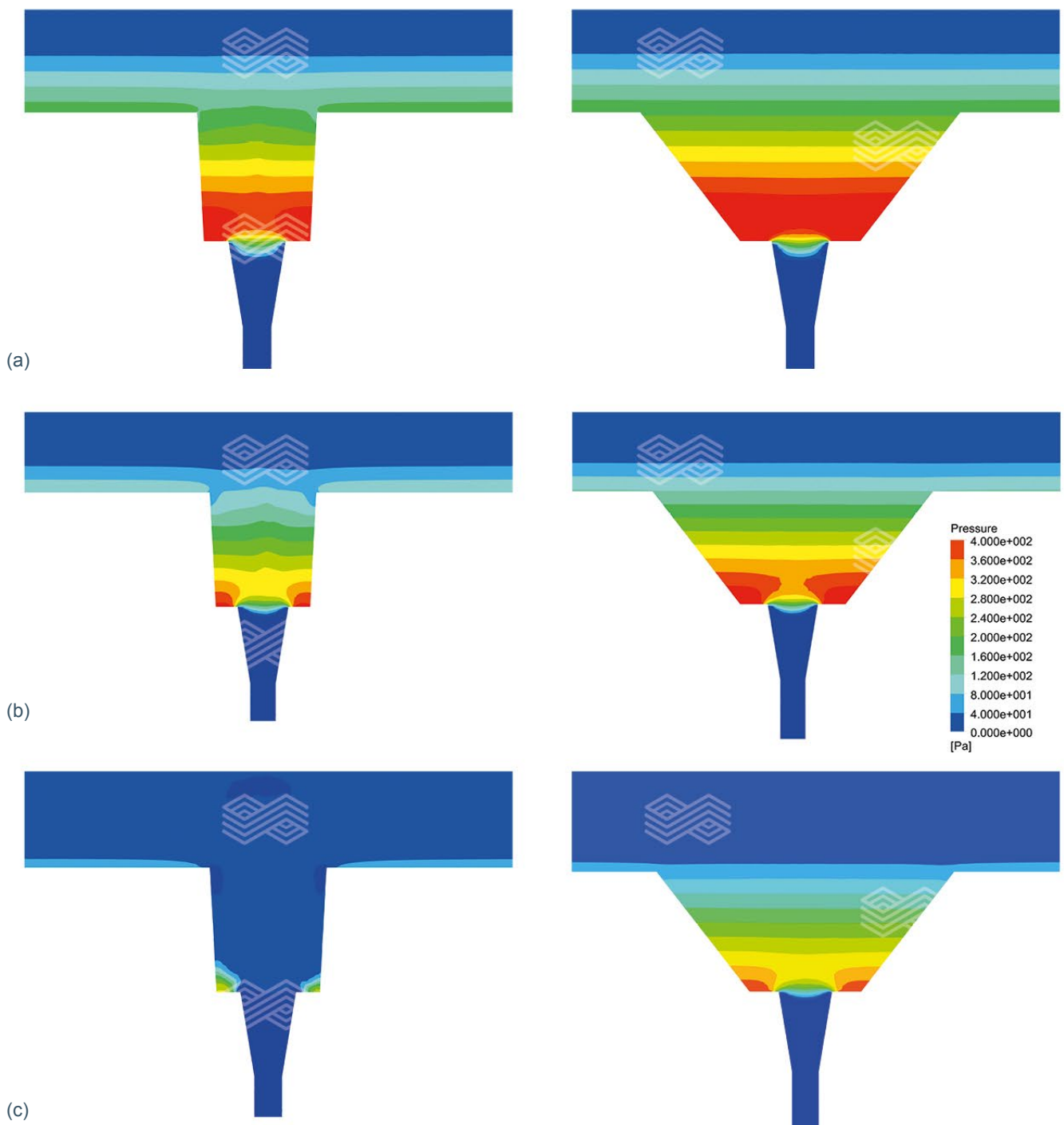


Figure 7.

Pressure distribution for three water level condition, showing a) 17 mm, b) 10 mm, and c) 5 mm.



Conclusion

With all presented it can be concluded, that the new well block configuration leads to, for all flow rates, a significant reduction of the H_C value. This could represent an increase in the metallic yield of a ladle draining operation. The new well block design displayed opportunities to increase the maximum flow rate for the same upper nozzle/plates bore size that could represent gains in sliding gate refractory performance. It also showed that air injection was not effective in reducing the H_C value. However, no air entrapment was observed showing potential in inclusion removal. The mathematical model showed very good agreement with the physical model, and thus provides a very important tool for a more rapid and customer-tailored development solution.

Future Work

Based on the very convincing results of this numeric modelling and the promising tests in the water model the new well block design has potential to be tested in the steel industry.

References

- [1] Hammerschmid, P. Vortex Formation during Drainage of Metallurgical Vessels. *Ironmaking and Steelmaking*. 1984; 11(6): 332–339.
- [2] Sankaranarayanan, R, Guthrie, R. Slag entrainment through a “funnel” vortex during ladle teeming. In: The Metallurgical Society of the Canadian Institute of Mining and Metallurgy. Steelmaking Conference; 1992; Ontario, Canadá. 655–64.
- [3] Davila, O, Morales, R. Mathematical Simulation of Fluid Dynamics During Steel Draining Operations from a Ladle. *Metallurgical and Materials Transactions*. 2006; 37B: 71–87.
- [4] Kato, H. Quality improvement of unstable zone by ladle slag detection system for continuous casting. *ISIJ International*. 1992; 5: 54–59.
- [5] Santos, S. Estudo do Mecanismo de Formação de Vórtice Durante a Etapa de Vazamento do Aço da Panela para o Distribuidor do Lingotamento Contínuo da CST Através da Modelagem Física [master thesis]. Ouro Preto: Universidade Federal de Ouro Preto; 2006.
- [6] Kojola, N. Prediction and Disarming of Drain Sink Formation during Unsteady-State Bottom Teeming. *ISIJ International*. 2009; 49:1–9.
- [7] Mazzaferro, G. Experimental and numerical analysis of ladle teeming process. *Ironmaking Steelmaking*. 2004;31(6):503–508.
- [8] Sankaranarayanan, R. *Ironmaking Steelmaking*. 2002; 147: 234–240.
- [9] Lange, M. Clean Steel Block - New developments towards clean steel. *La Revue de Métallurgie-CIT*. 2003.6:577–582.
- [10] Morales, O, Davila M. Physical and Mathematical Models of Vortex Flows During The Last Stages of Steel Draining Operations from a Ladle. *ISIJ International*. 2013. 5: 782–791.
- [11] ANSYS. Turbulence and Wall Function Theory [help system CD-ROM]. 2015.
- [12] ANSYS. Multiphase Flow Theory [help system CD-ROM]. 2015.

The TMM magazine just answered me saying there is no problem to publish the paper at the RHIM Bulletin. They have only requested to say the original source of the paper => TMM Magazine (ABM).

Authors

Paulo Vinícius Souza da Conceição, RHI Magnesita, Contagem, Brazil.
 Carlos Antônio da Silva, University of Ouro Preto, Ouro Preto, Brazil.
 João Victor Gomes Guimarães Ananias, University of Ouro Preto, Ouro Preto, Brazil.
 Alexandre Dolabella Resende, RHI Magnesita, Contagem, Brazil.
 Marcelo Borges dos Santos, RHI Magnesita, Contagem, Brazil.
 Adi Mehmedovic, RHI Magnesita, Leoben, Austria.

Corresponding author: Paulo Vinícius Souza da Conceição, paulo.souza@rhimagnesita.com



Gregor Arth, Daniel Meurer, Manfred Kappel, Peter Loop and Bernd Petritz

Tundish Technology and Processes: Ladle to Mould Systems and Solutions (Part III)

The installation of tundish furniture to control fluid flow and reduce turbulences at casting start and ladle change as well as calming the flow during steady state conditions is known to have the potential to improve casting performance. It is known, that the impact area is crucial at casting start regarding turbulence and reoxidation potential and, during ladle change with respect to slag emulsification. Impact plates, pads, pots, and boxes with special surface structure and design variations, typically based on previous fluid flow simulations to achieve optimized fluid flow at steady state conditions are state-of-the-art to minimise previous mentioned factors. Part III of this publication series continues the topic of impact pot parameter variations with focus on material selection on defined areas of the impact pots, namely the TUNFLOW™.

Introduction

Part I of this publication series [1] dealt with an overview of shrouding approaches during the ladle-to-tundish transfer, ensuring little to no reoxidation of the steel and thus guaranteeing a high cleanliness level. Part II [2] focused on the design variations of impact pots in the impact area below the ladle shroud inside the tundish. The interaction between refractory and steel/slag, especially under extremely turbulent conditions, is an ongoing topic of research for many years, mainly dealing in the area of the tundish wear

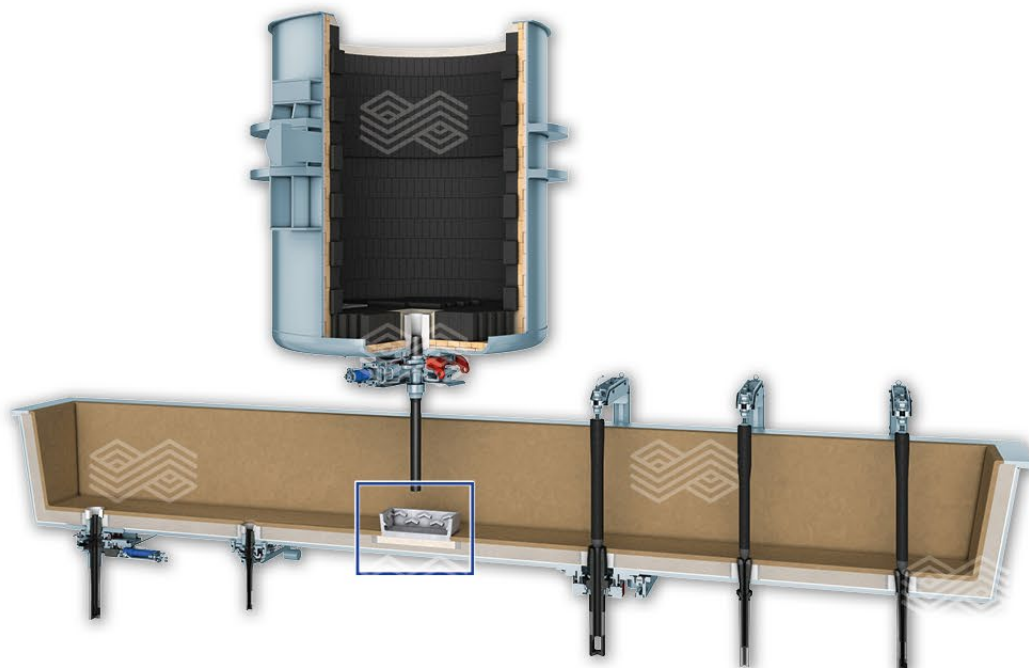
lining and slag band materials in isostatically pressed products. The wear mechanisms in the impact area are a mixture of several ones like chemical attack by emulsified tundish slag or carry over slag from the ladle, as well as mechanical attack due to the high steel velocity and pressure. This article, like Part II also addresses the impact pot, however goes into more detail regarding the material selection to enhance casting performance, in regards to what this means to the customer.

A schematic drawing of several ladle-to-mould solutions is presented in Figure 1. Part III of this publication series focuses on the blue edged section, namely the impact area.

A general overview on influencing factors on steel cleanliness and solutions has been published in [3], also discussing the effect of an impact pot, namely the TUNFLOW™, regarding turbulence, as well as hydrogen and nitrogen pick-up. The influence of impact pot design on steel bulk flow and residence time, surface turbulence and open-eye formation was discussed in detail in Part II of this series [2]. In addition one chapter dealt with the mechanical stresses on the impact pot bottom and walls and were estimated using computational fluid dynamics (CFD). This article goes one step further and reveals the potential of material selection to enhance the casting performance. The following chapters provide an insight into material selection and material combination potentials.

Figure 1.

Ladle to mould systems and solutions.



Overview on Impact pot Evolution

Impact plates / Safety plates

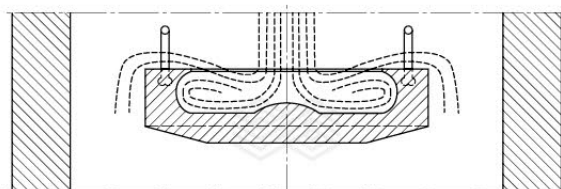
During the ladle to tundish transfer the steel impinges the impact area with high velocity as well as high pressure, leading to the highest refractory erosion inside the tundish. As a potential countermeasure very dense and chemically stable refractory plates or pour pads are placed in this impact area with mainly flat shape, to resist the present forces and prevent a break out [4]. Currently, impact plates are still used inside the tundish for safety reasons, placed below a turbulence inhibitor and often in combination with a thermocouple acting as a break-out detection device. Some steel producers also place used slide gate plates in the impact area, with the drawback of a local weakness, namely the hole of the plates. Others also apply MgO-C bricks taken out of an aggregate from secondary metallurgy processes, with the disadvantages on one hand of the gaps between the bricks, and the used material itself on the other. Typical brands for impact plates are listed in Table I.

Table I. Examples for impact plate grades.

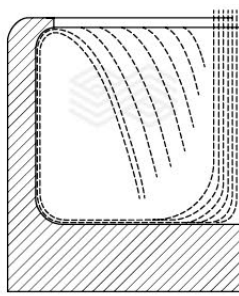
Brand	MgO	Al ₂ O ₃	SiO ₂	CaO	Fe ₂ O ₃	TiO ₂
ANKOFORM M90	92.0	0.2	3.8	1.8	1.0	–
ANKOFORM S90	–	80.5	12.0	1.8	1.7	3.0

Figure 2.

Showing pouring pads used for ingot casting in the late 1960's (a,b) [6] and (c) modern pad design.



(a)



(b)



(c)

Impact pads / Pouring pads

First attempts to influence the flow of the steel stream started in the ingot casting industry in the late 1960's, where a block was placed inside the mould to calm the flow during pouring [5,6]. The proposed design appeared similar to the later published first impact pots for the tundish, as will be presented afterwards. Distributing the flow of the incoming stream towards the walls, which then redirected the flow towards the steel stream coming from the ladle and helped to decrease the turbulence and reduce the kinetic energy.

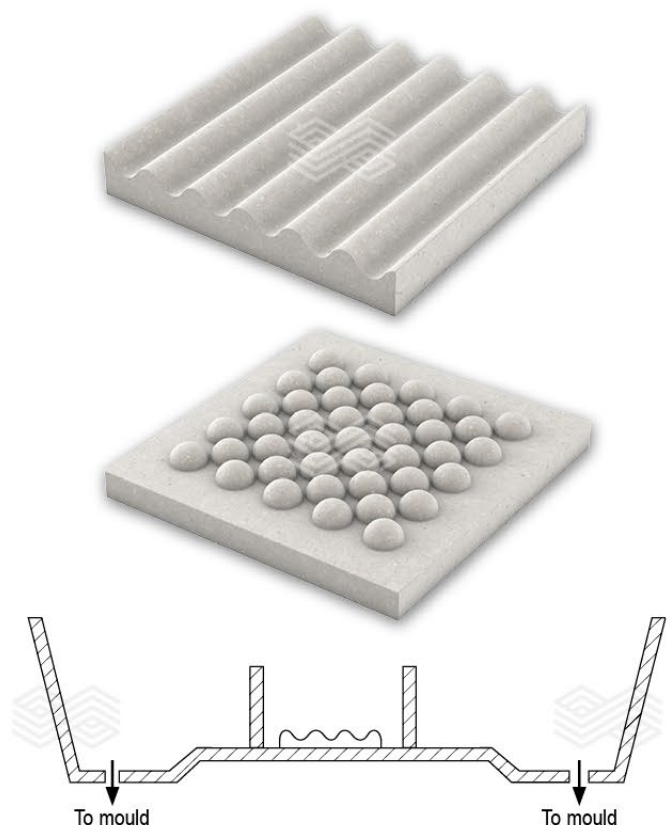
Modern pouring or impact pads in the tundish differentiate from impact pots mainly due to their wall height, which is significantly lower than for typical turbulence inhibitors like the TUNFLOW™. Impact pads aim primarily on redirecting the flow in certain directions roughly perpendicular to the incoming steel stream and to withstand the present forces. It can be seen as an intermediate step between no turbulent inhibitor installation and the application of an advanced impact pot, but with the drawback of low splashing reduction during the casting start. The main advantage is, depending on design, a modified flow and a slightly enhanced break-out safety. Figure 2 shows the evolution of pouring pad design changes from the 1960's, [6], to the present.

Impact pots

In the early 1990's a first structured pouring pad for the tundish impact area was patented, in combination with dams and sidewalls with a similar appearance to an impact pot (Figure 3) [7].

Figure 3.

First approaches towards impact pots inside the tundish [7].



Shortly afterwards another approach was published by the Bethlehem Steel Corporation (Figure 4), using the impact pot design to guide the majority of the steel stream in a defined direction, while calming the turbulence by redirecting the remaining steel towards the incoming one [8]. From this time on it seems that the interest in turbulence inhibitors increased drastically with a break-through around the millennial change, where previous findings were used to develop enhanced designs. In addition to safety issues, further benefits regarding the production of clean steel came into play. [9–11]

Since this time several novel designs were created, made available by CFD assisted modelling as well as the provision of new production techniques. Several variations of impact pots are depicted in Figure 5 in an approximate chronological order of development.

Impact Boxes / Delta Box

Impact pots typically show best performance if the ladle shroud is vertically aligned and the incoming steel stream is focused on the centre of the baseplate. Unfortunately, this is rarely the case for several reasons, such as old collector nozzles, steel splashes or even a bent ladle bottom. If only a slight misalignment is present, advanced designs like the TUNFLOW™ CHEVRON are still good turbulence inhibitors, as can be seen in previous publications [2, 13]. If a customer suffers from high wall erosion in the tundish bay, caused by a severe shroud misalignment, so called impact boxes can help to reduce the wear in this area.

Depending on the tundish geometry one or more walls are elongated towards the upper side of the tundish, the tundish box provides greater wall thickness and safety against break outs. The selection of an impact box is a case by case decision, with enhanced safety on the one hand, and the increased box weight and costs on the other, as well as the requirements of experienced workers during placement and connection with the tundish lining. Different designs of a tundish impact box are presented in Figure 6.

Figure 4.

Impact pots designs for 1 strand tundishes [8].

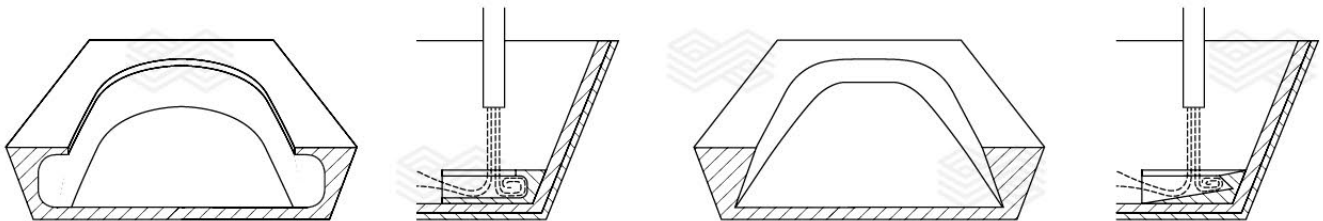


Figure 5.

Impact pot designs for different continuous casting tundishes showing the evolution of design [12].



RHI Magnesita offers combined solutions to help the customers calming the flow using designs like the TUNFLOW™ CHEVRON as basis, elongating one or more side walls to decrease break out probability due to a misaligned shroud, as well as localized material selection to ensure highest wear resistance, exactly where it is needed the most, the so-called HYBRID TUNFLOW™.

Experimental Results

As previously mentioned in Part II of this publication series [2], the selection of the best material according to the customer's process is a key to obtain the demanded casting goals. Optimal performance is gained from the selective material concepts and impact pot design, cross-checked with test results under similar process conditions carried out in the Technology Center, located in Leoben, Austria. One example of such test application is the production of different TUNFLOW™ materials and testing against varying ladle and tundish slags in a small high frequency induction furnace (HF-ITO). During this test 4 refractory samples of defined geometry are immersed in liquid slag at constant temperature and kept in rotation over the testing period. A detailed description as well as images out of this test can be found in [2].

To visualize the importance of correct material selection, different grade variations were investigated using the above mentioned set-up, varying slag composition, refractory grades (casted or pressed), and testing time. The chemical composition of 3 slags is provided in Table II, the calculation of the basicity was carried out after $B = (\text{CaO} + \text{MgO}) / (\text{SiO}_2 + \text{Al}_2\text{O}_3)$. Due to the fact that impact pots are typically casted products, mainly these grades were investigated. In addition some brick qualities were also tested under same conditions (10 minutes exposure time, pure slag, 1560 °C) and also with enhanced exposure time (60 min exposure time, pure slag, 1560 °C).

Magnesia Products

Examples from these laboratory trial results are presented in Figure 7. The influence of MgO with respect to olivine content on the refractory wear can easily be seen on these samples, as well as the higher resistance of pressed magnesia products when compared to the cast grades.

Table II. Chemical composition and calculated basicity of the applied slags

	MgO	CaO	SiO ₂	FeO	Al ₂ O ₃	basicity
Slag A	8.5	39.0	45.2	0.4	5.9	0.9
Slag B	4.2	30.4	8.0	0.9	55.4	0.5
Slag C	7.6	45.2	0.3	0.2	46.5	1.1

Figure 6.

Showing (a) historical tundish box design [6], (b) tundish box with elongated side walls, and (c) combined RHI Magnesita solution (CHE51P).

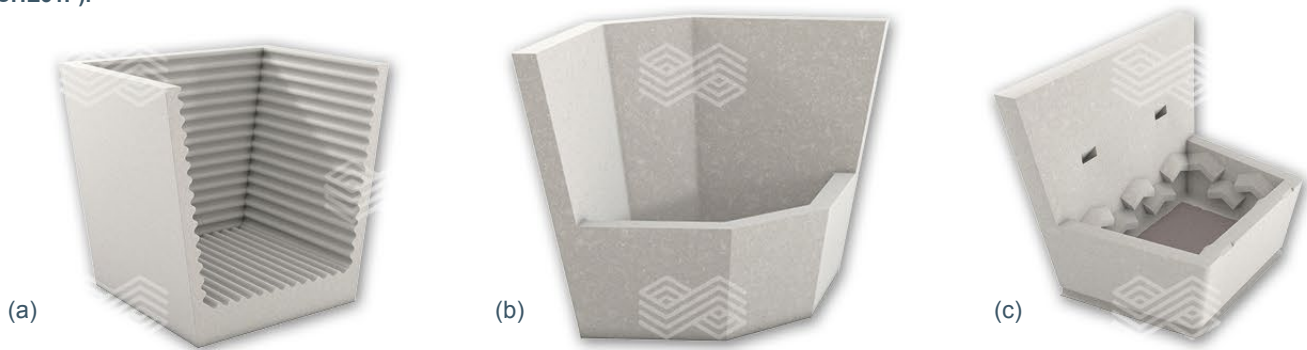


Figure 7.

Refractory samples based on magnesia, Sample 1–4 after 10 minutes exposure time to pure slag, sample 5 after 60 minutes.



These results were found to be consistent over all tests with the 3 slags used and the amount of corroded refractory is presented in Figure 8. To determine the amount of corrosion, the samples were first cut in half along the rotational axis and the resulting area was investigated. Using a defined geometrical mesh, the difference between the initial sample geometry and the remaining refractory shape was measured. No wear of the pressed magnesia was found during contact with any of the 3 slags after 10 minutes, only after an increase in residence time in the liquid slags to 60 minutes a higher corrosion was observed, however at very low levels.

A thermodynamic calculation series using FactSage 7.1 was carried out to compare the laboratory results with the estimated chemical stability of the refractory in contact with liquid slag. Although these calculated results are assumptions under thermodynamic equilibria, and no kinetic effects are considered, a similar tendency regarding the refractory wear was found for the cast magnesia products, namely lower liquefied refractory with decreasing olivine content (Figure 9).

Alumina Products

Due to the fact that TUNFLOW™ products are also available based on alumina, different grades were tested with the same 3 slags, under same test conditions as magnesia samples, for both cast and pressed qualities. Samples of alumina are presented in Figure 10, the enhanced performance of pressed alumina over cast grades is clearly visible, even after increased exposure time to the slags. Measured values of the corroded refractory are depicted in Figure 11, the influence of higher refractory quality of cast grades on corrosion tendency is again clearly visible. This tendency is also estimated using the thermodynamic calculations, seen in Figure 12.

Figure 8.

Influence of olivine content on refractory wear by different slags.

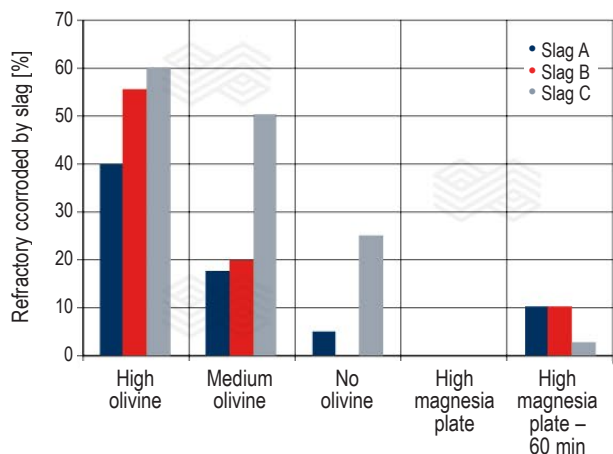


Figure 9.

Calculated liquefied magnesia grades by slags A–C.

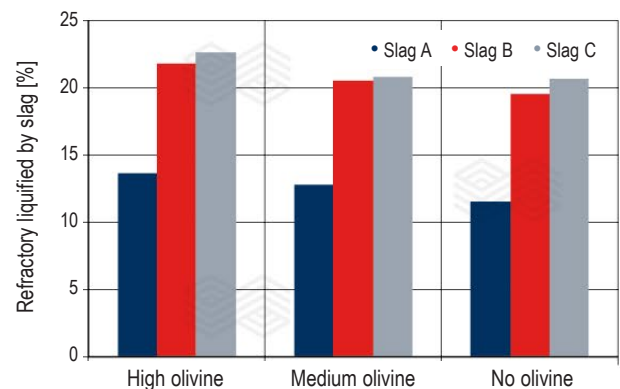


Figure 10.

Refractory samples based on alumina, Sample 6–8 after 10 minutes exposure time to pure slag, sample 9 after 60 minutes.



HYBRID TUNFLOW™

The different stress scenarios on impact pots presented previously [2] and the results of laboratory trials, thermodynamic calculations, and customer reports now clarify the view on impact pot design and grade selection. In addition to the highest impact pressure and steel velocity, the bottom of the impact pot is also attacked by slag – ladle carry-over or tundish, at an elevated level. To counteract the increased wear rate in this area, increased bottom thickness, or complete grade change are typical approaches by impact pot providers. This leads in one way or another to increased costs, impact pot weight and manipulation problems for the customer. The raw material crisis recently underlines this even more. Furthermore production limits regarding the maximum refractory thickness exist, thus preventing the enhancement of the inhibitors life and tundish safety.

A change of the whole impact pot material from magnesia to alumina or vice versa can lead to a positive effect with respect to performance and lifetime, as already proven by different customers. The results of laboratory trials as well

as thermodynamic calculations presented earlier confirm this. When comparing the different effects of slag A to C on alumina and magnesia refractories it is clear that slag variation from A to C has an escalating effect on the wear of magnesia products (A – lowest wear; C - highest wear), this effect is the opposite in alumina products (A – highest wear; C - lowest wear).

RHI Magnesita now combines these insights to a completely novel and cost-effective impact pot design series, the TUNFLOW™ HYBRID. This series utilises cost-effective body materials, in combination with a high-performance bottom. It is a potential combination of different adjustments:

- Main body material – magnesia or alumina.
- Bottom material – magnesia or alumina.
- Bottom manufacturing technology.
 - > cast or pre-shaped.
 - > resin-, ceramic, or cement-bonded.

Some variations of the novel TUNFLOW HYBRID design is given in Figure 13.

Figure 11.
Influence of alumina content on refractory wear by different slags.

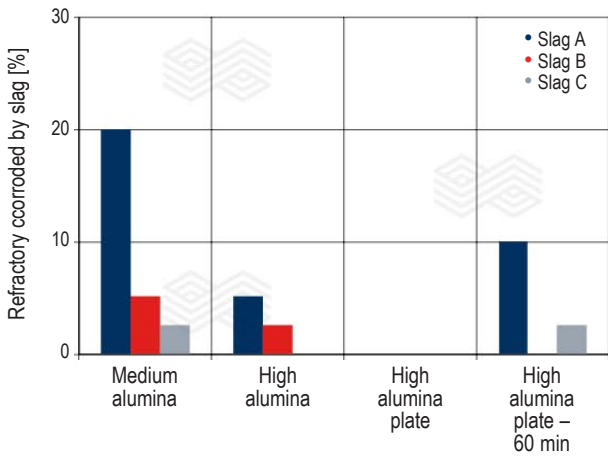


Figure 12.
Calculated liquefied alumina by slags A–C.

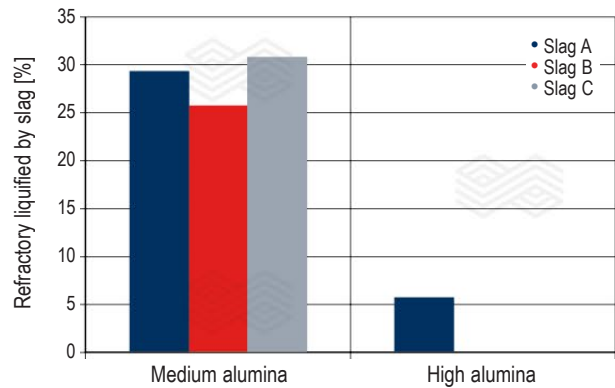
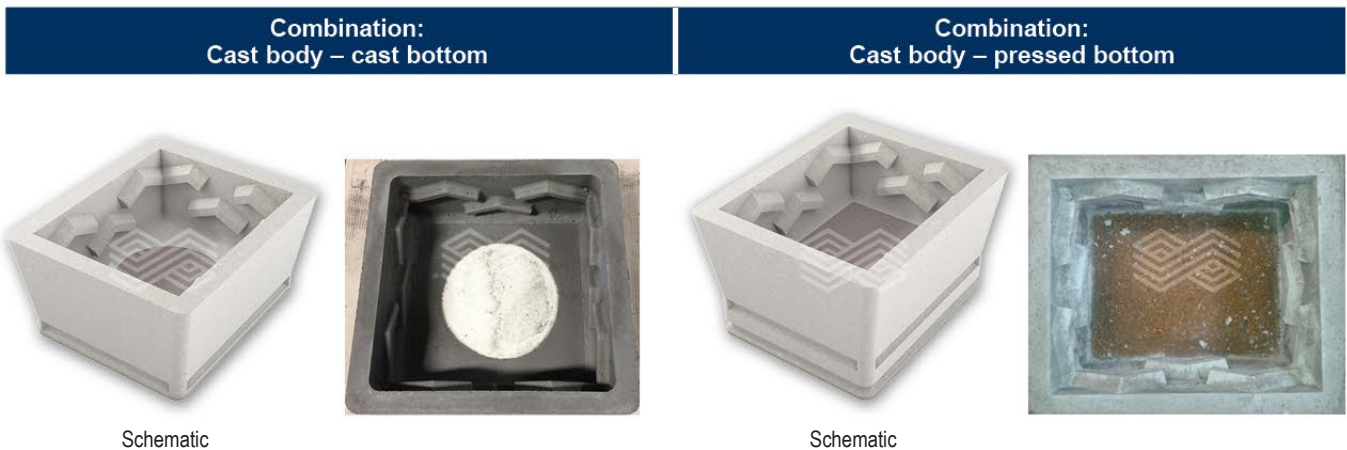


Figure 13.
Examples of the novel TUNFLOW™ HYBRID



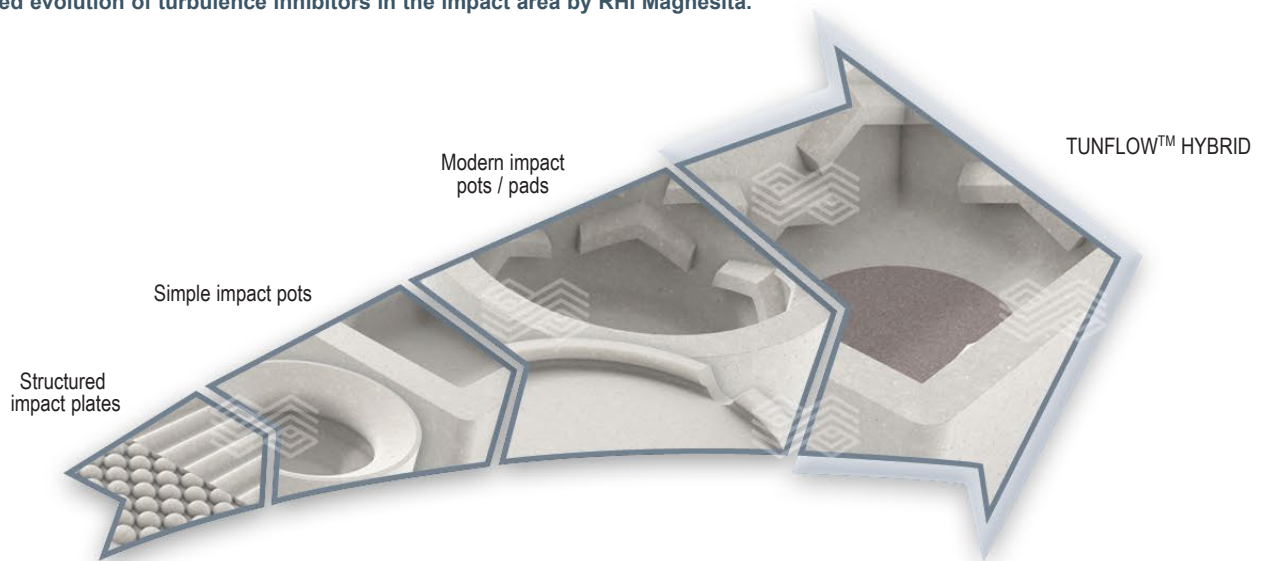
Summary and Outlook

An overview of the turbulence inhibitor evolution was presented in the beginning of this publication, starting in the late 1960's in the foundry sector, concluding the chapter with the current status of modern impact pots used in continuous casting machines. As was illustrated in the experimental section, refractory materials based on different raw materials provide varying performance when in contact with miscellaneous slags. This was demonstrated by laboratory methods as well as thermodynamic calculations, making the importance of correct material selection even more evident.

Due to the proven limits regarding typical applied manufacturing techniques of refractories, especially of the turbulence inhibitors for the continuous casting tundish, a novel approach was developed to overcome these drawbacks. RHI Magnesita now combines benefits of different manufacturing and bonding techniques, as well as material grades to produce the novel TUNFLOW™ HYBRID. The reduced weight, enhanced safety, and increased lifetime with the consequential advantages, as well as the now even more customer tailored product design elevates the HYBRID brand to a powerful tool to fulfil the customer's demands. Figure 14 shows a range of impact area turbulence inhibitors, which provide individual solutions for each customer.

Figure 14.

Updated evolution of turbulence inhibitors in the impact area by RHI Magnesita.



References

- [1] Arth, G., Viertauer, A., Hackl, G., Krumpel, G., Petritz, B. and Meurer, D. Tundish Technology and Processes: Ladle to Mould Systems and Solutions (Part I), RHI Bulletin (2016), 1, pp. 38–44.
- [2] Arth G., Meurer, D. Tang, Y., Hackl, G. and Petritz, B. Tundish Technology and Processes: Ladle to Mould Systems and Solutions (Part II), RHI Bulletin (2017), 1, pp. 60–66.
- [3] Secklehner, B.A., Casado, M.T., Viertauer, A. Wappel, D. and Brosz, B. Tundish Technology and Processes: A New Roadmap, RHI Bulletin (2015), 1, pp. 68–77.
- [4] Sahai, Y. and Emi, T. Tundish Technology for Clean Steel Production, World Scientific Publishing, 2008.
- [5] Daussan, H. J. Improvements in or relating to a method and a device intended for the improvement of the contexture of cast metals, Patent GB1126922.
- [6] Hajduk, M. Impact Pad, DPMA Erfinderaktivitäten, Publikation Deutsches Patent - und Markenamt, vol. 2003, 2004. pp 40-44.
- [7] Soofi, M. Tundish Impact Pad, US5072916.
- [8] Schmidt, M. and Newman S. B. Impact Pad for a Continuous Caster Tundish, US5169591.
- [9] Saylor, K.J. Turbulence Inhibiting Tundish and Impact Pad, EP0729393.
- [10] Zacharias, D.R. Tundish Impact Pad, EP 0790873.
- [11] Brecka, G., Pirkner D., Gamweger K. and A. Retschnig. Pralltopf, DE10143396.
- [12] Patent applications and patent pending.
- [13] Arth, G., Tang Y., Schwalm B., Marques A. and Ozorio D. RHI's solutions to reduce steel defects, ABM 2017 (2-6. Oct. 2017), 48th Steelmaking Proceedings, Sao Paulo, Brasil.

Authors:

Gregor Arth, RHI Magnesita, Leoben, Austria.
 Daniel Meurer, RHI Magnesita, Leoben, Austria.
 Manfred Kappel, RHI Magnesita, Leoben, Austria.
 Peter Loop, RHI Magnesita, Leoben, Austria.
 Bernd Petritz, RHI Magnesita, Leoben, Austria.

Corresponding author: Gregor Arth, gregor.arth@rhimagnesita.com





RHI MAGNESITA



We have
a vital job
to do



Alexandre Dolabella Resende, Rodrigo Nazareth Borges, Rubens Alves Freire and Ramon Fraga Resende

Tundish Furniture Optimisation Through Mathematical Modelling

The flow pattern in the tundish is critical to achieving high steel quality. In order to achieve desirable flow patterns in the tundish, different furniture options are commonly used, e.g., impact pots, weirs, and dams. Nevertheless, for weir and dams to be effective, it is imperative that the positioning and size are optimised for the specific tundish in consideration. In this study, a mathematical model to optimise the tundish furniture is presented. It consists of solving the flow in the tundish through a computational fluid dynamics (CFD) model coupled with an optimisation model combining a design of experiments method with response surface generation. The optimisation model was adopted to maximize the steel residence time in two different slab tundishes and the results are presented in this study.

Introduction

The tundish is an important vessel in the continuous casting process, linking the incoming steel from the ladle to the moulds. For many years, the tundish role was limited to the distribution of molten metal to the strands, allowing the continuity of the casting process even between successive ladle changes. As the demand for quality became more stringent, flow control in the tundish gained more attention, as steelmakers worked to make this vessel a place of further refining of the molten steel, instead of only a reservoir. To obtain the best tundish performance, the tundish furniture should be carefully designed. Consequently, RHI Magnesita has developed a mathematical model to predict the optimum configurations of weir and dam arrangements for maximum steel cleanliness.

Effect of Tundish Furniture on the Flow

The flow pattern in the tundish is significantly influenced by its furniture. An example of how fluid flows in the tundish impact on the final product was given by [1] who reported a rise of the reject rates of slabs from a steel company from 0.7% to almost 50% due to an improper placement of an impact pad. Another study [2] compared inclusion removal in a delta shaped four strand tundish under different impact pad and dam configurations. It was found that, depending on the position and height of the dams, the inclusion removal rate could be enhanced. However, for some cases, the steel quality could even be degraded. These studies reinforce the importance of developing a tool which is able to optimise the positioning and size of the furniture, particularly weirs and dams which have relatively simple geometries and are suitable for a parametric optimisation.

The definitions adopted in this work are from the combined model proposed by [3] to characterize the residence time distribution (RTD) of tundish flows. The model assumes that the total volume of the fluid in a tundish is divided into three regions: plug flow region, well mixed flow region and dead flow region. In the plug flow region, longitudinal mixing is nonexistent, however, transverse mixing may occur to any extent. In this flow region, all fluid elements have equal residence times in the tundish. In the well mixed flow region, on the contrary, the tracer dispersion occurs almost instantly, with the maximum possible mixing. Finally, the dead region is divided in two regions: in the first type, the fluid is considered to be completely stagnant, while in the second type, the fluid moves very slowly, causing some fluid to stay much longer in the vessel than the average residence time.

As the average residence time for a tundish at a constant flow rate remains unchanged, the longer residence time of the fluid in the dead region must be compensated by a shorter residence time of the fluid in the active flow region. This portion of fluid which stays in the vessel for a shorter time may not have enough time to separate and float out the nonmetallic inclusions. Furthermore, the melt in the dead region may lose too much heat and start to solidify prematurely. On the other side, higher values of plug flow are associated with enhanced steel cleanliness as it is associated with higher values of the molten steel minimum residence time, i.e., shortest time taken by a fluid element to travel from the inlet to the outlet of the tundish. Therefore, the best tundish performance is obtained when the dead volume is the smallest and the plug volume is the highest.

Optimisation Model Description

The weir and dam optimisation was performed through an adaptive single-objective optimisation method, which combines an optimal space-filling (OSF) design of experiments, a Kriging response surface and a mixed-integer sequential quadratic programming optimisation algorithm. The optimisation study was performed through ANSYS DesignXplorer. Further information about the optimisation methods can be found in [4]. The study variables were the position and size of the weir and dam, as shown in Figure 1.

The main key performance indicator (KPI) of the tundish flow performance chosen for the optimisation studies is the minimum residence time of the steel in the tundish, under steady-state flow conditions. It is expected that, by maximizing the minimum residence time, the plug flow fraction will be maximised and the dead flow fraction will be minimised, both of which are very important for improved steel cleanliness.

For each different combination of furniture parameters, a CFD model was performed and the minimum residence time was defined as the time taken by the first fluid streamline to reach the strand. Once the optimum parameters were obtained, a RTD study was performed to compare the optimum configuration against the reference in order to measure the benefits of the optimisation model.

In this work, the results obtained for two different slab tundishes will be presented. In the first case, the ladle shroud was centered relative to the impact pot. In the second case, the ladle shroud was significantly off-centered relative to the impact pot.

Case 1: Ladle Shroud Centered Relative to the Impact Pot

In the first configuration studied, the ladle shroud was perfectly centred with the impact pot, as shown in Figure 2. The results shown in this section are based on a previous study [5]. The geometry studied is a two-strand slab tundish, with a 73 tonne capacity and 5 tonne per minute flow rate per strand.

Figure 1.

Variables analysed in the optimisation model. P1: Weir submergence depth. P2: Dam height. P3: Distance from the ladle shroud axis to the weir. P4: Distance between weir and dam.

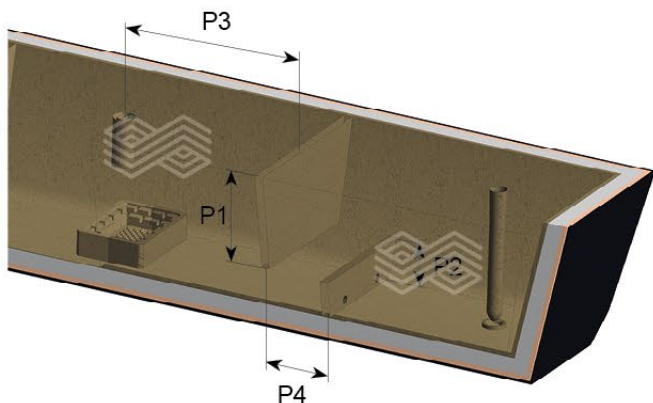
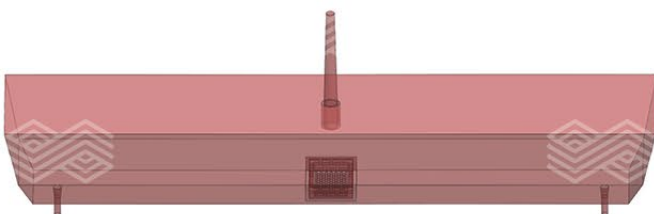


Figure 2.

Tundish geometry considered for the optimisation study (centred case).



Three different furniture configurations were compared for this case. First, a reference configuration with only an impact pot was simulated. Then, there were added weirs and dams according to a previous concept at the specific steel plant, without the optimisation model. And finally, an optimised configuration was proposed, obtained through the model developed by RHI Magnesita.

Figure 3 shows the flow streamlines for the three configurations. By optimising the furniture design, the recirculation zones and the flow velocities were reduced, which translates to better mixing efficiency in the tundish.

To obtain the optimised configurations, 99 simulations were necessary for this case.

Figure 3.

Flow streamlines for the centred case. Showing (a) impact pot only, (b) impact pot with weir and dam used before optimisation, and (c) Impact pot with optimised weir and dam.

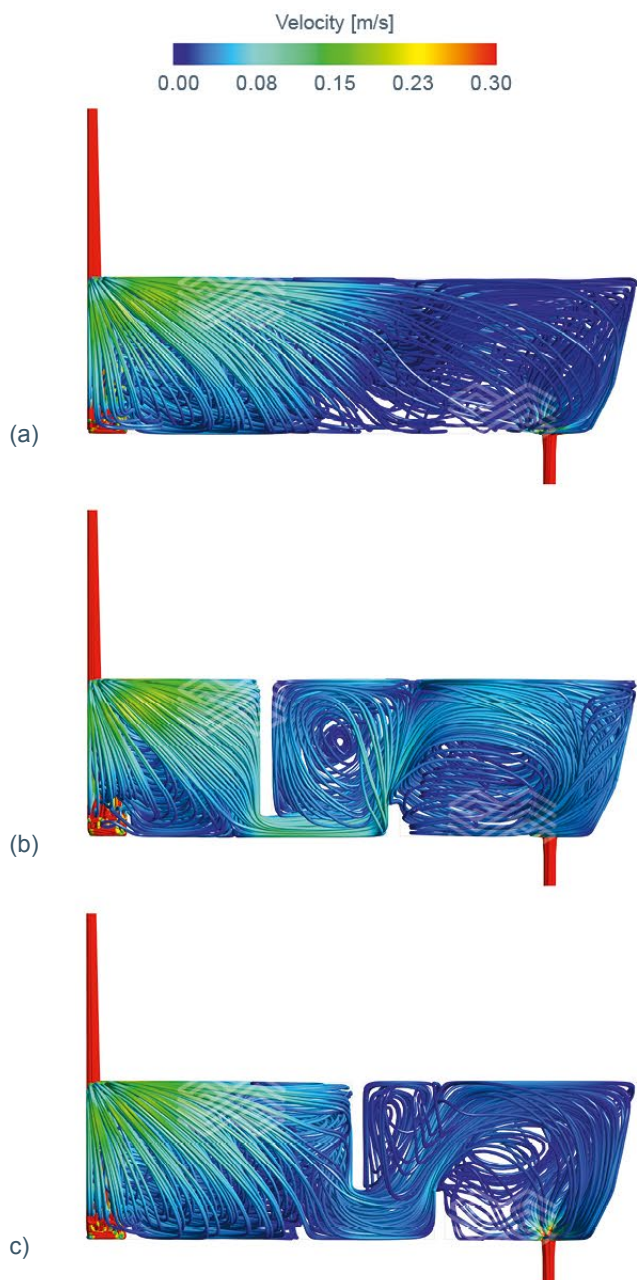


Figure 4 shows the evolution of the minimum residence time result as the optimisation study was conducted. The positive inclination of the trend curve shows the adaptive behaviour of the algorithm, which refines the domain as the study progresses, in order to find the global maximum. This means that, at later stages of the study, the computational efforts are concentrated on the parameter ranges which have shown the best results so far.

The importance of optimising the tundish furniture can be seen on the RTD results shown in Figure 5. The plug volume fraction has increased from 18% to 27% comparing the reference setup to the optimised one. In relative terms, it corresponds to a 50% improvement in performance, which is

Figure 4.
Results of minimum residence time for each simulated configuration in the optimisation study for case 01.

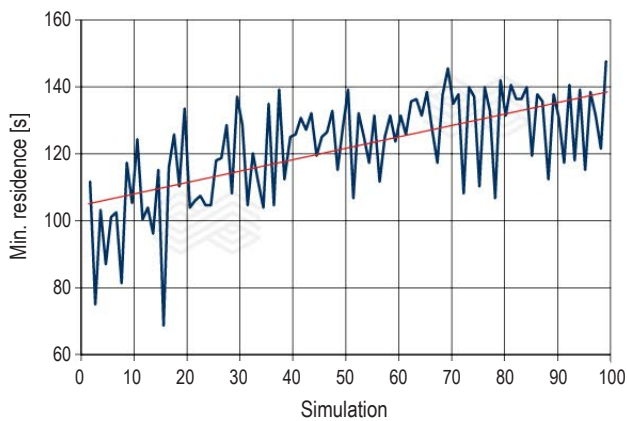
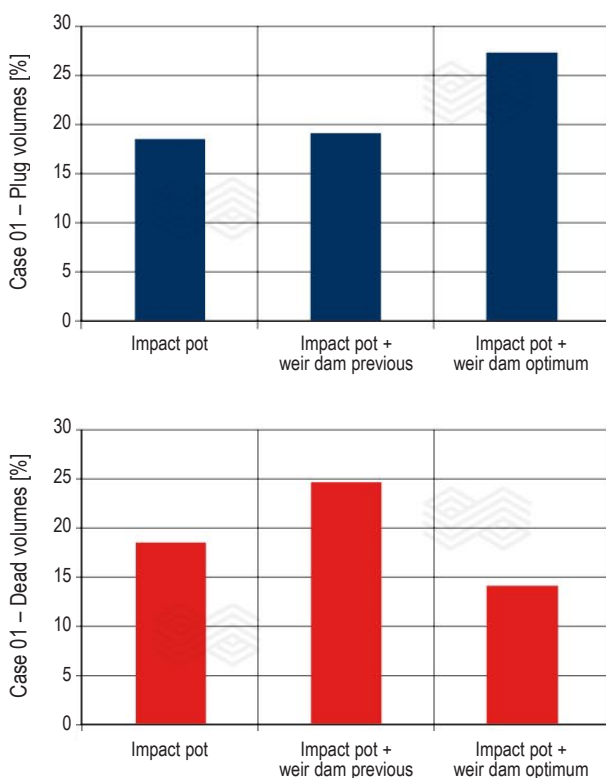


Figure 5.
RTD results comparing the different configurations for case 1.



very significant. The dead volume fraction was reduced from 18% to 14% between the reference and optimised configurations, which represents a relative reduction of 22%, also a very good result. It is interesting to notice that, by adding weir and dams in the nonoptimised configuration, the dead volume fraction actually increased, reaching 25%. This reinforces the importance of a careful assessment of the results through the simulations.

Case 2: Ladle Shroud Off-Centered Relative to the Impact Pot

For the second case studied, the ladle shroud was significantly displaced from the centreline of the impact pot. Although such a configuration is not ideal, it is important that the furniture design promotes the best performance as possible, even under adverse conditions. Figure 6 shows the tundish geometry for this case. It is an 80 tonne tundish with a flow rate of 3.4 tonne per minute per strand. The entry jet centreline is located at approximately $\frac{1}{4}$ of the impact pot length.

For this case, the optimised configuration was obtained after 32 simulations, as shown in Figure 7. The trend line shows again a positive inclination, emphasizing the adaptive behaviour of the optimisation algorithm.

Figure 6.
Tundish geometry considered for the optimisation study (off-centred case).

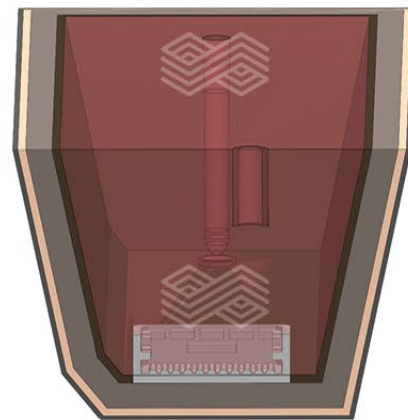
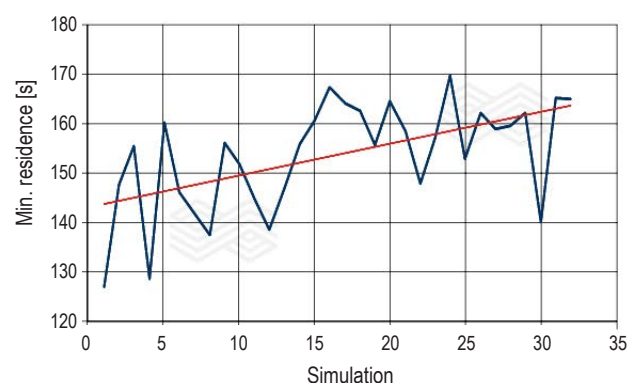


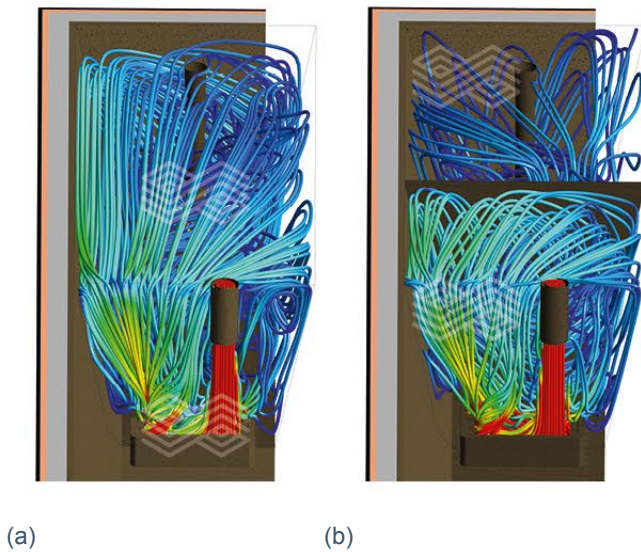
Figure 7.
Results of minimum residence time for each simulated configuration in the optimisation study for case 02.



For this case, there was no previous arrangement of weir and dam. Therefore only two configurations were compared: impact pot only (reference) and the optimised setup. Figure 8 shows the flow streamlines for each. It can be seen that, for the reference configuration, the off-centred entry jet caused the upward flow to concentrate on the opposite side, consequently causing a preferred flow path close to the wall.

Figure 8.

Flow streamlines for the off-centred case. Showing (a) impact pot only and (b) impact pot with optimised weir and dam.



However, the weir is able to break the preferred flow path, causing a complete redistribution of the flow, in the optimum case.

Figure 9 shows the evolution of the flow streamlines with the time. It can be seen how the preferred flow path along the wall causes a much shorter residence time. The effect of the flow modifiers is much more than just forcing the flow downwards and then upwards again. By interrupting the preferred flow path, the weir and dam force the fluid to be distributed over a larger portion of the tundish cross-section, thereby reducing its velocity. As a consequence, the steel residence time is much longer, providing benefits in terms of steel cleanliness and mixing efficiency.

Such improvement is quantified by the RTD results, shown in Figure 10. The plug volume fraction increased from 8% in the reference case to 21% in the optimised configuration, which is an increase of 162% in relative terms. The dead volume fraction reduced from 38% in the reference to 20% in the optimised setup, which is a relative decrease of 48%. It is particularly interesting to point that the magnitude of improvement was much higher for this tundish (off-centred) than for the one in Case 1 (centred). This shows that a well-designed tundish furniture provides even more benefit when the alignment of the shroud with the impact pot is not perfect. Taking into consideration that in actual plant operation misalignments are likely to occur, the optimisation model is a valuable tool to provide the best furniture design for each tundish, considering the specific operational conditions.

Figure 9.

Evolution of the flow with the time. (a) Flow at time = 50 seconds in the upper row. (b) Flow at time = 100 seconds in the middle row. (c) Flow at time = 200 seconds in the lower row.

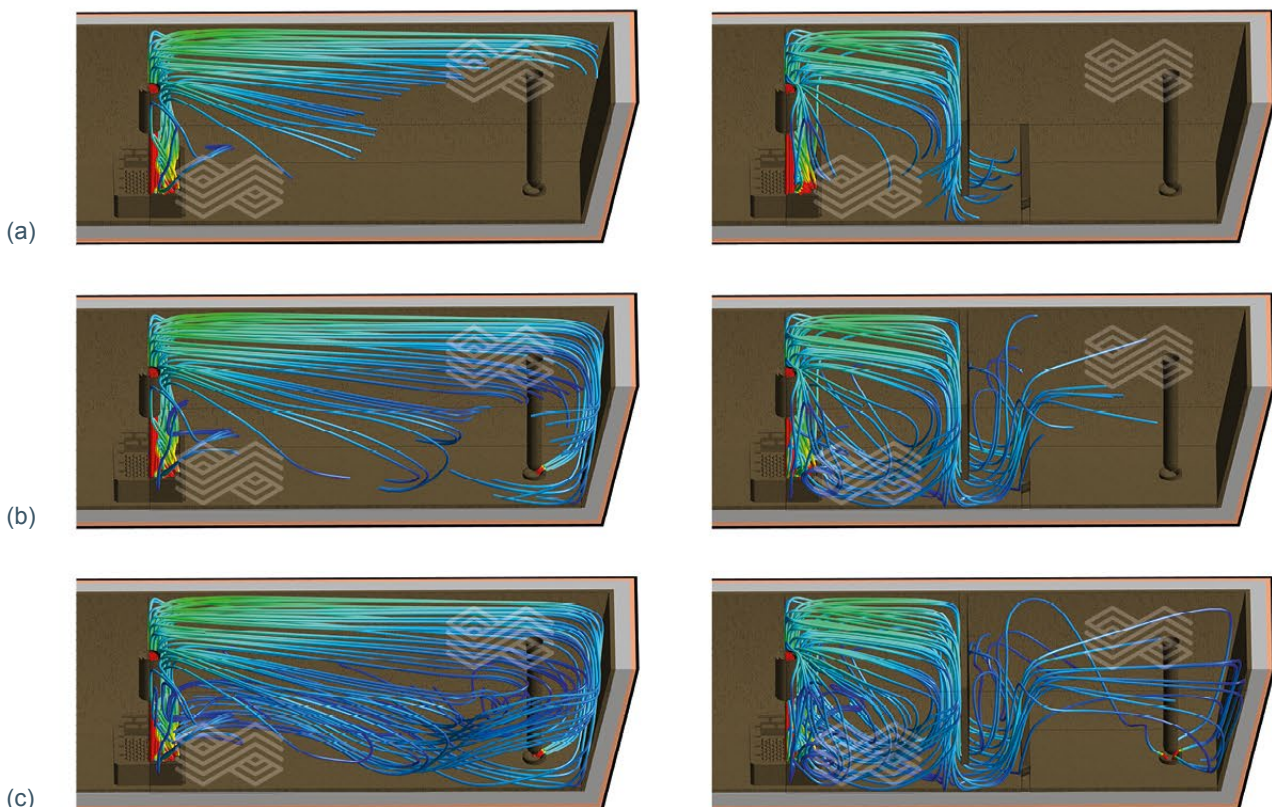
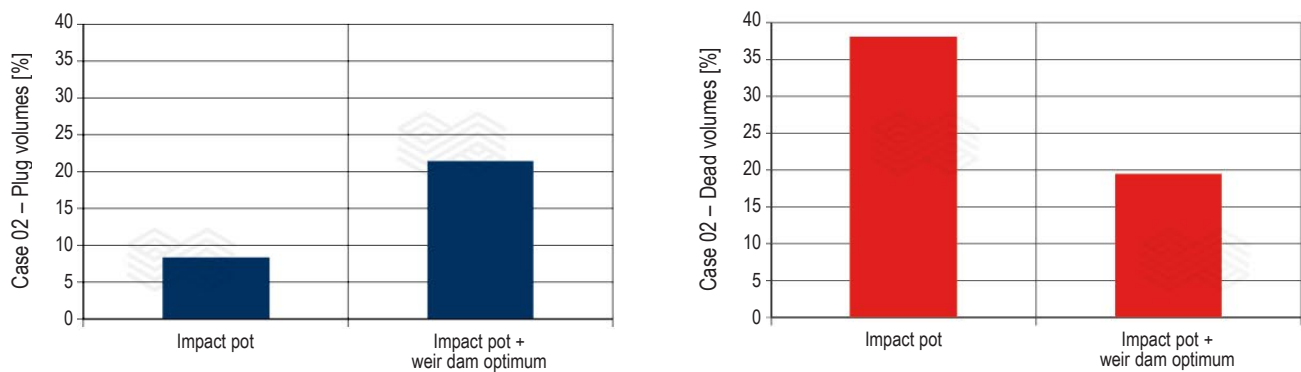


Figure 10.

RTD results comparing the different configurations for case 2.



Summary

In this work, RHI Magnesita's Optimisation Model for tundish furniture was presented. Through the mathematical model, it is possible to obtain the best combination of positioning and size for flow modifiers, such as weirs and dams, to maximize the performance of the equipment, in this paper defined as the minimum residence time. The optimisation model works in an adaptive way, narrowing the domain into the most promising parameter ranges as the study progresses, which provides faster and better results than if random samples were taken. Two different tundish geometries were studied through the model: one with perfect alignment between the shroud and the impact pot, and another with misalignment. The optimisation model provided significant improvement for both cases, with the misaligned geometry obtaining the greatest benefit from the optimised furniture. Therefore, the model is suitable to be applied to any tundish at any operational condition. By optimising the tundish furniture, significant improvements can be obtained in terms of steel cleanliness and mixing efficiency.

References

- [1] Guthrie, R.I.L. Fluid flows in Metallurgy – Friend or Foe?, *Metallurgical and Materials Transactions B*. 2004, 35B, 4171–437.
- [2] Chattopadhyay, K. Ph.D. Thesis, McGill University, Canada, 2011.
- [3] Sahai, Y. and Emi, T. Melt Flow Characterization in Continuous Casting Tundishes, *ISIJ International*. 1996, 36, 6671–672.
- [4] ANSYS, Release 17.2, Help System, Design Xplorer Theory, ANSYS, Inc., 2016.
- [5] Resende, A.D. and Freire, R.A. Tundish Furniture Optimization to Maximize Steel Quality. Presented at the 9th European Continuous Casting Conference, Vienna, Austria, June 2017, 801–810.

Based on a presentation given at 9th ECCC European Continuous Casting Conference – ECCC 2017, 26. June 2017 – 29. June 2017 in Vienna.

Authors

Alexandre Dolabella Resende, RHI Magnesita, Contagem, Brazil.

Rodrigo Nazareth Borges, RHI Magnesita, Contagem, Brazil.

Rubens Alves Freire, RHI Magnesita, Contagem, Brazil.

Ramon Fraga Resende, RHI Magnesita, Contagem, Brazil.

Corresponding author: Alexandre Resende, alexandre.resende@rhimagnesita.com





RHI MAGNESITA



There for you,
wherever
you need us





Taking innovation to 1200 °C and beyond

€37 m

Annual R&D
investment

>19000

Product recipes to
meet customers'
needs precisely

c.1900

Global patents
and patent
applications held

bulletin

2018

